

# Lawrence Berkeley National Laboratory

## Recent Work

### Title

HYDROCARBON INTERACTIONS WITH Ir, Ni, Si, AND NiSi<sub>2</sub> SURFACES

### Permalink

<https://escholarship.org/uc/item/7rb6r8z7>

### Author

Klarup, D.G.

### Publication Date

1985-10-01



# Lawrence Berkeley Laboratory

UNIVERSITY OF CALIFORNIA

RECEIVED  
LAWRENCE  
BERKELEY LABORATORY

NOV 18 1986

LIBRARY AND  
DOCUMENTS SECTION

## Materials & Molecular Research Division

HYDROCARBON INTERACTIONS WITH Ir, Ni, Si,  
and NiSi<sub>2</sub> SURFACES

D.G. Klarup  
(Ph.D. Thesis)

October 1986

**TWO-WEEK LOAN COPY**  
*This is a Library Circulating Copy  
which may be borrowed for two weeks.*



LBL-22249 c.2

## **DISCLAIMER**

This document was prepared as an account of work sponsored by the United States Government. While this document is believed to contain correct information, neither the United States Government nor any agency thereof, nor the Regents of the University of California, nor any of their employees, makes any warranty, express or implied, or assumes any legal responsibility for the accuracy, completeness, or usefulness of any information, apparatus, product, or process disclosed, or represents that its use would not infringe privately owned rights. Reference herein to any specific commercial product, process, or service by its trade name, trademark, manufacturer, or otherwise, does not necessarily constitute or imply its endorsement, recommendation, or favoring by the United States Government or any agency thereof, or the Regents of the University of California. The views and opinions of authors expressed herein do not necessarily state or reflect those of the United States Government or any agency thereof or the Regents of the University of California.

**Hydrocarbon Interactions with  
Ir, Ni, Si, and NiSi<sub>2</sub> Surfaces**

**Douglas Gordon Klarup**

**(Ph. D. Thesis)**

**Lawrence Berkeley Laboratory**

**and**

**Department of Chemistry**

**University of California**

**Berkeley, California 94720**

**This work was supported by the director, office of energy research, office of basic energy sciences, chemical sciences division of the U.S. Department of Energy under Contract Number DE-AC03-76SF00098.**

**Interactions of Hydrocarbons  
with  
Ir, Ni, Si, and NiSi<sub>2</sub> Surfaces**

**Doug Klarup**

**Abstract**

Thermal desorption spectroscopy was used to investigate interactions of organic adsorbate molecules on Ir(111), Ni(111), Ni(100), Si(111), Si(100), NiSi<sub>2</sub>(111), and NiSi<sub>2</sub>(100) surfaces. The decomposition of methyl-substituted benzenes was studied on Ir(111), Ni(111), and Ni(100), and the adsorption of acetylene, ethylene, benzene, and pyridine was studied on Si(111), Si(100), NiSi<sub>2</sub>(111), and NiSi<sub>2</sub>(100). The growth mechanism of NiSi<sub>2</sub> on Si was investigated as well. Factors such as adsorbate symmetry, surface geometry, and sub-surface composition are used to interpret the thermal desorption results.

Isotopic labeling studies show that methyl-substituted benzenes go through step-wise decomposition on Ir(100), Ni(111), and Ni(100). The methyl, or aliphatic, C-H bonds break prior to the aromatic C-H bonds. The thermal desorption spectra of *p*-xylene best demonstrate this regiospecific bond breakage, due to the high symmetry of the molecule compared to *o*- or *m*-xylene. Of the surfaces studied, Ni(100) spectra most clearly show regiospecific bond breakage of the adsorbate molecules, due to this surface's superior ability to break aliphatic C-H bonds and inferior ability to break aromatic C-H bonds compared to the (111) surfaces.

The thermal desorption results of acetylene, ethylene, benzene, and pyridine on Si and NiSi<sub>2</sub> surfaces show that Si atoms reside as the top layer on the NiSi<sub>2</sub> surface, that the underlying Ni atoms have only a small affect, if any, on the surface chemistry of the Si atoms in NiSi<sub>2</sub>(compared to pure Si), and that NiSi<sub>2</sub> islands form on both Si(100) and Si(111) surfaces when small amounts of

Ni are deposited and annealed. The implications of these results are discussed.

**To Amy**

## **Acknowledgement**

I would like to express my deepest gratitude to the following :

The late Dr. Earl Muetterties, whose kindness and unique approach to science made my introduction to surface chemistry exciting and interesting.

The Muetterties research group, in particular Dr. Ron Wexler, Dr. Kirk Shanahan, Dr. Tom Gentle, and Dr. Allen Johnson, for their invaluable assistance and advice.

Dr. Angelica Stacy, whose thoughtfulness, advice, encouragement, enthusiasm, and direction made my research environment very stimulating and pleasant.

The entire support staff of MMRD at LBL, particularly Mr. Weylond Wong, Mr. Herb Riebe, Mr. Jim Severns, and Mr. Hank Brendel. Maintaining and modifying ultra-high vacuum equipment would not have been possible without them. I would also like to thank Mr. Bill Wilkie in the ceramics shop, who was able to drill such small holes in something as brittle as a Si wafer.

The many co-workers I've had the opportunity to associate with. Especially Tom Rucker, Ken Lewis, Joe Womack, and Mike Kollrack, whose friendship, suggestions, and scintillating discussions, even if they weren't always about surface chemistry, made research a pleasure.

The friends and family I've been so lucky to be surrounded by: my grandfather, Elmer Klarup, whose interest and enthusiasm in science and education helped me make it through all the schooling. My parents, Donald and Phyllis Klarup and my sisters, Pam Klarup and Trish Hoffman, for keeping the faith and providing encouragement through the years. My mother-in-law, Carol Lynch, for being the wonderful person she is and raising such a great daughter. My own daughter, Erin Jean Lynch-Klarup, whose presence the last 17 months has made them the best months of my life. And finally my wife, Amy Lynch. Her love and support throughout my studies has and always will amaze me. I am a



lucky man.

This work was supported by the director, office of energy research, office of basic energy sciences, chemical sciences division of the U.S. Department of Energy under Contract Number DE-AC03-76SF00098.

## Table of Contents

Chapter One: Introduction .....	1
Thermal Desorption Spectroscopy .....	8
Figure .....	12
Chapter Two: Experimental .....	13
Chapter Three: Methyl Substituted Benzenes on Ir(111) .....	21
Results .....	21
Discussion .....	24
Figures .....	27
Chapter Four: Xylenes on Ni(111) and Ni(100) .....	45
Results .....	45
Discussion .....	48
Ni and Ir Comparisons .....	53
Figures and Table .....	55
Chapter Five: $\pi$ - Bonding to Si and NiSi <sub>2</sub> .....	72
Results .....	72
Si(100) .....	72
NiSi <sub>2</sub> (100) .....	73
NiSi <sub>2</sub> (100) Formation .....	75
Si(111) .....	76
NiSi <sub>2</sub> (111) .....	77
NiSi <sub>2</sub> (111) Formation .....	79
Discussion .....	80
Si(100) and Si(111) .....	80
NiSi <sub>2</sub> Formation .....	85
Critical Thickness .....	89
Metal-Silicon Interaction .....	90
Island Formation .....	92

Summary -----	94
Bulk NiSi <sub>2</sub> -----	<b>95</b>
NiSi <sub>2</sub> Surfaces -----	96
NiSi <sub>2</sub> (111) vs. Si(111) -----	97
NiSi <sub>2</sub> (100) vs. Si(100) -----	98
NiSi <sub>2</sub> (111) vs. NiSi <sub>2</sub> (100) -----	100
Figures and Tables -----	102
Chapter Six: Conclusions -----	132
References and Notes -----	134

## Chapter One

### Introduction

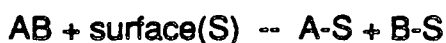
This thesis examines the interaction of organic adsorbate molecules on both metal(Ni,Ir, and NiSi<sub>2</sub>) and semiconductor(Si) surfaces. The variety of surfaces studied allows for comparisons involving surface geometry, surface reactivity(the ability of a surface to bond to an adsorbate), and film growth on surfaces. The experiments reported and discussed here contribute to the growing discipline of surface chemistry.

There are many reasons that surfaces are an interesting field for study. Since they are not described by isolated molecules or bulk characteristics, they pose fundamental chemical questions. Technologically, the traditional force behind surface science is heterogeneous catalysis, where the chemistry of a surface is so important. Another area where the understanding of surfaces is crucial is in the electronics industry. Here surface behavior is important not only from a physics point of view, where surfaces and interfaces provide unique and interesting electronic properties, but understanding how surfaces act and react with the surrounding environment is also critical. Questions concerning surface stability under different atmospheres are relevant to device longevity and use, and surface behavior is an important consideration for many manufacturing steps, i.e., etching, passivation, and thin film growth. In this thesis these two areas of surface chemistry are explored. Catalytic factors are investigated in the Ni and Ir work and the surface chemistry of two electronic materials, Si and NiSi<sub>2</sub>, is studied as well.

The question that immediately arises is what is the nature of the surface-adsorbed matter(adsorbate) interaction? What role does the surface play in catalysis, corrosion, device failure, and thin film growth? For some reactions that occur on a surface, all the surface does is simply reduce the dimensionality of the problem for one reactant A to find another reactant B in order to form AB. One estimation is that this step takes about 1/30 the time in two dimensions than

in three.<sup>1</sup> Thus layered solids like clays should be good catalysts, and this is true in some cases.<sup>2</sup> However, the chemical role the surface plays in such instances is minimal--it does not interact to any great extent with the adsorbates--and is also less interesting. All that is needed is some non-interacting surface, any non-interacting surface, and once this requirement is fulfilled there is little else to do.

The much more interesting case to study is the interacting surface--the surface with sites where chemistry occurs. A simple example of this type of surface is given by the scheme where the surface acts as a dissociation agent:



In this situation the type of surface is critical and this then lends itself to substantial study and consideration.

One way to gain insight into surface-adsorbate chemistry, or chemisorption,<sup>3</sup> is to study the decomposition of hydrocarbons on the surface. An example of this type of study is presented in chapter three, where the decomposition of methyl-substituted benzenes on Ir(111) is reported. This system has two advantages: (1) by investigating the interaction of dimethyl benzenes, or xylenes, one has the advantage of being able to look at three different isomers, and use their subtle geometric differences to help point out different types of adsorbate/surface interactions, and (2) by selective substitution of deuterium for either the aliphatic or aromatic hydrogen atoms, the decomposition mechanisms of methyl benzenes on metal surfaces can be studied. This is not the first instance of using isotopic substitution in surface chemistry. For example, the Muetterties group used this technique for several years and it has proven to be one of the most illuminating ways to study

decomposition mechanisms on metal surfaces.<sup>4</sup>

A refinement of the study of methyl-benzene decomposition on metal surfaces was to study these processes on surfaces of different crystallographic orientation. This study is presented in chapter four, where the two surfaces chosen were Ni(111) and Ni(100). The different orientations of these two surfaces allow some very interesting conclusions to be made concerning the role surface geometry plays in hydrocarbon chemisorption and decomposition. All three of these variations--surface crystallography, isomer variations, and isotopic substitutions--help point out what the important factors are in metal surface - hydrocarbon interactions.

The above mentioned projects all deal with pure metal surfaces, which have the advantage of simplicity. However, many "real" surfaces are not pure, but are oxides, silicides, or alloys. One way to approach this problem of the "impure surface" is to study the surface chemistry of a binary compound, in this case NiSi<sub>2</sub>. This system can help shed light on phenomena like the strong metal-support interaction, which is a reduction in chemisorption on certain supported metal catalysts after particular treatments. The effect has been attributed to the movement of support on top of and into the metal catalyst particles<sup>5a</sup> or alloy formation between metal and support. For example, Ni on SiO<sub>2</sub>, when reduced at high temperatures, forms Ni-Si alloys and the catalytic activity of the Ni is reduced.<sup>5b</sup> The study of a crystalline Ni-Si compound, NiSi<sub>2</sub>, may give insight into how this occurs or what the resultant alloy is; investigating NiSi<sub>2</sub> surface chemistry should shed light on the strong metal-support interaction.

Another aspect of "impure" surfaces is the effect that adatoms have on the surface chemistry. It has been shown that various adatoms can alter significantly the reactivity of a particular surface.<sup>6</sup> Therefore, the study of "impure" surfaces provides very good opportunities for improvement of "real" catalyst surfaces or helping pinpoint why certain catalysts are poisoned in a particular process. The study of NiSi<sub>2</sub>, a binary compound, contributes to this knowledge of how one

atom may affect another's surface chemistry. This should assist in a better understanding of "real" catalyst surfaces.

Another area of technological import which concerns "impure" surfaces is the field of oxide surface chemistry. Particularly for the refractory metals, which are cheaper and more abundant than the noble metals, the corresponding oxides temper the extreme reactivity of the pure metal surface hence making them much more useful catalysts. To study these oxides, it is common practice to oxidize the first few layers of the metal surface to attain the desired oxide (it is often very difficult to grow or obtain large single crystal oxides), but it is not clear whether this thin oxide layer accurately portrays the "real" oxide catalyst. The dependence of chemisorption on the thickness of  $\text{NiSi}_2$  films on Si was investigated here, and should lend insight into the metal/metal oxide case.

There are many other advantages to using the  $\text{NiSi}_2/\text{Si}$  system. It has importance in the catalytic field due to SMSI, and both  $\text{NiSi}_2$  and Si are used in the electronics industry. A metal ( $\text{NiSi}_2$ ) on a semiconductor (Si) creates an electronic barrier at the interface. By studying chemisorption on  $\text{NiSi}_2/\text{Si}$ , the effect this barrier has on chemisorption can be explored.

Another advantage of the  $\text{Si}/\text{NiSi}_2$  system is that it is possible to grow epitaxial  $\text{NiSi}_2$  on both Si(111) and Si(100). There is only a .4% lattice mismatch between Si and  $\text{NiSi}_2$ . This sidesteps the difficulties of trying to grow large single crystals of a binary compound. Although some large crystal work has been done, on ZnO, for example,<sup>7</sup> and reports of "quasi-crystalline"<sup>8,9</sup> alloys have been made, in general there are not many well defined surfaces of binary compounds that have been studied. It also leaves one with a crystalline face to study, which is very important as far as data interpretation is concerned.

A side benefit of studying this system is that one can investigate the growth mechanism of  $\text{NiSi}_2$  on Si from the first few Ni atoms on up. Investigating growth mechanisms of metal films on semiconductors is very important to the electronics

industry, where ultra-thin metal layers and their interactions with Si are important aspects to consider in device manufacture. In fact, NiSi<sub>2</sub> is often one of the silicides chosen for use in chip manufacture because of its small lattice mismatch (allowing for very sharp interfaces with Si), its ability to act as a diffusion barrier, and its stability.

In this thesis an emphasis was placed on  $\pi$ -bonding between the adsorbate and the silicon and silicide surfaces. These types of chemisorption systems have not been studied as much as other systems on silicon, such as H<sub>2</sub>O, H<sub>2</sub>, and O<sub>2</sub>, because they do not play as important a role technologically. They do, surprisingly, prove to be good probes for determining the similarities and differences between Si and NiSi<sub>2</sub> surface chemistry. Also, because of the  $\pi$ -bonding that does apparently occur, study of the systems presented stimulates speculation of how these molecules do bind to the Si and NiSi<sub>2</sub> surfaces.

Chemisorption of acetylene, ethylene, benzene, and pyridene on Si and NiSi<sub>2</sub> surfaces was investigated, and is reported in chapter five.

To provide a framework from which chemisorption may be understood, many theoretical models have been proposed. They either describe chemisorption as a local interaction, involving only one or at least a small number of substrate atoms, or as a non-localized system involving large numbers of substrate atoms. The former outlook has the advantage of simplicity and has correlations in transition metal complexation chemistry. The non-localized approach (using bands instead of discrete orbitals) gives ranges of energies (due to the larger number of atoms considered) for chemisorption bonds. This may be a more realistic approach, since more particles are considered.

Non-localized theories give very general descriptions of chemisorption. One example of this type of approach with chemisorption on metals, is viewing chemisorption through d-band vacancies.<sup>10</sup> Here chemisorption is favored by 1) large values of the exit work function--this favors electron donation to the metal 2) large (+) values of the density gradient at the Fermi level<sup>11</sup> and 3) presence of



d-band vacancies. Under these conditions, it is favorable for electrons to enter the metal and for an increasing number of states to accommodate them. The power of this model for chemisorption is in its simplicity and ability to predict general trends. For example, it predicts that the transition metals at the left side of the periodic table will be more reactive than those on the right side, and this is, in general, true. A disadvantage of this theory is that it does not adequately account for  $\pi$  back bonding from the metal to the adsorbate.

Another band-theory for chemisorption, concerning semiconductors, is the boundary layer theory.<sup>10,12</sup> Consider ion adsorption on an n-type semiconductor. There are two cases or types of chemisorption. If the adsorbate is adsorbing as an anion, electrons are donated from the conduction band until all the conduction electrons in the near surface region are removed. This is called depletive chemisorption. If the adsorbate is adsorbing as a cation, electrons are donated to the conduction band--accumulative chemisorption. If depletive chemisorption is the case, one should see a decrease in conductivity with increasing coverage of the adsorbate on the semiconductor. The opposite should be true for accumulative chemisorption. This is a very appealing theory for chemisorption but it suffers two major drawbacks. The first is that it deals only with ion adsorption, and this is not usually the case for chemisorption on semiconductors--especially hydrocarbon adsorption. The second drawback is that this model does not do much to explain the geometry of the chemisorbed molecule on the surface nor does it hint at what, other than charge transfer, are the important factors in the adsorbate/surface interaction.

Localized theories for chemisorption allow much greater insight into the adsorbate-surface interaction. In the case of metals, there is a large body of knowledge of ligand-transition metal bonding that can be correlated to surface bonding. For example, if one is studying the interaction of carbon monoxide with a surface, it is useful to picture the CO molecule binding to the surface as it would to a transition metal atom-- $\sigma$  bonding through the C atom and backbonding from the metal into the  $\pi^*$  orbital of the carbon monoxide. The picture can then be

expanded somewhat to include more substrate atoms, creating bands instead of orbitals because of the wider range of energies involved.<sup>13</sup> Another example might be dibenzenechromium(see figure 1-1), where the benzene rings are parallel to each other and where it is believed the main interaction of the benzene and Cr atom is through  $\pi$ -bonding using the metal d orbitals. If a similar interaction occurs on a metal surface, the benzene ring should chemisorb parallel to the surface, and this is usually the case.

A localized theory for chemisorption also may be more appropriate for semiconductors than a non-localized theory like the boundary layer theory. This possibility arises when one looks at what constitutes localized bonding--a strong interaction between an adsorbate molecule and one(or at most just a few) surface atom(s). The interaction must be stronger than the substrate atom's interaction with its neighbors. This is certainly the case for hydrogen atom adsorption on Si(111). For example,after enough H exposure,  $\text{SiH}_4$  forms and desorbs from the surface.<sup>14</sup> Clearly the Si-H interaction is stronger than the Si-Si interactions. Another situation that leads to localized bonding is the existence of surface states, electronic states that are unique to the surface. The energy of surface states is very narrow(because it involves so few atoms) and lies outside the bands formed by the bulk of the substrate, hence it is detectable.<sup>15,16</sup> Chemisorption naturally involves these surface states, either causing them to disappear or forming new ones, indicative of localized bonding occurring at the surface. Indeed, these surface states often are connected with the famous "dangling" bonds which project from the surfaces of covalent solids.<sup>17,18</sup> In silicon these dangling bonds are highly directional  $\text{sp}^3$  hybrids and are involved in Si surface reconstruction as well as Si surface chemisorption. If atomic orbitals, like  $\text{sp}^3$  hybrids, can account for the surface states observed, a localized bonding picture can be employed and the details of the chemisorption event(mechanism, bonding geometry) can be speculated upon.

For the studies reported in this thesis, adsorption of hydrocarbons on metal and silicon surfaces, localized bonding theories provide more insight into the

specific interactions than non-localized theories. It is more useful to consider the binding of the adsorbate to one or just a few of the surface atoms than to consider the entire system of all of the substrate atoms and adsorbate atoms.

Understanding of the chemistry taking place is clearer using a localized bonding picture. This is partly the case because localized theories provide a better connection to simpler chemical systems where few atoms and molecules are involved. However, localized theories are also more useful because of the current understanding of surface chemistry. As more information and knowledge accumulates concerning adsorbate-adsorbate interactions and long range surface-adsorbate effects non-localized type theories should become more important and useful.

### **Thermal Desorption Spectroscopy**

Studying adsorption on Ir, Ni, Si, and NiSi<sub>2</sub> surfaces requires a technique which can provide useful information on these systems. There are a plethora of surface science techniques to choose from, too many to cover in this thesis. One group of techniques involves vibrational and photoemission spectroscopies, and are probably at the forefront of chemisorption investigation. These techniques (for example electron energy loss spectroscopy and ultra-violet photoemission spectroscopy) lend direct information on the bonding of the adsorbate to the surface. Thus they are very powerful tools. However, they are best used for simple adsorbates, diatomic molecules for instance, because then detailed and useful interpretation is possible. For more complex molecules, such as the xylenes, direct interpretation of the spectra obtained is difficult, especially when the decomposition of the molecule is considered, though advances are being made.<sup>19</sup>

There are also diffraction spectroscopies, low energy electron diffraction is probably the best known example, but these are somewhat limiting for large molecules as well. For one thing, ordering of the adsorbate molecules is

necessary in order for periodic patterns to occur. This is not much of a problem for small, simple molecules, but it is more difficult for the larger molecules. Furthermore, without the use of intensity-voltage curves, which involve complex mathematical interpretations, one is limited to two dimensional information, and it is unclear how the ordered adsorbate layer is interacting with the surface.

The technique that was used in the studies presented in this thesis is thermal desorption spectroscopy. This is actually a form of mass spectroscopy, where one monitors the gasses that desorb from the surface of the sample as it is heated. As far as chemisorption is concerned, this technique does have some disadvantages. For one thing, the information obtained is indirect; it is obtained *after* the chemisorption bond has been broken. Another small disadvantage is that the introduction of significant amounts of thermal energy perturb the system. This is manifested most often in the subsequent decomposition of the adsorbate, which is necessary if one is studying the decomposition mechanism of an adsorbate on a surface but is otherwise an unwelcome side-effect. It is true that no technique leaves a system unperturbed--interference is necessary to probe the chemisorption bond--but thermal desorption spectroscopy introduces a very large perturbation indeed.

A big advantage of thermal desorption spectroscopy is that some idea of the adsorbate-surface bond strength can be obtained. At the very least relative bond strengths can be calculated, since the bond strength is related to the temperature at which the adsorbate molecule desorbs. However, there also exist methods<sup>20-26</sup>, using thermal desorption spectroscopy, by which absolute heats of adsorption can be calculated, though there are limits to the reliability of these calculations.<sup>26</sup> The calculations work best if the desorption mechanism is known. The rate determining step must be the desorption of the molecule itself from the surface. This is most certainly true for molecular adsorption and desorption, but may not be true for cases involving dissociative adsorption, where recombination is required for desorption, or adsorbate decomposition, where the gasses desorbing have formed from the adsorbate decomposition. Also, the

order of the desorption can be determined from the shape and characteristics of thermal desorption curves. For instance a 2nd order desorption is characterized by a decreasing peak maximum temperature (the temperature at which the maximum number of gas particles is detected desorbing from the surface) with increasing coverage. The same result, however, can be obtained if a coverage dependent activation energy of desorption is involved. In addition, because it is the activation energy of *desorption* that is obtained from the thermal desorption curves, another assumption must be made in order to find the heat of *adsorption*. This assumption is that the adsorption is non-activated. Whereas this might be true for adsorbates on metal surfaces, this is clearly not the case for hydrogen adsorption on Si, where predissociation of the H<sub>2</sub> molecule is necessary before any hydrogen atoms will bind to the silicon surface.

Despite these interpretational difficulties, thermal desorption spectroscopy was used in these investigations. This is partly because it was a readily available technique that is relatively simple to execute. However, it was also because the systems studied involved complex molecules as adsorbates, so more direct techniques were not feasible due to worse interpretation problems. The thermal desorption spectra give relative adsorbate-surface bond strengths and, where feasible, absolute heats of adsorption have been calculated and reported. Since trends were of interest here, the most simple formula following Redhead<sup>20</sup> was used. For a first order reaction:

$$E/RT_p^2 = (v/\beta)\exp(-E/RT_p)$$

where  $E$  is the activation energy of desorption,  $T_p$  is the peak maximum temperature,  $v$  is the frequency factor, usually taken to be on the order of molecule vibration on the surface, or  $10^{13} \text{ sec}^{-1}$ ,<sup>27</sup> and  $\beta$  is the heating rate. The heats of adsorption calculated from this formula at least give some idea of the bond strength between the adsorbate molecule and the surface.

The studies presented in this thesis all are designed to elicit the important factors in adsorbate-surface interactions, or chemisorption. The

methyl-substituted benzenes on metal surfaces experiments are an attempt to determine, at least partially, the decomposition mechanism of these complex molecules on metal surfaces. The role different crystallographic orientations play on these decompositions also are considered. They are presented in chapters 3 and 4. The unsaturated hydrocarbons on Si and NiSi<sub>2</sub> are designed to bring out similarities and differences between adsorption on a pure element, Si, and a binary compound, NiSi<sub>2</sub>. The effect of different crystallographic orientations is considered here as well. A side investigation concerns the growth mechanism of NiSi<sub>2</sub> on Si. These results are presented in chapter 5. Some general conclusions are presented in chapter 6.

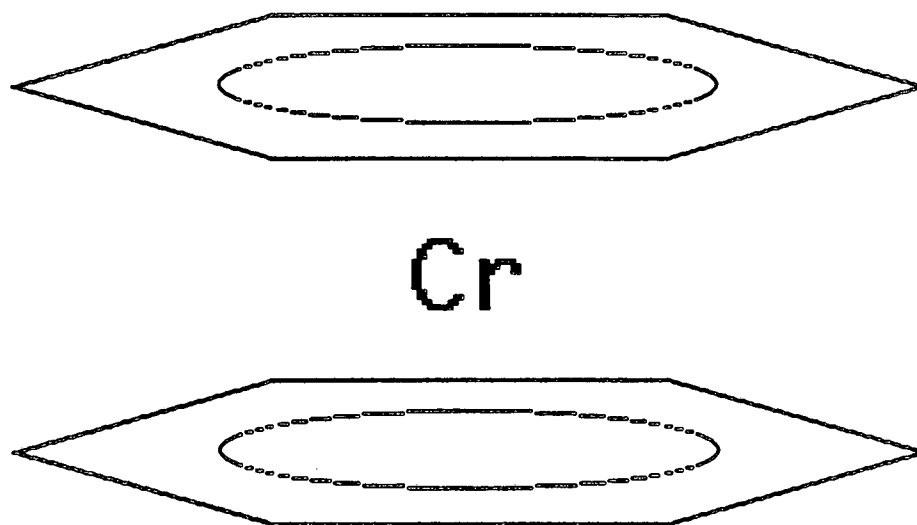


Figure 1-1. Dibenzenechromium. The benzene rings are parallel to one another.  $\pi$ -bonding between the metal d orbitals is believed to be the primary mode of bonding in the molecule.

## Chapter Two

### Experimental

Because low pressures are required for surface cleanliness and electron beams are used for surface analysis, all experiments were performed in a Varian ultra-high vacuum chamber equipped with five 40 liter/sec ion pumps and a titanium sublimation pump. Rough pumping was accomplished using two oil-free liquid nitrogen cooled sorption pumps. An auxiliary turbo pump (Pfeiffer) was used during Argon ion sputtering to allow a flow of Ar through the chamber and aid in its removal. Base pressures were always less than  $5 \times 10^{-10}$  torr and usually less than  $2 \times 10^{-10}$  torr. The major background contaminants were  $H_2$ , He,  $H_2O$ ,  $CH_4$ , CO,  $N_2$ , Ar, and  $CO_2$ .

The UHV chamber was equipped with various surface science techniques. These included low energy electron diffraction (LEED), which gives information concerning the periodicity of the surface, Auger electron spectroscopy (AES), using a 4 grid retarding field analyzer, for surface composition analysis, and Argon ion bombardment to assist in cleaning the surface. A quadrupole mass spectrometer (Uthe Technology International) also was attached to the chamber and was used to monitor background gases as well as gases desorbing during the thermal desorption experiments. For experiments with the Ni(100), Ni(111), and Ir(111) surfaces a single stainless steel plate with a small hole cut in the center of it was placed in front of the mass spectrometer ionizer. For experiments with the Si(111) and Si(100) surfaces, two such plates, spaced about 1/2 inch apart, were used, with the holes lined up. With the crystal surface properly aligned in front of the holes, only the gasses actually desorbing from the surface of interest reached the quadrupole--cutting down on background interference. A dedicated computer was used to control the mass spectrometer so that several masses could be monitored simultaneously. Two variable leak valves were positioned between the gas introduction manifold and a "dosing needle" which extended into the UHV chamber. The end of the "dosing needle" was on the



same plane as the crystal, so the crystal face could be exposed to large effective pressures without backfilling the chamber. Single crystal samples were mounted on a rotatable manipulator with a 2 1/2 inch offset that extended down into the UHV chamber from above. The manipulator also had a vertical flip mechanism that allowed the crystal surface to face downward.

For nickel deposition onto the Si surfaces, a 2 kW electron beam evaporator (VG instruments) was used. This was positioned in the lower half of the chamber so the Ni evaporated up to the crystal. For deposition, the crystal was flipped approximately  $70^\circ - 80^\circ$  ( $20^\circ - 30^\circ$  from horizontal) and maneuvered close to a quartz crystal film thickness monitor so that the amount of evaporant could be monitored. Both the monitor and the crystal were located 9 inches above the evaporator. To prevent Ni deposition over the entire chamber, a cylinder of stainless steel was placed in a vertical fashion on the evaporator, thus restricting the evaporant to a small area above the opening of the cylinder which was approximately 2 1/2 inches below the film thickness monitor. For further protection against Ni deposition, as well as protection against unwanted sputtered deposition during Ar ion sputtering, a stainless steel plate was placed in front of the LEED optics. This shield could be rotated away from the LEED optics when necessary. Pressures during Ni evaporation were usually around  $1 \times 10^{-8}$  torr.

The various single crystal samples looked at (Ni(111), Ni(100), Ir(111), Si(100), and Si(111)) all were mounted on the manipulator in some fashion. The Ni crystals and the Ir(111) crystals were spot welded directly to heater leads for their support and then were heated directly by running current through the sample. The Si samples were heated indirectly. They were first mounted on a thin Ta foil and held in place with the use of small Ta prongs attached to the Ta foil. The Ta foil was then spot welded to the heater leads and heated by passing current through the foil. This in turn heated up the silicon samples. These methods of heating the samples allowed for fairly linear heating rates, at least in the regions of interest. Cooling was accomplished through the use of a liquid nitrogen sink that extended into the chamber from above. A Cu braid extended

from the sink to the sample holder assembly. This allowed rapid cooling of the samples (which is important to avoid surface contamination) and maximum low temperatures of about  $-125^{\circ}\text{C}$  for the metal surfaces and about  $-60^{\circ}\text{C}$  for the Si surfaces.

Rapid temperature measurement of the samples was crucial for the thermal desorption spectroscopy experiments and was accomplished through the use of Chromel-Alumel thermocouples. For the metal samples, the thermocouple was simply spot welded onto the edge of the crystal. For the Si samples, this was not possible, and alternative methods of attachment were investigated. What worked best was first drilling a .015 inch hole in the Si single crystal, then passing both thermocouple leads through this hole and spot welding the leads together. The thermocouple leads are .005 inches in diameter and when spot welded together form a junction that is usually around .015 inches in diameter. Thus the thermocouple junction could be drawn back into the hole in the Si crystal and wedged into place. Reproducibility from one crystal to another indicated that the thermocouple junction was in good thermal contact with the sample.

Several different chemicals and materials were used in these studies. The  $\text{d}^{10}$  o-xylene,  $\text{d}^{10}$  p-xylene,  $\text{d}^6$  p-xylene, mesitylene, and perdeutero pyridine were purchased from the Aldrich Chemical Company. The perdeutero m-xylene and benzene were purchased from Fisher Scientific Co., and the  $\text{C}_6\text{H}_5\text{CD}_3$  and  $\text{C}_6\text{D}_5\text{CH}_3$  purchased from Merck and Co. The  $\text{d}^6$  o-xylene and the  $\text{d}^6$  m-xylene were prepared by Robert Lum of the Muetterties research group in the University of California laboratories. The  $\text{C}_2\text{D}_2$  and  $\text{C}_2\text{D}_4$  were purchased from Merck, Sharp and Dohme. All samples were put through at least three freeze-pump-thaw cycles on a mechanically pumped glass vacuum line in order to remove unwanted air. Purity of the samples was checked using the mass spectrometer. Argon and oxygen (Matheson) were introduced directly from pressurized tanks into the gas introduction manifold of the chamber. The Ni used in the silicide studies was purchased in the form of .5 mm wire, grade 1, from Puratronic.

The single crystal samples used in these studies also had several different sources. The Ni crystals were first cut as wafers, using spark erosion, from a Ni single crystal rod(99.999%--Materials Research Corporation). These wafers then were mounted on a goniometer and oriented in the desired manner using Laue x-ray back diffraction. Once oriented, the wafers were ground down, using SiC paper, so that the desired face of the crystal was exposed. The wafer then was turned around, and the orientation and grinding done on the opposite side so that what was left was a thin single crystal wafer with two parallel sides of the desired orientation. The wafers were mounted in Koldmount for easy handling and polished further. This involved first polishing on 4 different grades of SiC paper(0,00,000,0000) for a rough polish, then placing them on a diamond paste polishing wheel, first with 6 micron, then 1 micron diamond paste to achieve a finer polish. Finally, they were given a finishing polish using .05 micron Alumina in water in a vibrating tank.

The remaining crystals used in these studies were kindly provided by various people. The Ir(111) crystal was lent by Professor Thor Rhodin of Cornell University. The Si crystal wafers were given by Dr. David Hodul of Varian Corporation. The Si(100) crystal was p-type, 4-6 ohm-cm, and about .4 mm thick. The Si(111) crystal was also p-type, 10-12 ohm-cm, and about .3 mm thick. All crystals borrowed or received from outside sources already were polished and were used as received.

$\text{NiSi}_2$  can be grown epitaxially on Si single crystals as has been shown by several investigators.<sup>28,29</sup> The procedure is quite simple-- first evaporating a desired amount of Ni onto the Si surface and then annealing at about 750°C for sufficient time to form  $\text{NiSi}_2$ . The amount of Ni deposited onto the surface of the Si was monitored by the quartz crystal microbalance, though absolute calibration of this microbalance was non-trivial. Just using the density of bulk Ni, one Å of Ni deposited onto the crystal corresponds to  $9.13 \times 10^{14}$  atoms/cm<sup>2</sup> of Ni. This is then 1.35 monolayers on the Si(100) surface(one monolayer is the number of surface atoms present on the ideal surface-- $6.78 \times 10^{14}$ /cm<sup>2</sup> for Si(100) and 7.84

$\times 10^{14}/\text{cm}^2$  for Si(111)) and 1.16 monlayers on the Si(111) surface. However, the LEED pattern of the Si(111) surface does not disappear until 5 Å of Ni have been deposited onto the Si surface, according to the film thickness monitor, and the Auger signal versus amount deposited, on the Si(111) surface, shows a break around 4-5 Å. This, however, corresponds to  $4.11 \times 10^{15}$  atoms/cm<sup>2</sup> (again, according to the film thickness monitor), which is 5.24 monlayers. What may be complicating the situation, besides the possibility that the film thickness monitor may not be calibrated properly (the Ni bulk density may be an inappropriate value to use), is that the first Ni atoms deposited may be slipping under the Si surface and/or forming three dimensional islands on the surface (which is discussed later in this thesis). This would obviously affect any calibration done using AES or LEED, making absolute calibration difficult. Therefore, for the purposes of this thesis, one monolayer will be taken as the number of Si atoms present on that particular Si ideal surface ( $6.78 \times 10^{14}$  for Si(100) and  $7.84 \times 10^{14}$  for Si(111)) and the bulk density for Ni will be used with the film thickness monitor to give at least some relative values of the amount of Ni deposited on the Si surfaces.

Once mounted on the manipulator and introduced in the UHV chamber, the surfaces of the various samples needed to be cleaned of contaminants. This was accomplished using both oxygen treatments and Argon ion sputtering depending on the crystal and contaminant. The main contaminants on the Ni crystals were carbon and sulfur. Carbon was removed using an oxygen pressure of  $1 \times 10^{-7}$  torr while heating the Ni crystal at 650°C for two minutes. This was repeated until no further carbon was seen in the Auger spectrum. The remaining oxygen on the surface was removed by simply annealing the sample an additional minute at 650°C. Sulfur was removed by bombardment with 500-eV Ar<sup>+</sup> ions followed by annealing to restore surface order. Carbon and sulfur were also the main contaminants on the Ir surface, and these were removed using more intensive oxygen treatments. The Ir crystal was heated at 800°C while an oxygen pressure of  $2 \times 10^{-7}$  torr was maintained in the chamber. Two minutes of such treatment

was usually sufficient to remove carbon and sulfur. The remaining oxygen was removed from the Ir surfaces by annealing at 1100°C. Ar<sup>+</sup> ion bombardment was used to remove less common contaminants such as Ca and Si.

The Si samples used, when first placed in the chamber, had a native oxide layer present on the surface. This was removed by heating the crystals at 850 - 900°C for several minutes. The remaining contaminant was carbon, some of which was removed using Ar ion bombardment (1000 eV beam,  $3.5 \times 10^{-5}$  torr Ar). It was extremely difficult to remove all remaining traces of carbon, so many of the experiments reported here were done on a surface slightly contaminated with carbon (the ratio of the C<sub>273</sub> to Si<sub>91</sub> Auger signals was always less than .01). However, experiments done with essentially no C and those done with a slight amount of C showed no discernable difference. The main contaminant on the NiSi<sub>2</sub> surfaces was, again, carbon, and this was removed using Ar ion bombardment as well (600 eV beam, 30 minutes).

The cleanliness of the crystal surface was verified with both Auger electron spectroscopy (AES) and low energy electron diffraction (LEED). The AES spectrum showed only peaks attributable to the pure sample under study except for Si, which often had trace amounts of carbon present (the intensity of the C signal was always < .01 that of the Si signals). LEED patterns characteristic of the clean sample surfaces were always obtained: the Ir(111), Ni(111), and NiSi<sub>2</sub>(111) surfaces showing sharp hexagonal patterns, the Ni(100) showing a square, four-fold pattern, the NiSi<sub>2</sub>(100) showing basically a four-fold pattern but with off integral spots indicating some reconstruction, the Si(100) showing a 2 x 2 pattern attributed to two domains of the 2 x 1 reconstruction, and the Si(111) surface showing the famous 7 x 7 reconstruction characteristic of sputtered and annealed Si(111) surfaces.

Once the surface had been cleaned, thermal desorption experiments were carried out with the various samples using different adsorbates. The procedure for the thermal desorption experiments follows. The sample first was flashed to

remove all traces of adsorbates from the surface, then cooled down to adsorption temperature ( $-90^{\circ}\text{C}$  for Ir and Ni and  $-50^{\circ}\text{C}$  for Si and  $\text{NiSi}_2$ ). Once adsorption temperature was reached, the crystal sample was placed in front of the dosing needle connected to the leak valve through which the adsorbate of interest was introduced. Using the ion gauge in the chamber and a stopwatch, various amounts of the adsorbate were directed to the sample face. The ion pumps remained on during the dosing process. After the dose was completed, the remaining gas was pumped away until the pressure reached that present just prior to dosing. Then the sample was positioned in front of the mass spectrometer and heated rapidly ( $25^{\circ}\text{C}/\text{sec}$  for Ir and Ni and  $30\text{-}40^{\circ}\text{C}/\text{sec}$  for Si and  $\text{NiSi}_2$ ) and linearly while monitoring, with the mass spectrometer, various desorption products. The data then was printed out on a chart recorder.

After the thermal desorption spectrum was completed, the sample surface was checked for contamination using AES and then, if it was Ni(100) or Ir, the surface recleaned. The Ni(111) surface usually did not require cleaning: the C evidently diffused into the bulk of the crystal during the thermal desorption experiment. The Si and  $\text{NiSi}_2$  surfaces often were not cleaned between thermal desorption spectra done on the same day for two reasons: 1) often cleaning was not needed, since these surfaces did not always decompose the adsorbates placed upon them and 2) the only way to clean these surfaces, at least of C, is through sputtering with  $\text{Ar}^+$  ions, and after cleaning in this manner the chamber needed to rest overnight in order to regain a sufficiently low base pressure. After the surfaces were cleaned (if they were to be cleaned), the crystal was cooled for another thermal desorption spectrum.

The exposure of adsorbate gas to the crystal was calibrated by facing the crystal away from the dosing needle and backfilling the chamber to a desired pressure. In this way the pressure at the crystal face should have been close to that of the ion gauge reading. In the subsequent flash the amount that desorbed from the surface was compared to thermal desorption spectra obtained using the dosing needle and in this manner the amount actually introduced to the sample

face using the dosing needle was obtained.

Changes in the LEED pattern due to adsorption of the gasses studied was checked for in the following manner. After cleaning the surface, the sample was placed in front of the LEED screen to insure that a clean surface LEED pattern was obtained. The crystal face then was rotated to in front of the appropriate dosing needle, and a known(usually large) amount of the adsorbate was introduced to the sample face. The sample then was rotated back to in front of the LEED screen and quickly checked for any change in the LEED pattern. If none appeared, which was always the case, the sample was heated slowly and then recooled and its LEED pattern rechecked. None of the systems studied showed any significant change in the LEED pattern--only a general increase in background intensity was observed--indicating that the adsorbates did not order on the surface. Only quick checks were done to avoid electron beam damage to the adsorbates on the surface. For similar reasons, AES were kept to a minimum and never done prior to a thermal desorption unless additional decomposition did not matter. Particularly for semi-conductor surfaces, electron beam induced decomposition of the adsorbates can be quite a problem.<sup>30,31,32</sup>

## Chapter Three

### Methyl-Substituted Benzenes on Ir(111)

#### Results

This section deals with the thermal desorption spectra of benzene, toluene and the xylenes on Ir(111). Using isomers and isotopic labelling, the decomposition mechanism of methyl substituted benzenes on Ir(111) were investigated. The results of these experiments are reported below.

Since the focus of this study was on methyl-substituted benzenes, the logical place to start was with benzene itself. The results of the thermal desorption spectra of benzene are shown in figure 3-1. Here five different initial coverages were tried, and various possible desorption gasses were monitored with a quadrupole mass spectrometer.

Different behavior was observed at different coverages. At low coverages, the only detectable desorption product was H<sub>2</sub>, indicating complete decomposition of the benzene molecule on the Ir(111) surface. The H<sub>2</sub> intensity graphs are characteristic of those found for aromatic hydrocarbons. There is a low temperature region containing relatively sharp, resolved peaks and a higher temperature region characterized by a broad desorption intensity. For benzene, at low coverages, the initial low temperature H<sub>2</sub> maximum occurs at about 135°C, and the high temperature, broad desorption centers around 330°C.

Starting with higher coverages of benzene, interesting modifications to the low coverage results are seen. A distinct shoulder begins to grow in on the low temperature side of the 135°C peak. Furthermore, at near saturation coverage, molecular benzene is seen desorbing from the Ir(111) surface, around 72°C. This is much lower than found by Nieuwenhuys, et. al.,<sup>33</sup> or Mack, et. al.,<sup>34</sup> but this may be due to lower adsorption temperature or different heating rates. Obviously benzene decomposition itself yields a relatively complicated thermal



desorption spectrum. Going on thermal desorption experiments alone, it is impossible to say what types of intermediates are involved in benzene decomposition.

To help elucidate the decomposition mechanism of aromatic hydrocarbons on surfaces, benzene rings with various degrees of methyl substitution were tried, the first one being toluene. The thermal desorption results for four characteristic experiments with toluene, starting with different initial coverages, are shown in figure 3-2. Unlike benzene, toluene (as well as the xylenes) showed no molecular desorption peaks.<sup>35</sup> However, with toluene, at least qualitatively, the thermal desorption spectra appear similar to those of benzene; while monitoring H<sub>2</sub> desorption, a low temperature region characterized by relatively sharp peaks followed by a high temperature, broad desorption is found. At low coverages, the H<sub>2</sub> desorption peak maximum occurs, roughly, around 100°C. At near saturation coverage (2.5 Langmuir exposure), the H<sub>2</sub> thermal desorption graph becomes very complex and intriguing, with three distinct peak maxima occurring in the low temperature region around -18°C, 40°C, and finally 110°C. Also, it should be mentioned here that although not depicted in figure 3-2, there was a very small amount of gas with a mass of 78 amu detected with a peak maximum at 110°C.

Given the complex low temperature region in the thermal decomposition of toluene on Ir(111), it was decided that using isotopically labeled molecules may lend insight into the decomposition mechanism taking place. Hence CD<sub>3</sub>C<sub>6</sub>H<sub>5</sub> and CH<sub>3</sub>C<sub>6</sub>D<sub>5</sub> were tried. The results were complementary with each other. Figure 3-3 depicts the results for one such characteristic (using CH<sub>3</sub>C<sub>6</sub>D<sub>5</sub>) thermal desorption. Here a near saturation coverage was used and masses 2, 3, 4, and 83 amu were monitored. These correspond to H<sub>2</sub>, HD, D<sub>2</sub>, and C<sub>6</sub>D<sub>5</sub>H. H<sub>2</sub> desorption occurs initially, with peak maxima at -17°C and 28°C. There is a small amount of HD desorption occurring in this temperature region as well. Finally, at about 105°C, we find H<sub>2</sub>, HD, and D<sub>2</sub> desorbing simultaneously.

The next step was to investigate the xylenes. The thermal desorption results for perdeutero ortho-xylene are shown in figure 3-4 (deuterated compounds were used, when available, to avoid interference from background  $H_2$ ).  $D_2$  was the only detectable desorption product. Note that now the low temperature region has two closely spaced, sharp peaks at  $32^\circ C$  and  $73^\circ C$ . Again the high temperature region is broad and ill-defined. The results for the thermal desorption experiment starting with a near saturation coverage of specifically labeled *o*- $(CD_3)_2C_6H_4$  are shown in figure 3-5. Here, the only detectable gasses desorbing from the surface were  $H_2$ , HD, and  $D_2$ . There is little  $H_2$  desorption occurring in what may be taken as the first peak region ( $0-20^\circ C$ ), but there is substantial H present as HD.  $D_2$  is desorbing over the entire low temperature range, but most of the D has desorbed either as  $D_2$  or HD by  $100^\circ C$ .

The thermal desorption results for perdeutero meta-xylene are shown in figure 3-6. Here the low temperature region is characterized by two well separated, sharp peaks at  $-32^\circ C$  and  $136^\circ C$ . The thermal desorption experiment for the specifically labeled compound, starting with near saturation coverage, is shown in figure 3-7. Note that the initial peak maximum has moved up to about  $18^\circ C$  from  $-32^\circ C$  for the perdeutero meta-xylene.  $H_2$ , HD, and  $D_2$  desorb at all peak maxima temperatures in the thermal desorption spectrum of *m*- $(CD_3)_2C_6H_4$ .

The thermal desorption spectra of perdeutero para-xylene appear very similar to those of meta-xylene (see figure 3-8). There are two, low temperature desorption peak maxima occurring at  $-24^\circ C$  and  $142^\circ C$ . These peaks are well spaced and sharp. Integrating, one finds that the area under the first peak, if compared to the area under the rest of the spectrum, yields a ratio of 2 : 8. A similar result was found for meta-xylene.

Thermal desorption spectra with *p*- $(CD_3)_2C_6H_4$  are exemplified in figure

3-9. There is no H<sub>2</sub> desorption until the second peak maximum region, and very little HD desorption until this point as well. The intensity of the HD signal in the temperature region of the first peak maximum is small enough to be attributed to background. There is background H on the surface to scavenge D atoms once methyl C-D bonds break, thus HD desorbs. D<sub>2</sub> desorbs primarily in the first temperature region, though there is some in the second as well as a substantial amount of HD.

## Discussion

There is no question that regiospecific bond breakage is occurring in the decomposition of methyl-substituted benzenes on Ir(111) (Regiospecific bond breakage is the sequential decomposition of the molecule by type of bond, in this case aliphatic vs. aromatic). Some portion of the methyl C-H bonds break first, followed by general decomposition of the molecule, involving methyl C-H, aromatic C-H, and C-C bond breakage (for likely intermediates involved in aromatic ring decomposition see Koel, et. al.<sup>19</sup>). Regiospecific bond breakage is most probably happening to all methyl-substituted benzenes studied, but it is most clear for toluene and para-xylene.

Looking at figure 3-3, it is apparent that toluene undergoes regiospecific bond breakage in its decomposition. Consider the high temperature region, where broad, low hydrogen desorption is the norm. The primary gas desorbing from the surface is D<sub>2</sub>, though some HD is also present. At this temperature most of the methyl C-H bonds have broken, leaving primarily aromatic C-D bond-containing species. An interesting fact to point out is the presence of benzene, C<sub>6</sub>D<sub>5</sub>H, desorbing at 1050°C. Admittedly, there is only a very small amount present, but the fact that it appears indicates that there is some C-C bond breaking occurring in the same temperature region as C-H bond breakage. The methyl carbon is breaking away from the aromatic ring. In the toluene case,

therefore, the initial step is in breaking one or more methyl C-H bonds, followed by indiscriminate bond breaking of C-D, C-H and even some C-C bonds. It is difficult to say from the thermal desorption data why there are two H<sub>2</sub> peak maxima prior to aromatic C-D bond breakage. Perhaps toluene is occupying more than one adsorbed state when the coverage is near saturation. Or perhaps there are lateral interactions causing two low temperature, methyl-related peaks at high coverage.

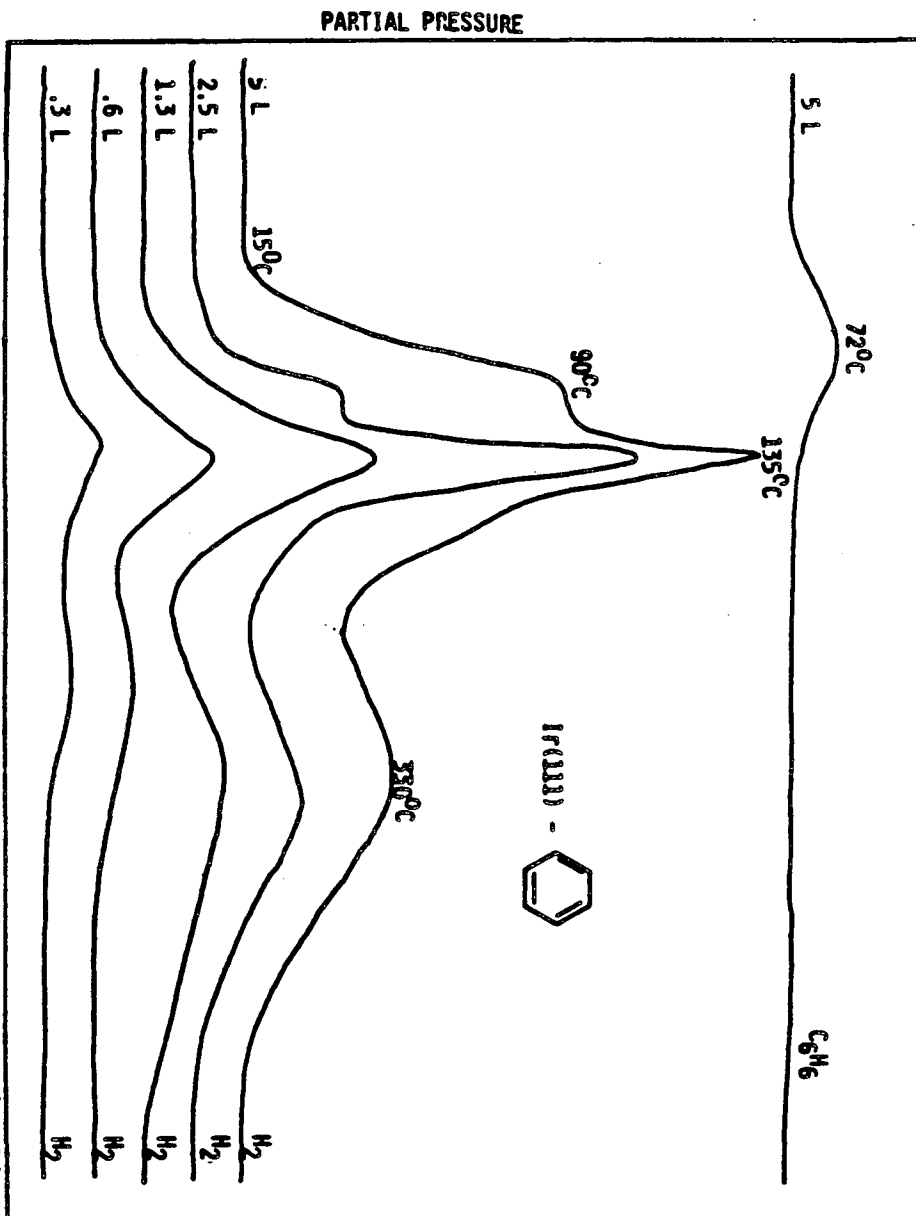
Of all the adsorbates studied, para-xylene most clearly demonstrates regiospecific bond breakage. The first step in its decomposition on Ir(111) is to break two methyl C-D bonds. The ratio of 2 : 8 suggests two C-D bonds break, and the thermal desorption spectrum of the isotopically labeled para-xylene (see figure 3-9) show they are methyl C-D bonds. It is interesting to speculate as to what the resulting intermediate would be. If the two C-D bonds were broken on the same methyl group, one might expect the resulting species to stand up on end. If one C-D bond breaks on each of the two methyl groups, then the resulting intermediate should be flat, with the benzene ring parallel to the Ir(111) surface.

There are other interesting questions to consider. Why is para-xylene the xylene that most clearly exhibits regiospecific bond breakage as its first decomposition step? The first D<sub>2</sub> peak maximum occurs, for the specifically labeled compounds, at 20°C for ortho-xylene and 18°C for meta-xylene, yet at a much lower temperature (-24°C) for para-xylene. Thus there are two C-D bonds of para-xylene that are weakened more, hence break sooner, than with meta or ortho-xylene. Why should this be so? Perhaps it is due to its methyl groups falling over the right spots on the Ir(111) surface--either above a single Ir atom or between two Ir atoms, to just mention two possibilities--which allow for the appropriate reaction to take place on each (assuming one C-D bond breaks on each methyl group). Another possibility is the higher symmetry of para-xylene. It has only two types of deuterium atoms, whereas ortho-xylene has three and meta-xylene (H atoms) four. This higher symmetry reduces the number of different interactions of the adsorbate with the surface, creating a more resolved

thermal desorption spectrum better able to exhibit regiospecific bond breakage.

Of relevance here, perhaps, is the temperatures at which  $H_2$  and  $D_2$  desorb. Off a clean Ir(111) surface, the peak maxima for  $H_2$  desorption occur between  $25^\circ\text{C}$  and  $59^\circ\text{C}$ . The peak maxima for  $D_2$  desorption occur between  $0^\circ\text{C}$  and  $50^\circ\text{C}$ . The presence of peak maxima much lower than these temperatures in the decomposition spectra of meta and para-xylene suggest the occurrence of other species (decomposition intermediates, for example) may be affecting the hydrogen desorption temperature. It is also conceivable that methyl C-H bond scission occurs at very low temperatures, even upon adsorption, and the subsequent  $H_2(D_2)$  desorption proceeds later.

Figure 3-1. Thermal desorption spectra of benzene off of Ir(111), starting with several different coverages. The number found at the beginning of each trace indicates the exposure (in Langmuir-- $10^6$  torr-sec) of adsorbate given the crystal. Only at high exposures (coverages) was any molecular desorption detected. The  $H_2$  traces are characteristic of thermal desorptions involving aromatic ring decomposition on Ir(111). There are two temperature regions, the first having relatively sharp, intense  $H_2$  peaks and the second having a broad, ill-defined  $H_2$  peak.



For other thermal desorption results of benzene  
on Ir(III) see:  
Hleuembuyse, B.R.; Hagen, D.I.; Bowler, G. and  
Somorjai, G.A., Surface Science, 59(1976) 155-176

NRL 841-407

Figure 3-2. Thermal desorption spectra of perproteo toluene off of Ir(111), starting with 4 different coverages. No molecular desorption was detected, indicating toluene completely decomposed on the surface. The spectra have two temperature regions. The low temperature region has sharp, intense peaks and the high temperature region has a single broad, ill-defined peak.



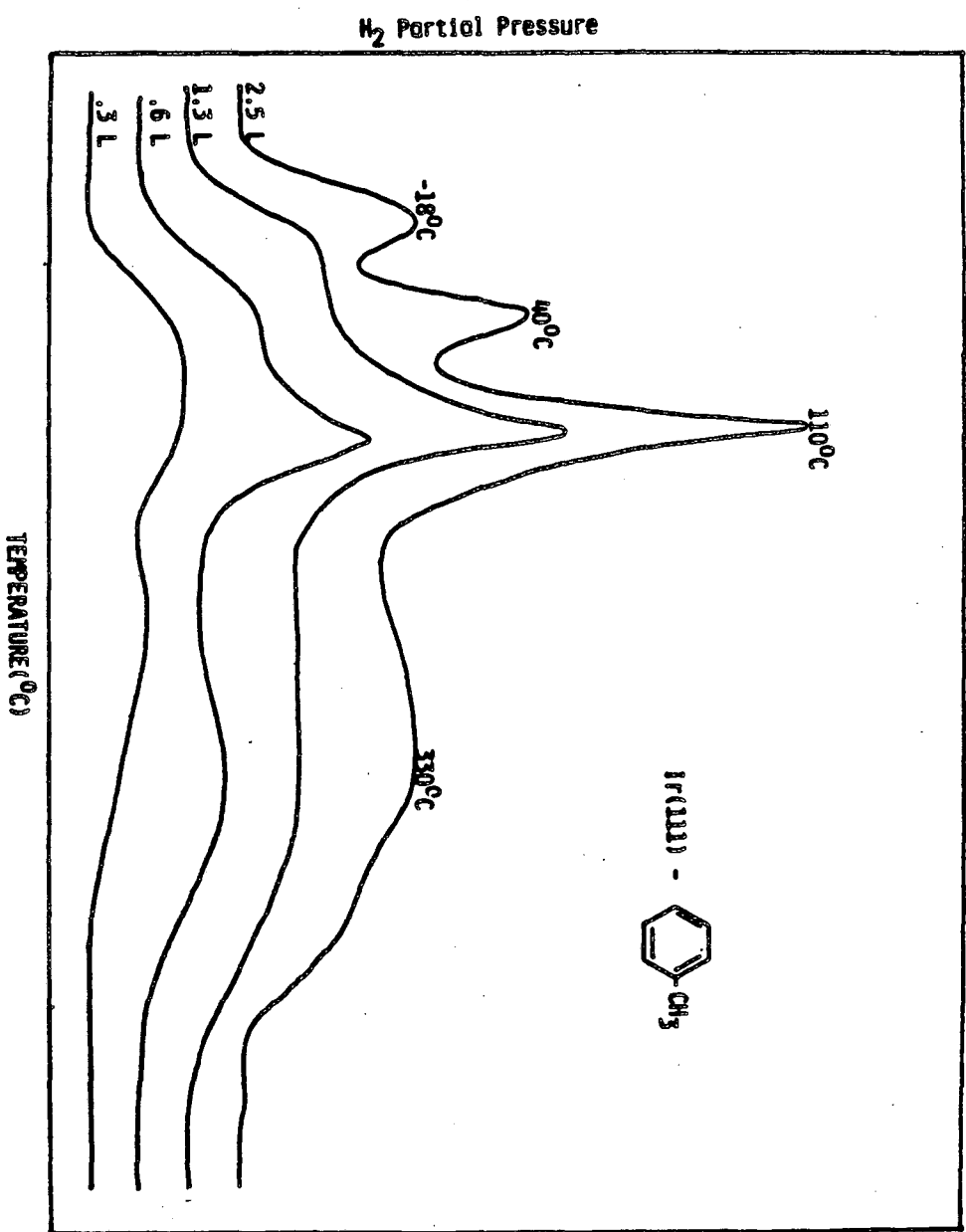


**Figure 3-3.** Thermal desorption spectrum of specifically labeled toluene,  $(\text{CH}_3)\text{C}_6\text{D}_5$ , starting with near saturation coverage. No molecular desorption was detected. All masses depicted were monitored simultaneously. Toluene demonstrates regiospecific bond breakage in its decomposition on Ir(111). Since the first peak in the toluene thermal desorption is  $\text{H}_2$ , the first step in toluene decomposition is breakage of a methyl C-H bond. The subsequent peaks are due to a combination of methyl and aromatic bond breakage ( $\text{H}_2$ , HD, and  $\text{D}_2$  all desorb in these regions). C-C bonds also are being broken at relatively low temperatures since desorption of a small amount of benzene,  $\text{C}_6\text{D}_5\text{H}$  was detected.

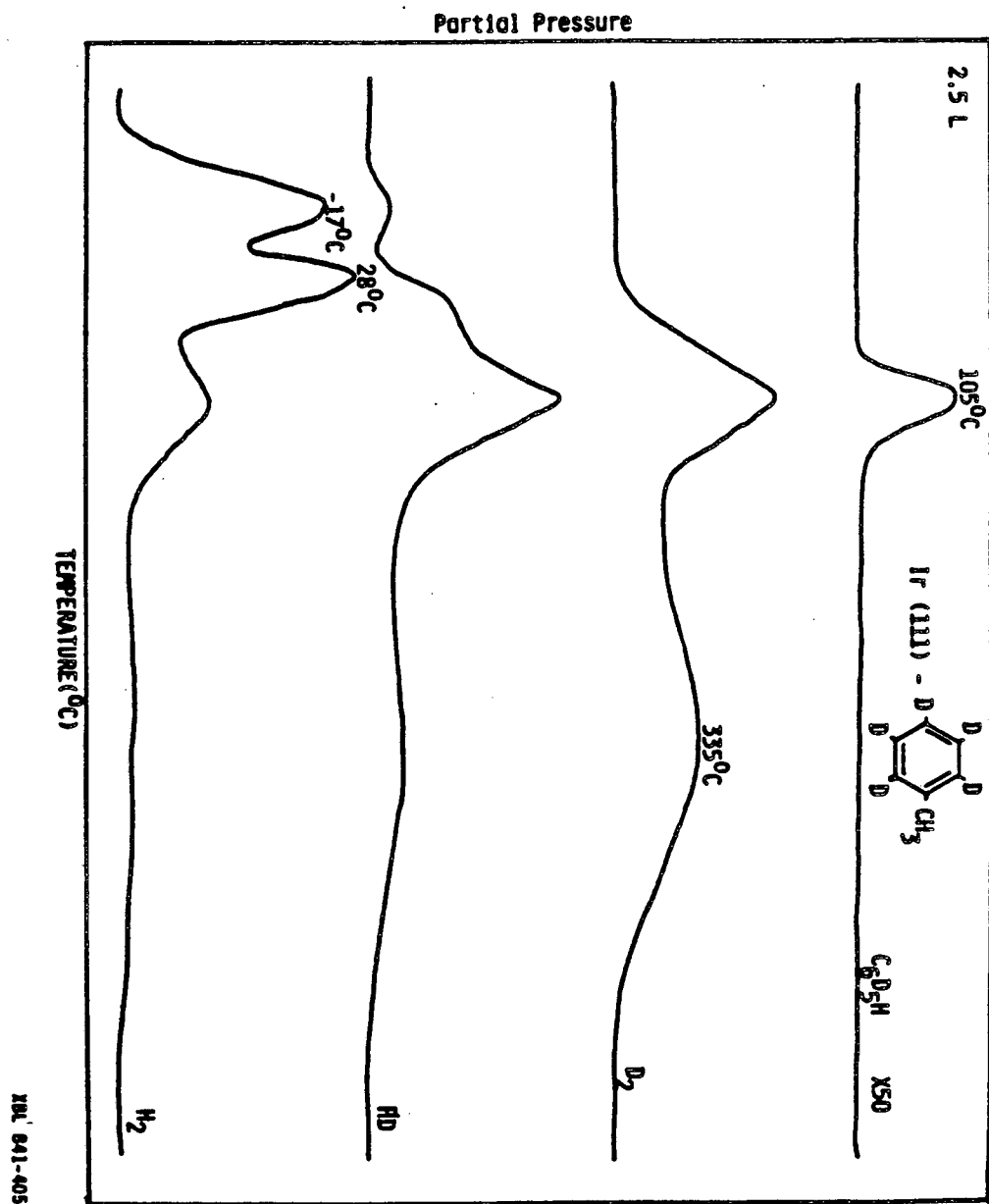


Figure 3-4. Thermal desorption spectra of perdeutero *o*-xylene off of Ir(111), starting with three different coverages. Only D<sub>2</sub> was detected desorbing from the surface, indicating complete decomposition of the molecule.

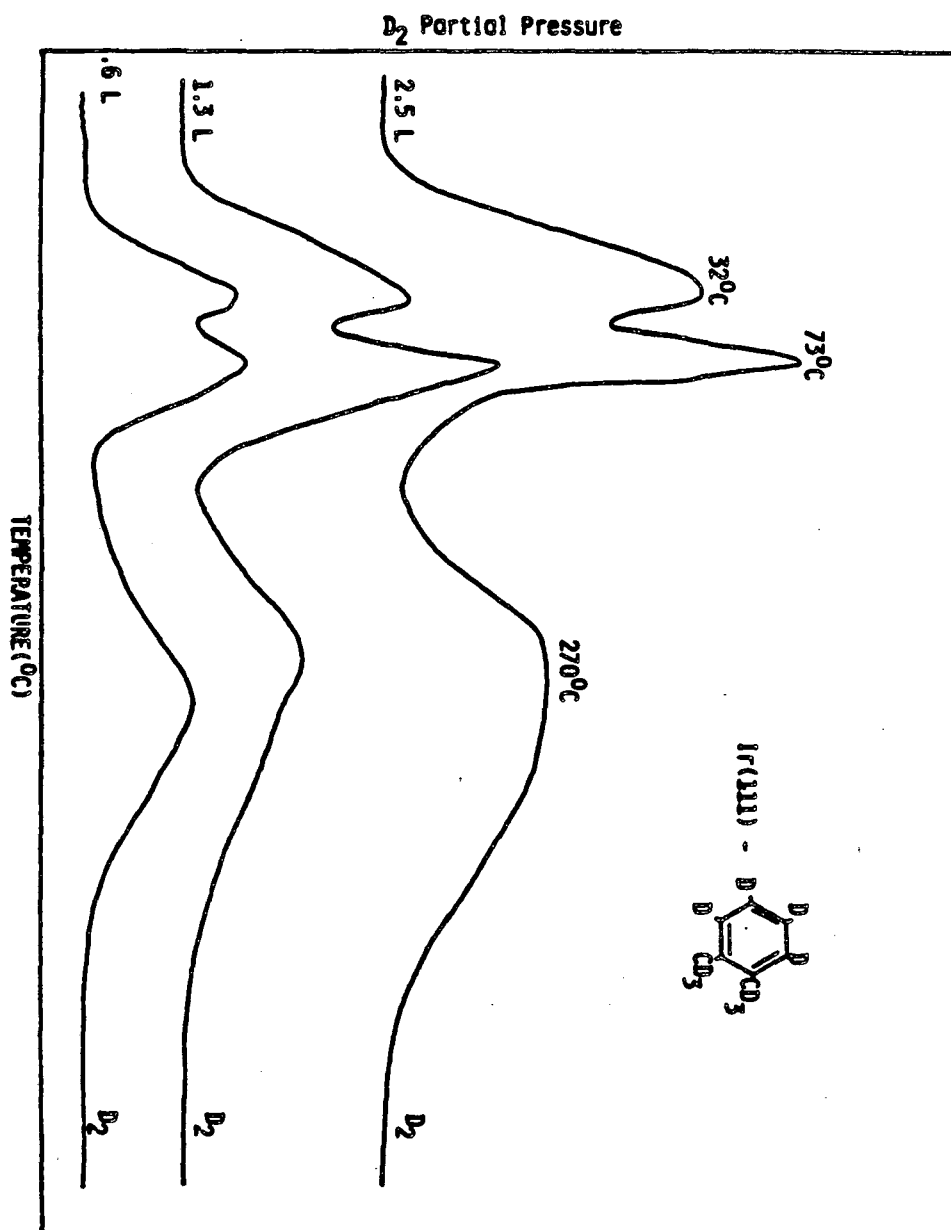


Figure 3-5. Thermal desorption spectrum of specifically labeled *o*-xylene,  $o - (\text{CD}_3)_2\text{C}_6\text{H}_4$ , starting with near saturation coverage. All masses were monitored simultaneously. The first peak is primarily  $\text{D}_2$ , though there is a significant amount of HD present as well. This hints at regiospecific bond breakage occurring (the breakage of methyl C-D bonds only) to create the first peak in the spectrum. Note the temperature of desorption for the first peak is 2 - 20°C.

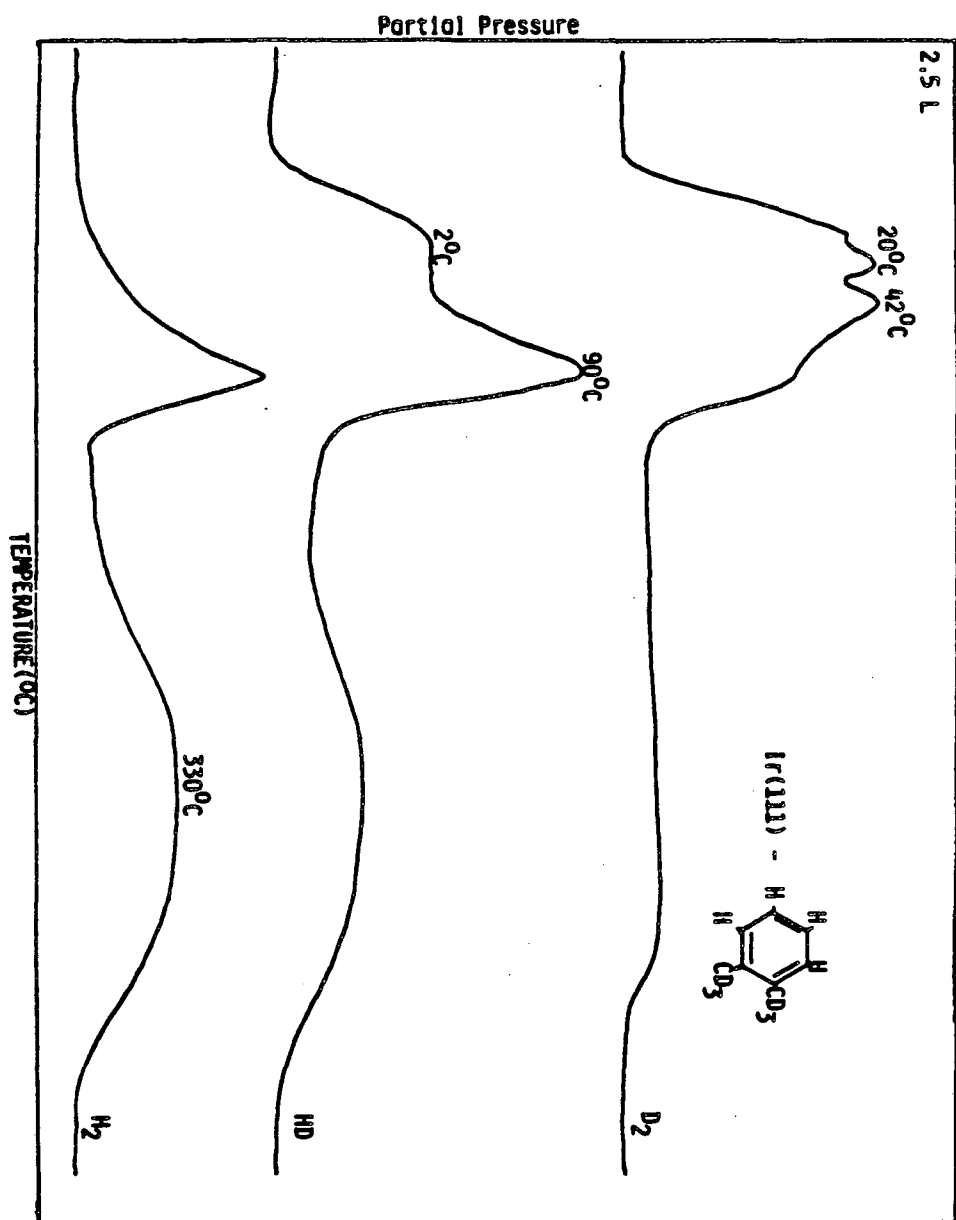


Figure 3-6. Thermal desorption spectra of perproteo *m*-xylene off of Ir(111), starting with four different coverages. Only H<sub>2</sub> was detected desorbing from the surface, indicating complete decomposition of the molecule.



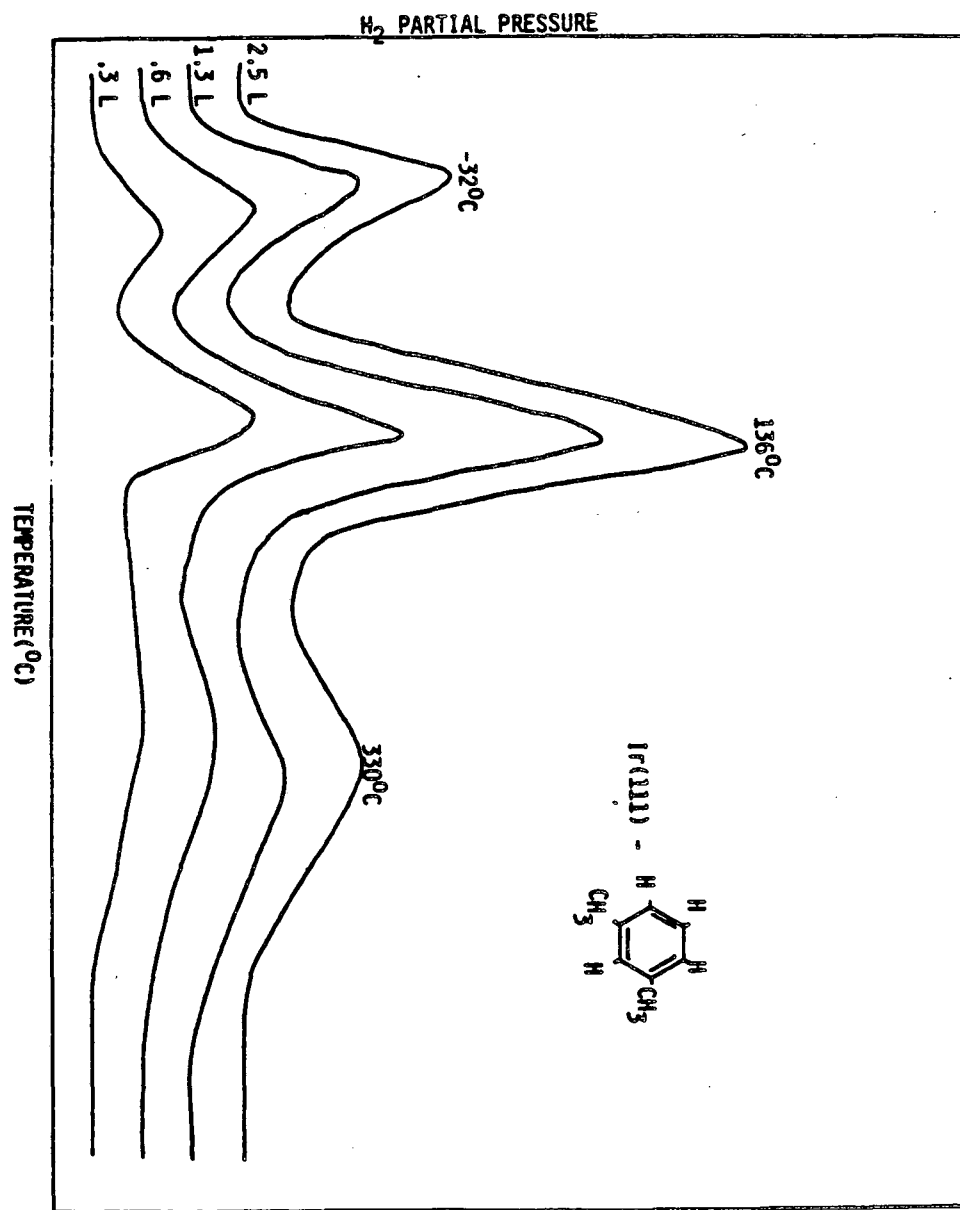


Figure 3-7. Thermal desorption spectrum of specifically labeled *m*-xylene,  $m - (\text{CD}_3)_2\text{C}_6\text{H}_4$ , starting with near saturation coverage. All masses were monitored simultaneously. The first peak is both  $\text{D}_2$  and HD, but very little  $\text{H}_2$ . This hints at regiospecific bond breakage occurring (the breakage of methyl C-D bonds only) to create the first peak in the spectrum. Note the temperature of desorption for the first peak is  $18^\circ\text{C}$ .

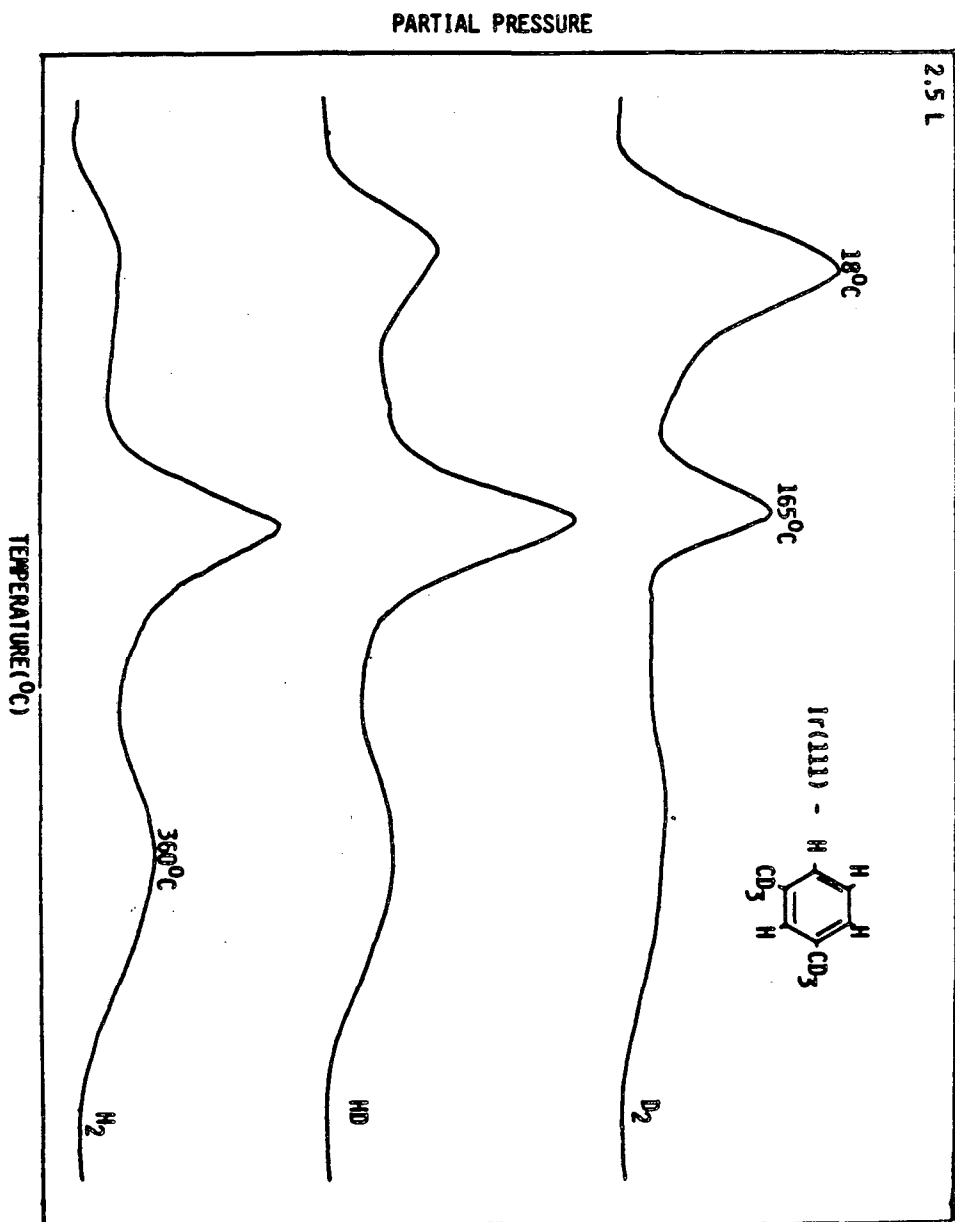


Figure 3-8. Thermal desorption spectra of perdeutero *p*-xylene off of Ir(111), starting with four different coverages. Only D<sub>2</sub> was detected desorbing from the surface, indicating complete decomposition of the molecule. The ratio of the area under the first peak to the area under the rest of the spectrum is 2 : 8, indicating two methyl C-D bonds break to cause the first D<sub>2</sub> peak.

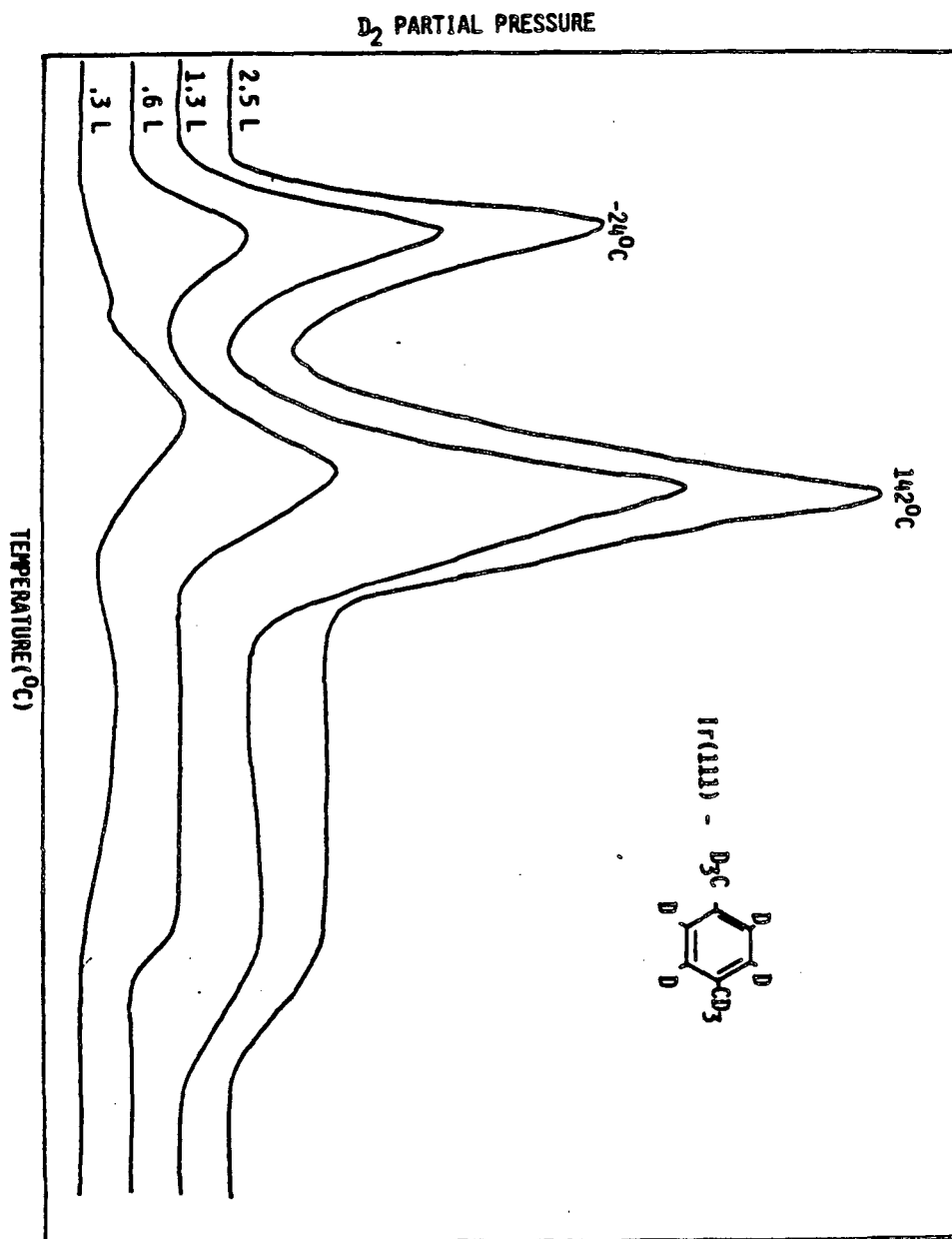
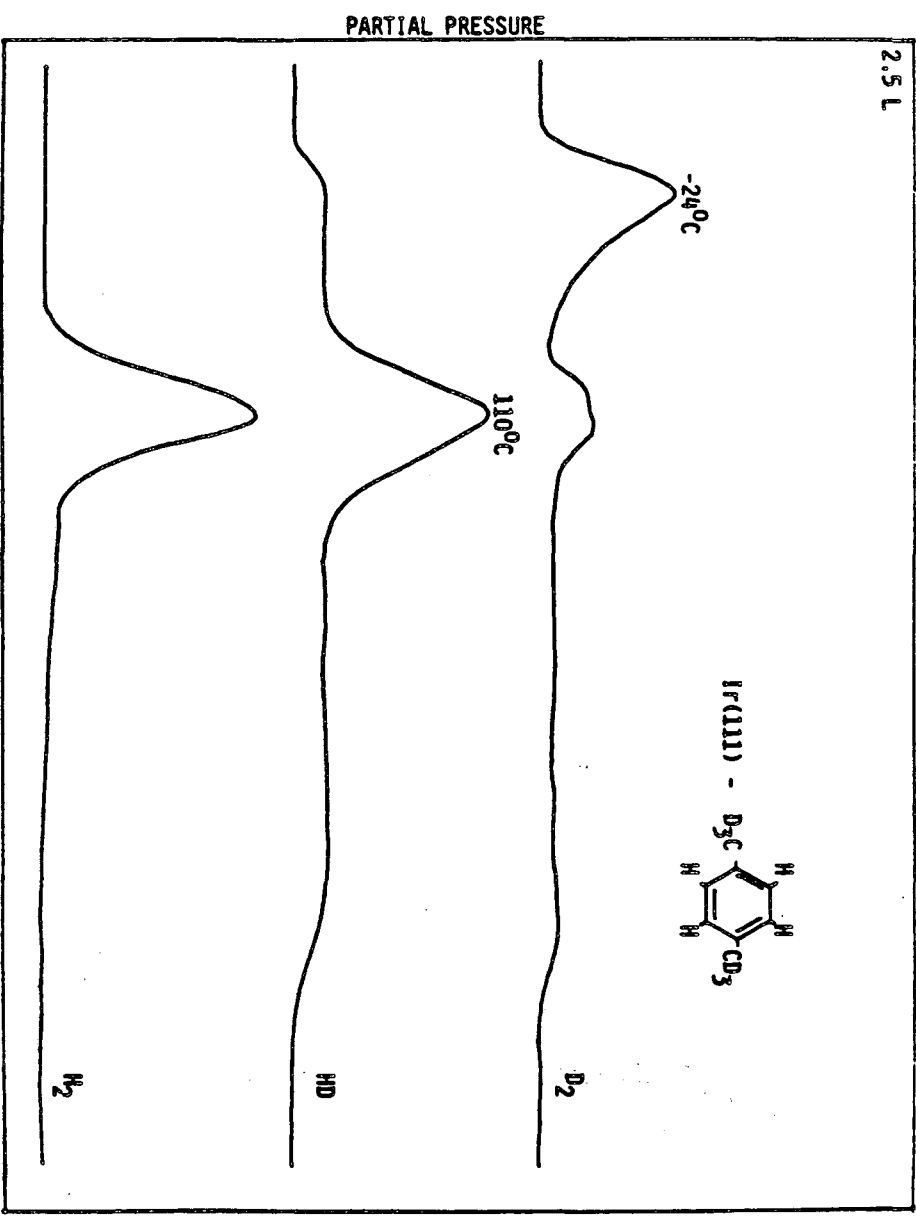


Figure 3-9. Thermal desorption spectrum of specifically labeled *p*-xylene,  $p - (\text{CD}_3)_2\text{C}_6\text{H}_4$ , starting with near saturation coverage. All masses were monitored simultaneously. The first peak consists only of  $\text{D}_2$  (the small HD signal seen could easily be due to background H atoms present on the surface). This clearly shows regiospecific bond breakage occurring (the breakage of methyl C-D bonds only) to create the first peak in the spectrum. Note the temperature of desorption for the first peak is  $-24^\circ\text{C}$ . This is much lower than is the case for *o*- and *m*-xylenes, which helps separate this peak from the subsequent peaks. This allows the clear demonstration of regiospecific bond breakage.



XBL 841-399

## Chapter Four

### Thermal Desorption Studies of the xylenes on Ni(111) and Ni(100) Surfaces

#### Results

The effect of two different surface orientations in adsorbate-metal interactions is the focus of this chapter. The two surfaces were Ni(111) and Ni(100), and their interaction with methyl-substituted benzenes was studied using thermal desorption spectroscopy. The results of these thermal desorption experiments are shown in figures (4-1 - 4-8).

The thermal desorption of perdeutero ortho-xylene off of Ni(111) is shown in figure 4-1. The only reaction product detected from the surface was hydrogen gas, in this case  $D_2$  (This was true of all methyl-substituted benzenes on all metal surfaces studied--hydrogen was the only reaction product detected, indicating complete decomposition of the adsorbate molecule.). Two desorption peaks are present in the thermal desorption spectrum of ortho-xylene on Ni(111), one at  $105^\circ\text{C}$  of relatively sharp intensity, and one around  $222^\circ\text{C}$ , which has a weaker and broader desorption shape. This desorption pattern is very common for methyl-substituted benzenes decomposing on metal surfaces.

If the aromatic hydrogen positions are occupied by hydrogen atoms, leaving the aliphatic positions with deuterium atoms, and this specifically labeled ortho-xylene is adsorbed on the surface, the thermal desorption shown in figure 4-1(b) is obtained. From this experiment it is apparent that the first peak in the thermal desorption spectrum of specifically labeled ortho-xylene is made up primarily of deuterium atoms, both as  $D_2$  and HD. However, there is also significant desorption of hydrogen atoms, whose source is the aromatic positions on the ring. This shows up primarily as HD, though some  $H_2$  also is desorbing at this low temperature. On the other hand, the high temperature peak is primarily



composed of H<sub>2</sub>, although some HD is desorbing in this temperature region as well.

A similar situation exists for meta-xylene on Ni(111) shown in figure 4-2. Here there are three peaks, at least at high coverage. Their locations are 110°C, 180°C, and 330°C. The 110°C peak is relatively sharp and has high intensity. The 180°C peak is primarily a shoulder on the lower peak. The 330°C peak is low and broad--characteristic of aromatic decomposition on metal surfaces. The thermal desorption of the specifically deuterated compound, *m*-(CD<sub>3</sub>)<sub>2</sub>C<sub>6</sub>H<sub>4</sub>, is shown in figure 4-2(b). Deuterium is the primary component of the first peak, present both as D<sub>2</sub> and HD. The second peak has both HD and H<sub>2</sub>, while the third is almost exclusively H<sub>2</sub>.

The case of para-xylene on Ni(111) is shown in figure 4-3. Figure 4-3(a) shows the results of the thermal desorptions of perdeutero para-xylene, starting with varying amounts of initial surface coverage. There are, once again, two temperature regions present in the spectrum. The first occurs with a peak maximum at 114°C, and the peak is relatively sharp. The second temperature region has a peak which is lower and broader than the low temperature one and it is centered around 223°C. The specifically labeled *p*-(CD<sub>3</sub>)<sub>2</sub>C<sub>6</sub>H<sub>4</sub> on Ni(111) thermal desorption is shown in figure 4-3(b). Here again it is primarily deuterium atoms in the first peak and hydrogen atoms in the second. In fact, the results from para-xylene are very nearly the same as ortho-xylene.

The thermal desorption of perproteo mesitylene was obtained as well, though no corresponding specifically labeled compound was available for comparison. The results of this spectrum are very similar to those already presented. There is a relatively sharp peak at 105°C followed by a long, broad area of H<sub>2</sub> desorption(see figure 4-4). Figure 4-5 depicts the thermal desorption of mesitylene on Ni(100). There is again the same general shape to the thermal desorption spectrum. Only H<sub>2</sub> is detected desorbing from the surface, and there

are two general regions of desorption. The first occurs at 60°C, and is a sharp, intense peak. This is followed by a second peak that maximizes at about 175°C, and then has a very long tail out to about 400°C.

The other substituted benzenes showed similar results on the Ni(100) surface as were found on the Ni(111) surface but the details were different. Figure 4-6 shows the thermal desorption spectra of ortho-xylene off of Ni(100). The two temperature regions are present, but they occur at different temperatures than on the Ni(111) surface. The first temperature region occurs around 75°C, and is sharp and intense. The second temperature region occurs around 180-250°C or so, and is once again broad and of low intensity.

The thermal desorption of the specifically labeled ortho-xylene, *o* - (CD<sub>3</sub>)<sub>2</sub>C<sub>6</sub>H<sub>4</sub>, is shown in figure 4-6(b). Deuterium atoms, from the methyl group of the xylene, are almost exclusively in the first temperature peak. Correspondingly, hydrogen atoms are almost all in the higher temperature region, though a large amount are found as HD, desorbing around 60°C, in the low temperature area.

Analogous experiments were done with meta-xylene for the Ni(100) surface, and these results are presented in figure 4-7. The low temperature peak occurs at 65°C, and is sharp and intense. The high temperature region occurs around 225°C. There is another peak in the case of meta-xylene which comes in around 150°C, in between the obvious high and low temperature cases. It is fairly sharp and intense, but not nearly so much so as the 65°C peak. The thermal desorption spectrum of specifically deuterated meta-xylene, shown in figure 4-7(b), indicates that this 150°C peak may be due to breakage of the methyl C-D bonds, as is the case with the 65°C peak. Deuterium is found, as D<sub>2</sub> and HD, in both peaks. The high temperature region, on the other hand, is almost exclusively H<sub>2</sub>, though a small amount of HD is present here as well.

The thermal desorption spectra of para-xylene on Ni(100) are depicted in figure 4-8. Figure 4-8(a) shows the perdeutero case. Here the two temperature regions are resolved very well --there is minimal overlap between them. The first

peak occurs at 75°C and is very sharp and intense. The second peak occurs around 290°C, and although sharp compared to the other xylenes and surface, is much less so than the low temperature peak. If one takes the area under the first peak, and compares it to the area under the rest of the spectrum, the ratio is greater than 6 : 4. The specifically labeled compound shows corresponding peaks in its spectrum(see figure 4-8(b)), with the low temperature peak consisting almost exclusively of D<sub>2</sub>. The small amount of HD present could be due to the scavenging of background H atoms by the deuterium atoms from the molecule's methyl groups. The high temperature region consists almost primarily of H<sub>2</sub>, with essentially no HD present.

Low energy electron diffraction experiments were attempted with each of the adsorbates involved on both Ni(100) and Ni(111). The only compound that gave any pattern was mesitylene on the Ni(111) surface, which gave a very weak (7)<sup>1/2</sup> by (7)<sup>1/2</sup>.

## Discussion

It is a fairly safe position to take that there exists regiospecific bond breakage in the decomposition of the xylenes and mesitylene on both Ni(111) and Ni(100) surfaces. The aliphatic hydrogen-carbon bonds, or at least some of them, break prior to the aromatic hydrogen-carbon bonds. This is consistent with findings of Friend and Muetterties concerning toluene on these surfaces.<sup>4</sup> However, the existence of regiospecific bond breakage becomes less apparent when the temperature regions where aliphatic C-H bonds and aromatic C-H bonds break overlap to any degree. It is true that there still exists sequential C-H bond breakage in general, but there is a temperature region where both types of bonds are being broken. In this region we find H atoms and D atoms, in the form of HD, desorbing from the surface in both high and low temperature regions. This is often the case on the Ni(111) surface.

For example, consider the thermal desorption experiments of ortho-xylene

on Ni(111)(see fig. 4-1). Here it can be seen that the deuterium atoms from the methyl, or aliphatic C-D bonds are desorbing from the surface prior to the hydrogen atoms from the aromatic ring. The most likely cause of this phenomena is that the C-H bonds of the methyl groups break prior to the C-H bonds on the aromatic ring. Thus sequential, step-wise decomposition is occurring. That there is HD present in both temperature regions does cause some ambiguity in this interpretation, but its presence is due mainly to the fact that the two temperature regions are relatively close together, and significant overlapping of their respective peaks occurs.(see figure 4-1(a))

A similar thing occurs for meta-xylene(see figure 4-2) and para-xylene(see figure 4-3) on Ni(111). The methyl C-D bonds break prior to the aromatic C-H bonds. The evidence for this is less clear cut for meta-xylene than for either ortho or para-xylene, for there are three peaks and they are very close together, giving rise to a larger amount of overlap between the temperature regions. It is not too surprising therefore to find a large amount of HD desorbing from the Ni(111) surface in the case of *m*-(CD<sub>3</sub>)<sub>2</sub>C<sub>6</sub>H<sub>4</sub>(see figure 4-2(b)). In general the thermal desorption spectra of the xylenes on Ni(111) hint at regiospecific bond breakage, but the two temperature regions are too close to demonstrate it clearly.

It is on the Ni(100) surface, where the two temperature regions are far enough apart, that this regiospecific bond breakage becomes most apparent. Note the results for *p*-xylene, shown in figure 4-8. In the perdeutero thermal desorption, the two peaks are widely separated and are each relatively sharp. Then looking to the specifically labeled compound, we find in the low temperature region that it is almost exclusively D<sub>2</sub> desorbing, whereas in the high temperature region it is almost exclusively H<sub>2</sub>. There is very little HD in this case. Given that the ratio of the first peak to the rest of the spectrum is greater than 6 : 4, the intermediate involved after the first peak must be devoid of methyl deuterium atoms. The thermal desorption spectra for *o*- and *m*-xylenes(see figures 4-6 and 4-7) do not demonstrate regiospecific bond breakage as well as *p*-xylene but, in general, show it better than the xylenes on Ni(111).

Another characteristic that is present in the thermal desorption spectra of the specifically deuterated xylenes off of Ni is that a small amount of HD is sometimes found desorbing at high temperatures, corresponding to aromatic bond breakage. It may be that this is just an indication of the amount of deuterium atoms that are occupying aromatic sites, or it may be due to H-D mixing occurring before the hydrogen desorbs. However, it may be due also to non-regiospecific behavior, i.e., methyl C-D bonds being broken in the high temperature region.

A fair question to ask at this point is whether the temperature at which  $H_2$ ,  $D_2$ , and HD desorb is really indicative of when their corresponding C-H bonds are being broken. In other words, are the desorptions limited by bonds breaking, or do these hydrogen gasses have some residence time of their own on the surface prior to desorption (the multiple peaks in the thermal desorption spectra are due then to the occupation of different binding sites on the surface). Thermal desorption experiments of  $H_2$  off of nickel surfaces<sup>36</sup> show that  $H_2$  desorbs over a very broad temperature range, depending on the coverage.  $H_2$  is desorbed, essentially completely, by  $150^\circ\text{C}$  in the case of Ni(111) and  $175^\circ\text{C}$  in the case of Ni(100). Thus the high temperature peak displayed in the thermal desorption spectra of the xylenes cannot be coming from hydrogen atoms which have remained on the surface long after their respective C-H bonds have broken. They would have desorbed prior to  $175^\circ\text{C}$  in that case. The high temperature peak must be due to the breakage of C-H bonds at those high temperatures, followed immediately by  $H_2$  desorption.

The low temperature peak is another matter, since it falls in a desorption area found with pure  $H_2$  off of Ni. This peak could be due to either recent methyl C-H bond cleavage, followed by  $D_2$  desorption, or it conceivably could be due to deuterium atoms which were liberated at a lower temperature--possibly even upon adsorption. The sharpness of the peaks presented here argues against this

latter possibility ( $H_2$  desorptions are broad), but it cannot be ruled out.

The multiple peaks observed for the hydrogen thermal desorption spectra of the xylenes on Ni naturally leads to a stepwise decomposition interpretation. The first step has been identified: the cleavage of the methyl C-D bonds mentioned earlier. The subsequent steps are more difficult to identify, and probably impossible using thermal desorption spectroscopy, but they are obviously further degradation of the aromatic ring, involving both C-H and C-C bond breakage. Electron energy loss spectroscopy studies, by Koel et. al., of benzene decomposition on Rh(111) have been done<sup>19</sup> and similar intermediate species (CH and  $C_2H$ ) found there could be expected here.

The thermal desorption spectra of methyl-substituted benzenes are, naturally, very similar. Para-xylene portrays the cleanest regiospecific bond breakage, and this may be due to the fact it is the most symmetric of the three--all of the aromatic hydrogen atoms are equivalent. Meta-xylene has three types of aromatic hydrogen, and this may account for the extra peak in the Ni(111) thermal desorption. The extra  $D_2$  peak in the thermal desorption of specifically deuterated meta-xylene indicates that not all methyl hydrogens are interacting in an equivalent manner on the Ni(100) surface.

A final question to consider is what is the reason these two surfaces differ in the degree to which they demonstrate regiospecific bond breakage? A useful and interesting way to approach this question is to compare the temperatures at which each surface is able to break methyl and aromatic C-H bonds (assuming they do not break at low temperatures or upon adsorption). This comparison is presented in Table 4-1. Note that in all cases the Ni(100) surface is able to extract the methyl H (or D) atoms at a lower temperature than the Ni(111) surface. This might be expected because of the more open surface of Ni(100). More open surfaces often allow stronger interactions with adsorbates, because a higher number of surface atoms can bond to the adsorbate molecule.

The aromatic C-H bonds, on the other hand, are more easily dissociated on the Ni(111) surface. The temperatures at which the aromatic hydrogen atoms

appear is always lower for Ni(111) than Ni(100). The most likely reason for this phenomena is the similar symmetry of both the six-member aromatic ring and the Ni(111) surface(see figure 4-9). They are both hexagonal. This probably allows for more interaction of the aromatic ring, or at least the hydrogen atoms located on the ring, with the Ni(111) surface than with the four-fold symmetry of the Ni(100) surface. This would be especially true if the six member ring assumed the same adsorption site on both surfaces. Jovic, et. al., argue that benzene assumes an adsorption site centered over one or two nickel atoms on both the Ni(111) and Ni(100) surfaces because of the similarity of their EELS(electron energy loss spectroscopy) spectra.<sup>37</sup> Investigating benzene adsorption on Ni(100) and Ni(111) using a variety of techniques, Bertolini et. al.<sup>38</sup> determined that benzene assumed a more "rigid" structure on Ni(111) than on Ni(100) indicating that it was interacting more with the Ni(111) surface. Friend and Muetterties investigated the thermal desorption of  $C_6D_6$  on these two surfaces and found that (1) molecular desorption off of Ni(100) was two times that off of Ni(111) (less decomposition on Ni(100)) and (2) the  $D_2$  peak due to decomposition was  $20^{\circ}$  to  $40^{\circ}C$  higher on Ni(100)( $200-220^{\circ}C$  versus  $180^{\circ}C$ ) than Ni(111).<sup>4</sup> All of these facts and data point to a higher interaction of the aromatic hydrogen atoms with the Ni(111) surface compared to the Ni(100) surface, most probably due to its similar symmetry. This then accounts for the results described and shown in Table 4-1.

It should be emphasized that this correlation between the aromatic ring symmetry and surface symmetry apparently is limited to the hydrogen atom removal only. Molecular benzene desorbs from Ni(100) at a higher temperature than Ni(111),<sup>4</sup> indicating that the molecule as a whole chemisorbs more strongly to Ni(100). This may be because the atomic orbitals on an individual Ni atom stick out at a greater angle on the (100) surface than on the (111) surface.<sup>10</sup> It is these orbitals that interact with the  $\pi$ -system of the aromatic ring, creating the chemisorption bond responsible for molecular adsorption. The hydrogen atoms of benzene are not significantly involved with the  $\pi$ -system of the molecule, so the

surface symmetry of the atoms themselves may play a more important role for hydrogen removal.

In summary, Ni(100)'s more open surface facilitates abstraction of the methyl hydrogens, and Ni(111)'s hexagonal symmetry facilitates dissociation of aromatic C-H bonds. The effect is most probably a kinetic one, and not thermodynamic. The Ni(100) surface lowers the activation energy for breaking the methyl C-H bonds, and the Ni(111) surface does the same for the aromatic C-H bonds. Surface orientation does, in general, affect kinetics significantly more than energetics.<sup>39,40</sup>

### **Ni and Ir TDS Comparisons**

Results from the thermal desorption spectra of the xylenes off of Ni(100), Ni(111), and Ir(111) are presented in figures 3-4 - 3-9, 4-1 - 4-3 and 4-6 - 4-8. Note that the basic character of the first peaks desorbing from the different surfaces are different. For one thing, in the thermal desorption spectra of Ir, the first temperature region usually consists of not just one but two different peaks. The first temperature region in the case of Ir extends beyond the second peak, even though they are at relatively high temperature compared to the first peak, because the second peaks are still very sharp and contain some deuterium atoms from the methyl groups of the xylene.

Comparing a specific adsorbate, para-xylene off of Ir(111) and Ni(100), it is clear that two different decomposition mechanisms are involved. For the Ni(100) case, the area under the first peak, compared to the rest of the spectrum, gives a ratio greater than 6 : 4. All of the methyl deuterium atoms are removed in the first step of the decomposition. This is supported by the specifically labeled thermal desorption experiment, where deuterium is seen only in the first peak and hydrogen only in the second. In the Ir(111) case, the integration ratio is 2 : 8, indicating that only two of the methyl deuterium atoms are removed in the first step of the decomposition. When looking at the specifically labeled thermal



desorption result, then, there is only deuterium in the first peak, but the second peak has both deuterium and hydrogen atoms appearing. At this temperature region both the rest of the methyl C-D bonds as well as the aromatic C-H bonds are breaking. Evidently the hexagonal Ir(111) surface facilitates the removal of aromatic hydrogen atoms so much that they compete with the removal of the remaining methyl deuterium atoms. Obviously there are two different intermediates involved on the two different surfaces, Ni(100) and Ir(111), hence there are different mechanisms to their respective decompositions. It is difficult to say what is the cause of two different decomposition mechanisms, but various differences between the two metals could possibly account for this phenomenon. Fermi level, the larger interatomic distances in Ir, and, at least when comparing Ni(100) and Ir(111), geometrical differences could all be factors influencing the different decomposition mechanisms of xylenes on these surfaces.

Figure 4-1. The thermal desorption spectra of (a) perdeutero *o*-xylene,  $(\text{CD}_3)_2\text{C}_6\text{D}_4$ , and (b) specifically labeled *o*-xylene,  $(\text{CD}_3)_2\text{C}_6\text{H}_4$ , off of Ni(111). In (a) each separate trace represents different thermal desorptions done with different initial exposures of the adsorbate to the surface. In (b) only one thermal desorption experiment is represented, and masses 2,3, and 4 ( $\text{H}_2$ , HD, and  $\text{D}_2$ ) were monitored simultaneously. Hydrogen was the only detected desorption product, indicating complete decomposition of the molecule. The spectra hint at the occurrence of regiospecific bond breakage, with methyl C-D bonds breaking prior to aromatic C-D(or C-H) bonds.

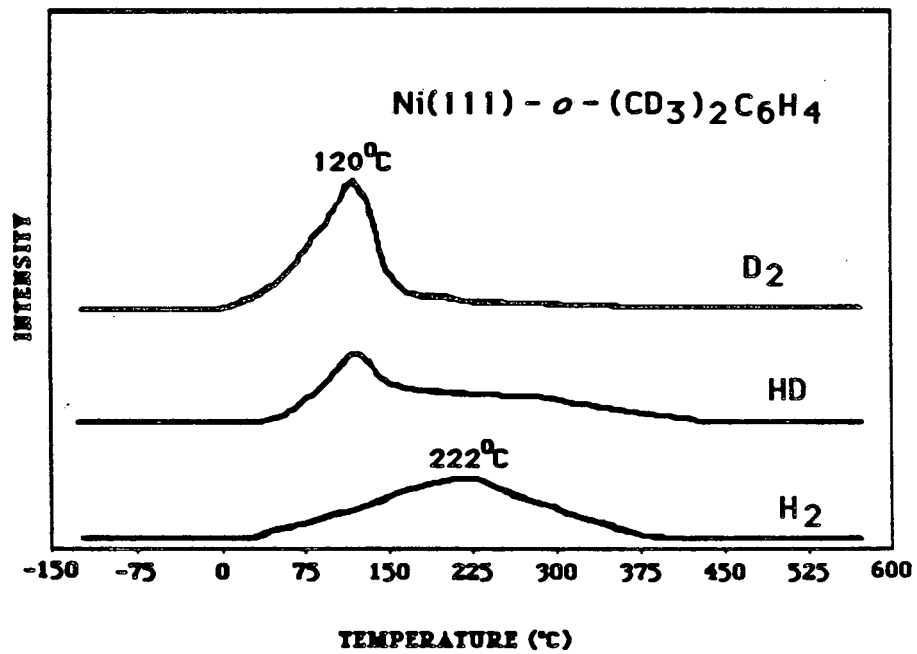
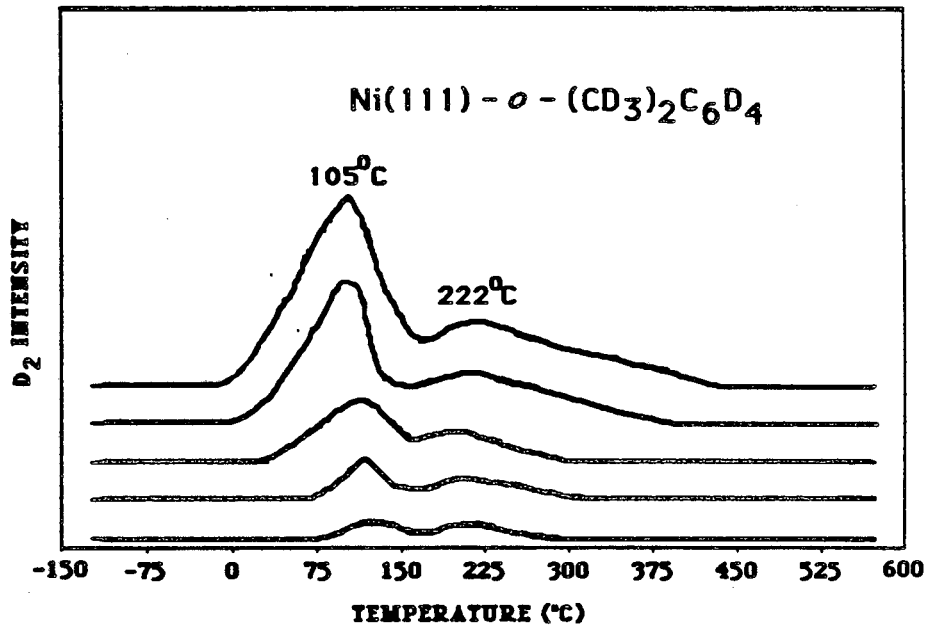


Figure 4-2. The thermal desorption spectra of (a) perproteo *m*-xylene,  $(\text{CH}_3)_2\text{C}_6\text{H}_4$ , and (b) specifically labeled *m*-xylene,  $(\text{CD}_3)_2\text{C}_6\text{H}_4$ , off of Ni(111). In (a) each separate trace represents different thermal desorptions done with different initial exposures of the adsorbate to the surface. In (b) only one thermal desorption experiment is represented, and masses 2,3, and 4 ( $\text{H}_2$ , HD, and  $\text{D}_2$ ) were monitored simultaneously. Hydrogen was the only detected desorption product, indicating complete decomposition of the molecule. The spectra hint at the occurrence of regiospecific bond breakage, with methyl C-D bonds breaking prior to aromatic C-D (or C-H) bonds.

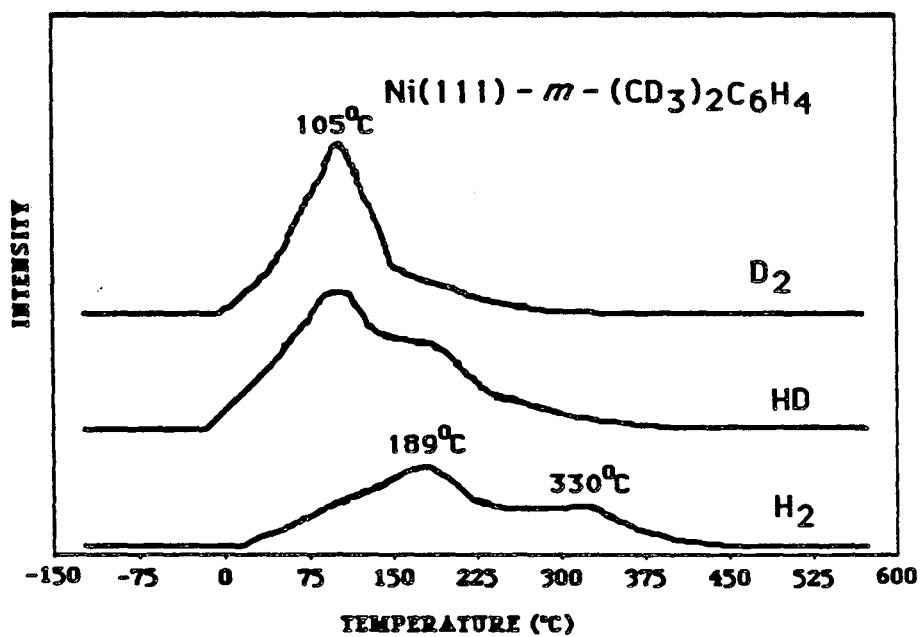
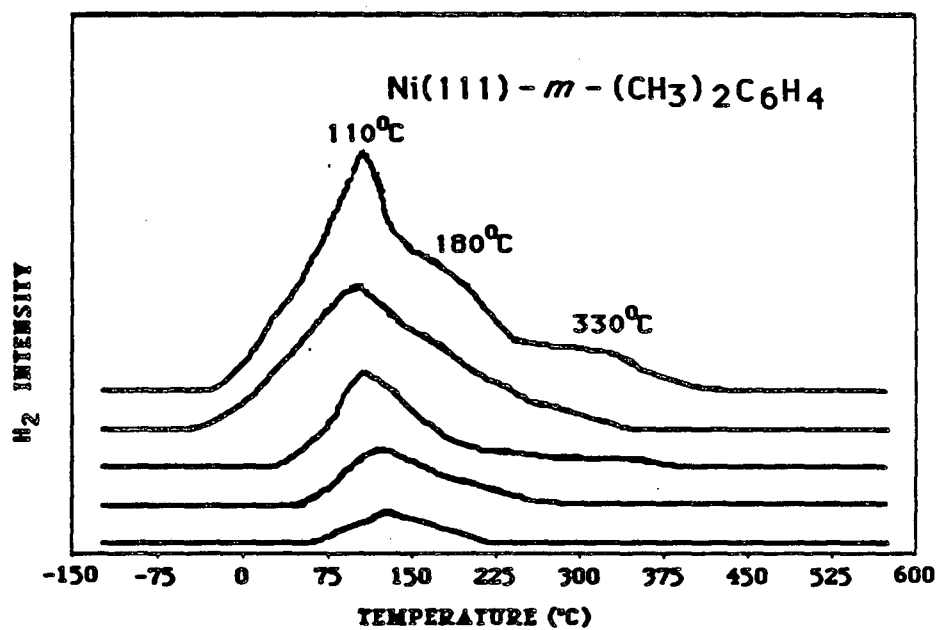
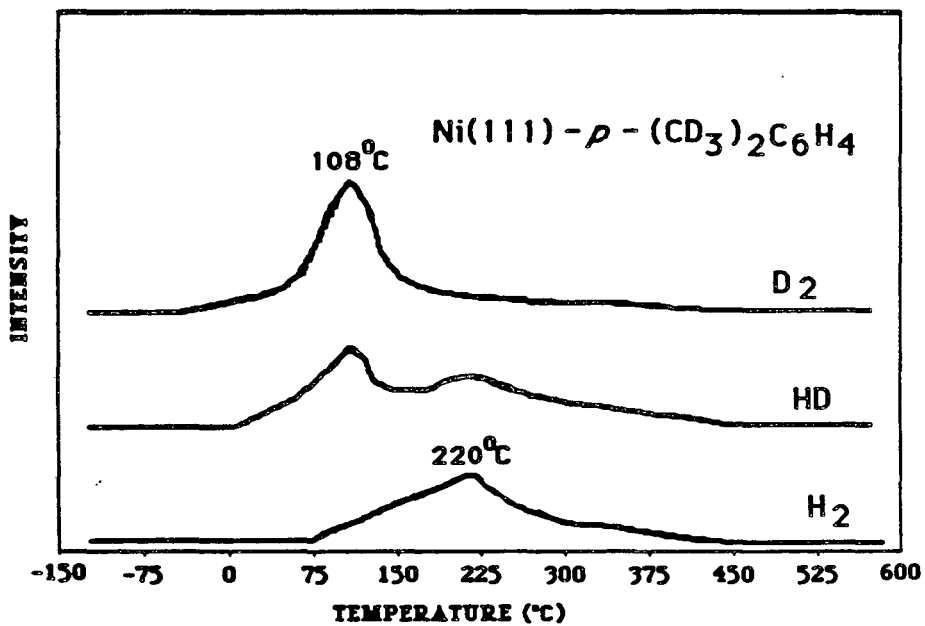
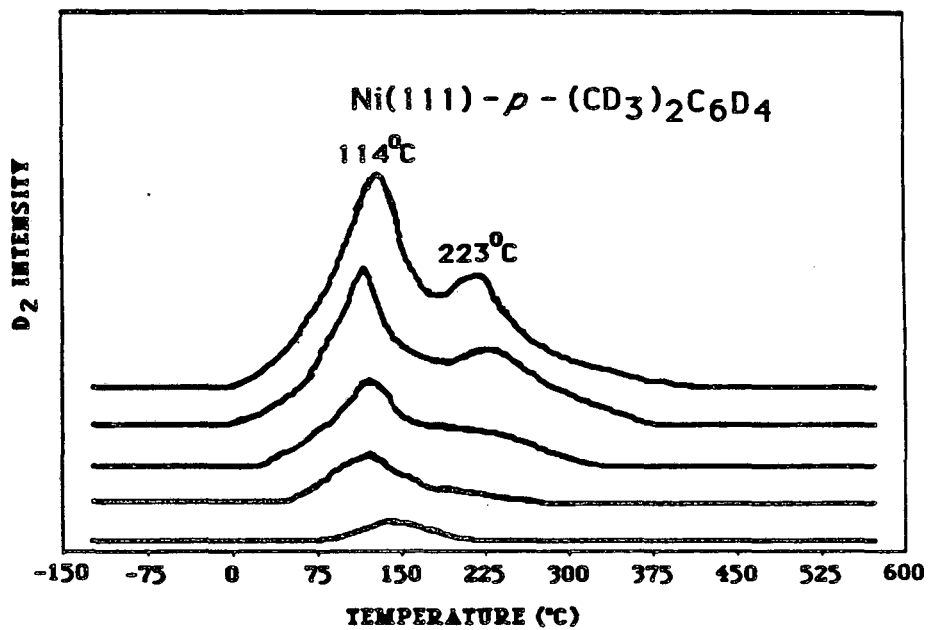


Figure 4-3. The thermal desorption spectra of (a) perdeutero *p*-xylene,  $(\text{CD}_3)_2\text{C}_6\text{D}_4$ , and (b) specifically labeled *p*-xylene,  $(\text{CD}_3)_2\text{C}_6\text{H}_4$ , off of Ni(111). In (a) each separate trace represents different thermal desorptions done with different initial exposures of the adsorbate to the surface. In (b) only one thermal desorption experiment is represented, and masses 2,3, and 4( $\text{H}_2$ , HD, and  $\text{D}_2$ ) were monitored simultaneously. Hydrogen was the only detected desorption product, indicating complete decomposition of the molecule. The spectra hint at the occurrence of regiospecific bond breakage, with methyl C-D bonds breaking prior to aromatic C-D(or C-H) bonds.



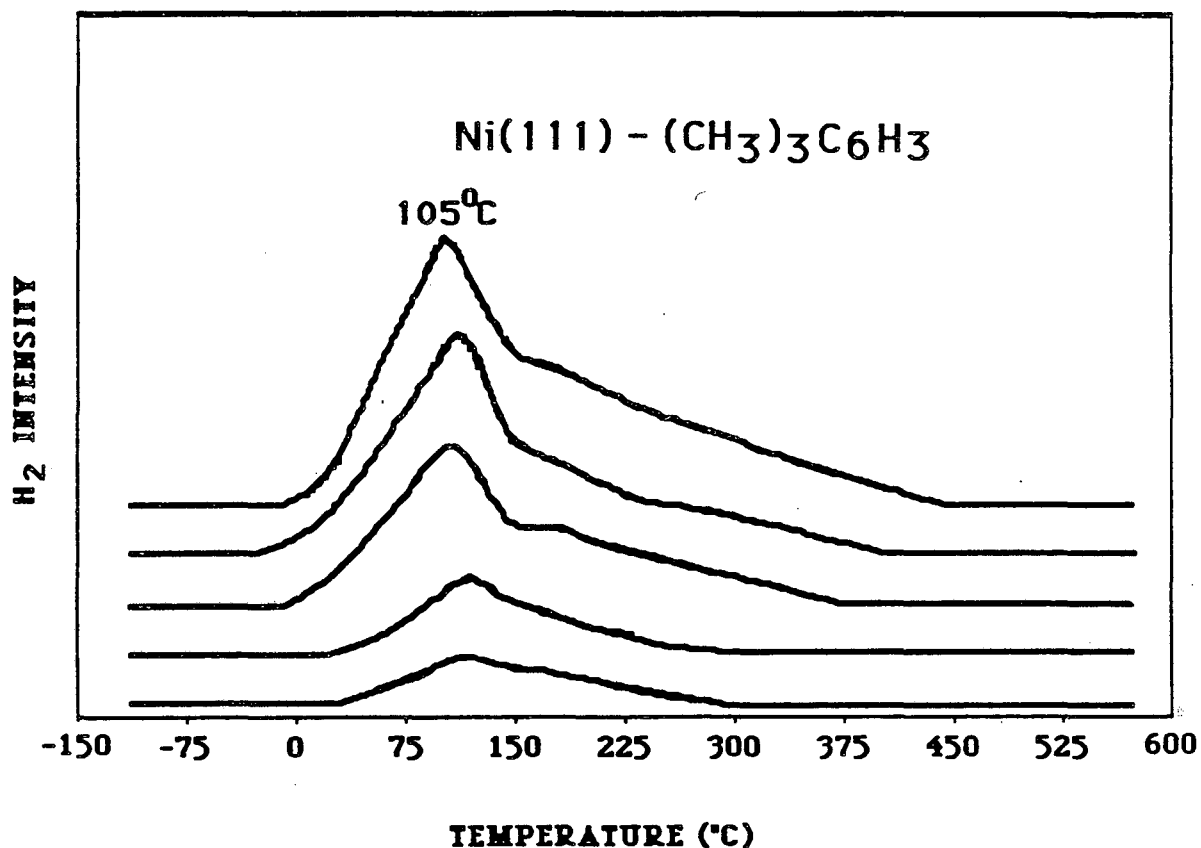


Figure 4-4. Thermal desorption spectra of perproteo mesitylene off of Ni(111), starting with several different initial coverages. Hydrogen was the only gas detected desorbing from the surface. In this case, the temperatures at which methyl and aromatic C-H bonds break are essentially the same.



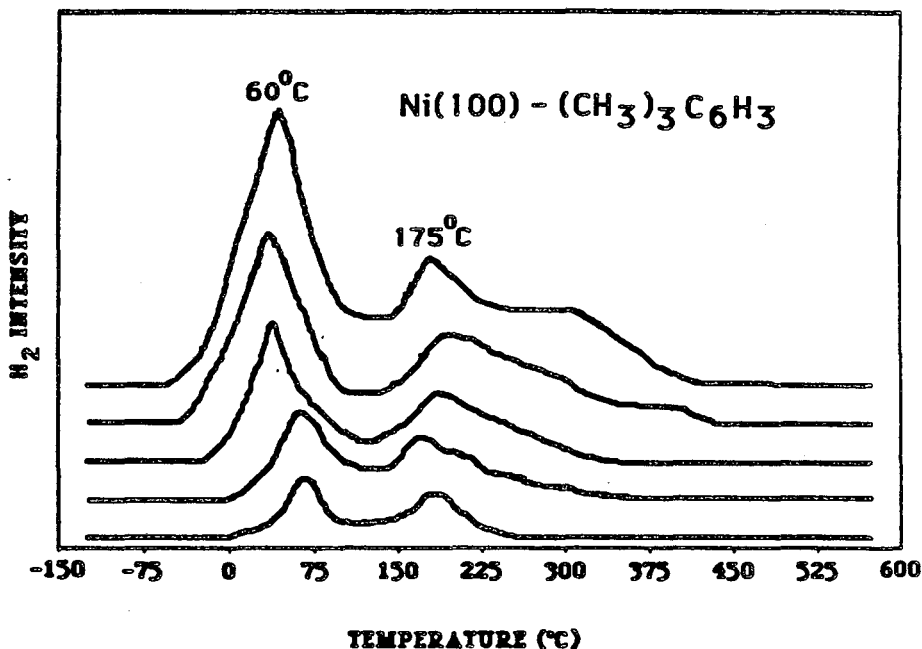


Figure 4-5. Thermal desorption spectra of perproteomesitylene off of Ni(100), starting with several different initial coverages. Hydrogen was the only gas detected desorbing from the surface. No specifically deuterated molecule was available for comparison, but spectra of other methyl benzenes suggest the first peak is due to methyl C-H bond breakage and the subsequent peaks are due primarily to aromatic C-H bond breakage. Note peak resolution is much better than the Ni(111) case, demonstrating Ni(100)'s greater ability to break methyl C-H bonds.

Figure 4-6. The thermal desorption spectra of (a) perdeutero *o*-xylene,  $(\text{CD}_3)_2\text{C}_6\text{D}_4$ , and (b) specifically labeled *o*-xylene,  $(\text{CD}_3)_2\text{C}_6\text{H}_4$ , off of Ni(100). In (a) each separate trace represents different thermal desorptions done with different initial exposures of the adsorbate to the surface. In (b) only one thermal desorption experiment is represented, and masses 2,3, and 4 ( $\text{H}_2$ , HD, and  $\text{D}_2$ ) were monitored simultaneously. Hydrogen was the only detected desorption product, indicating complete decomposition of the molecule. The spectra hint at the occurrence of regiospecific bond breakage, with methyl C-D bonds breaking prior to aromatic C-D(or C-H) bonds.

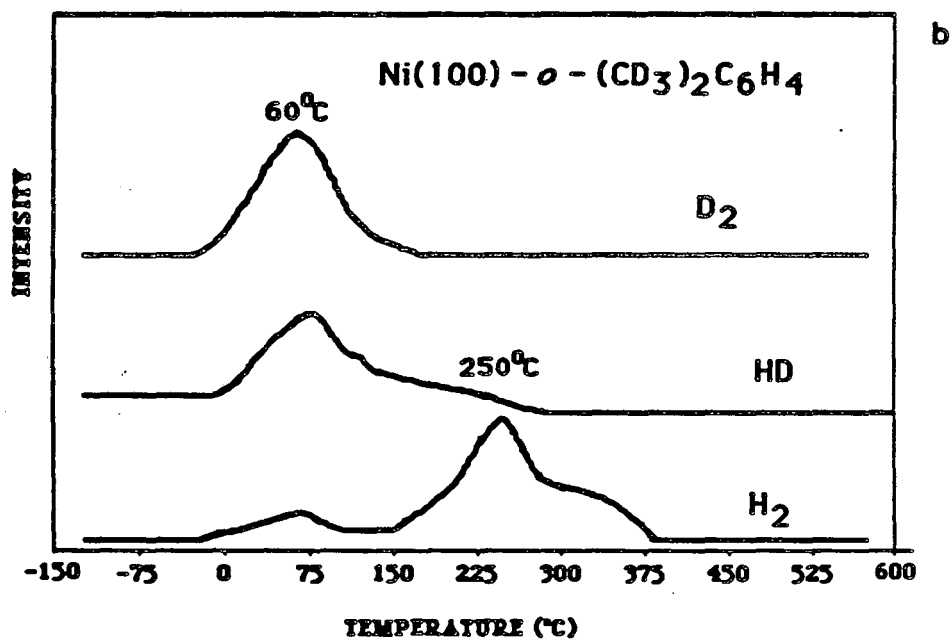
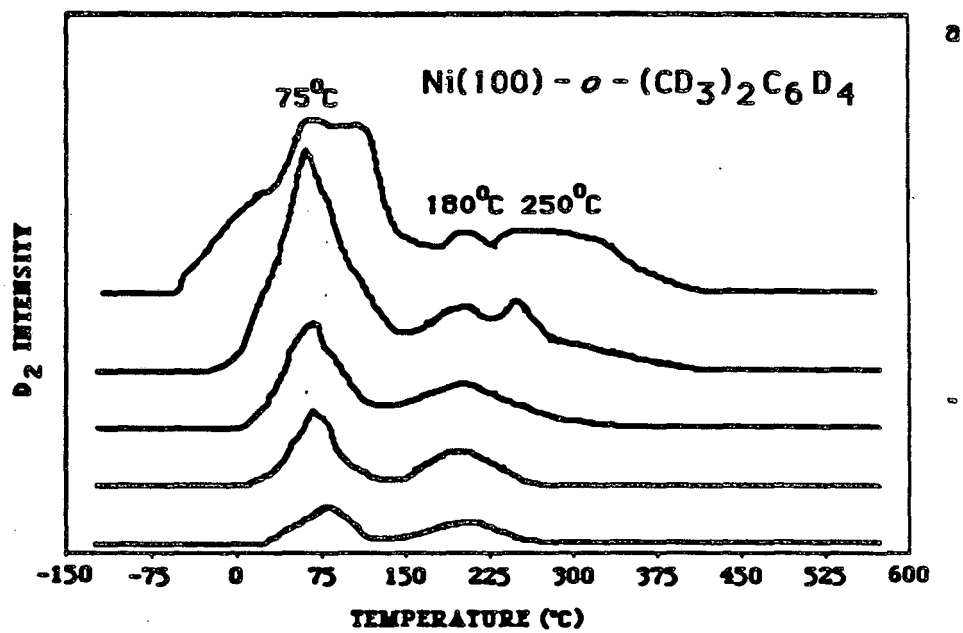


Figure 4-7. The thermal desorption spectra of (a) perproteo *m*-xylene,  $(\text{CH}_3)_2\text{C}_6\text{H}_4$ , and (b) specifically labeled *m*-xylene,  $(\text{CD}_3)_2\text{C}_6\text{H}_4$ , off of Ni(100). In (a) each separate trace represents different thermal desorptions done with different initial exposures of the adsorbate to the surface. In (b) only one thermal desorption experiment is represented, and masses 2,3, and 4( $\text{H}_2$ , HD, and  $\text{D}_2$ ) were monitored simultaneously. Hydrogen was the only detected desorption product, indicating complete decomposition of the molecule. The spectra hint at the occurrence of regiospecific bond breakage, with methyl C-D bonds breaking prior to aromatic C-D(or C-H) bonds.

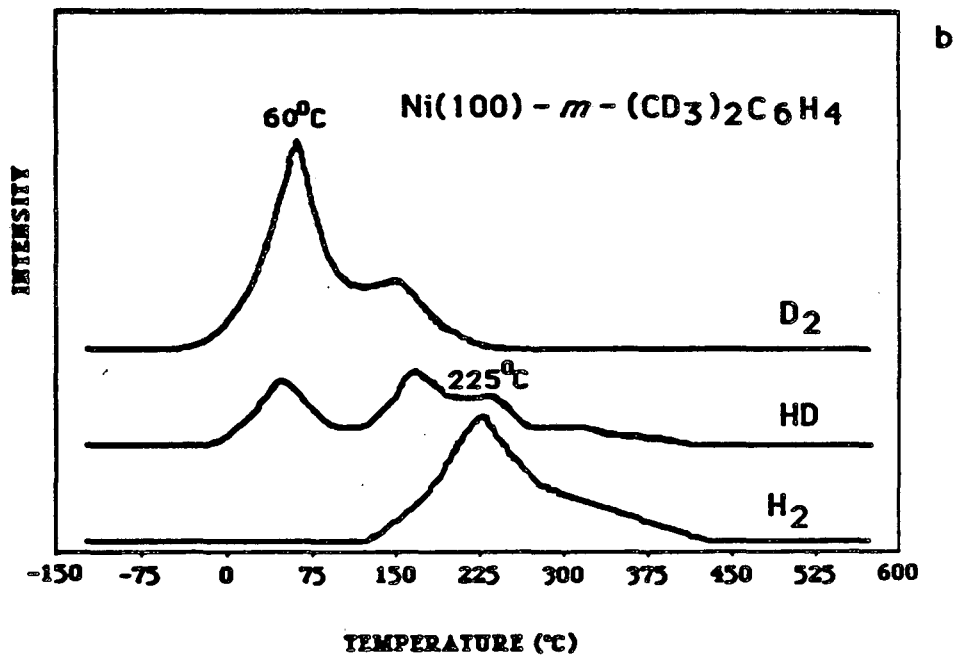
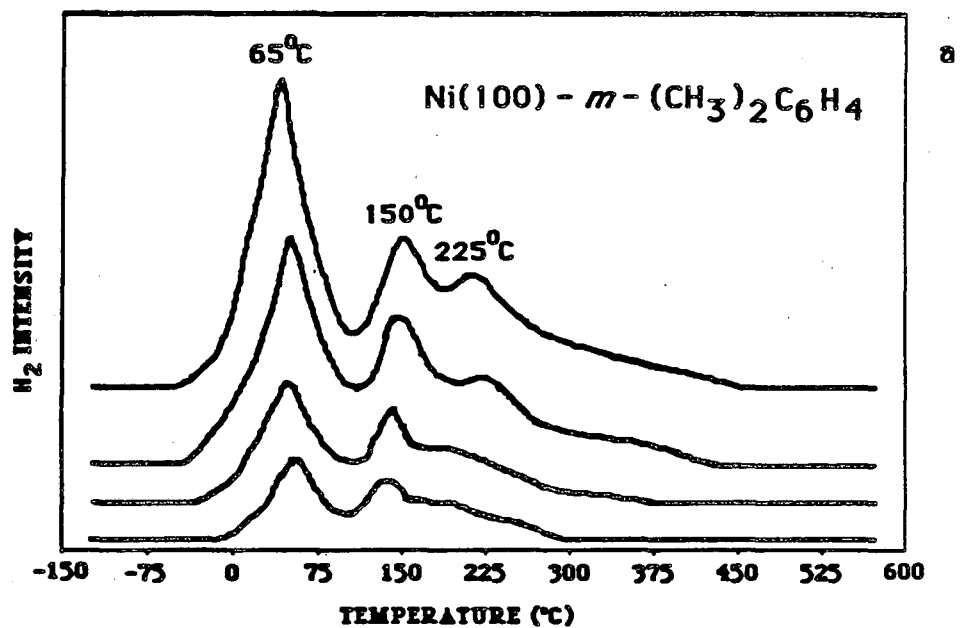


Figure 4-8. The thermal desorption spectra of (a) perdeutero *p*-xylene,  $(\text{CD}_3)_2\text{C}_6\text{D}_4$ , and (b) specifically labeled *p*-xylene,  $(\text{CD}_3)_2\text{C}_6\text{H}_4$ , off of Ni(100). In (a) each separate trace represents different thermal desorptions done with different initial exposures of the adsorbate to the surface. The ratio of the area under the first peak to the area under the rest of the spectrum is greater than 6 : 4, indicating all methyl C-D bonds break to cause the first  $\text{D}_2$  peak. In (b) only one thermal desorption experiment is represented, and masses 2,3, and 4 ( $\text{H}_2$ , HD, and  $\text{D}_2$ ) were monitored simultaneously. Hydrogen was the only detected desorption product, indicating complete decomposition of the molecule. The spectra show clear regiospecific bond breakage, with methyl C-D bonds breaking prior to aromatic C-D(or C-H) bonds.

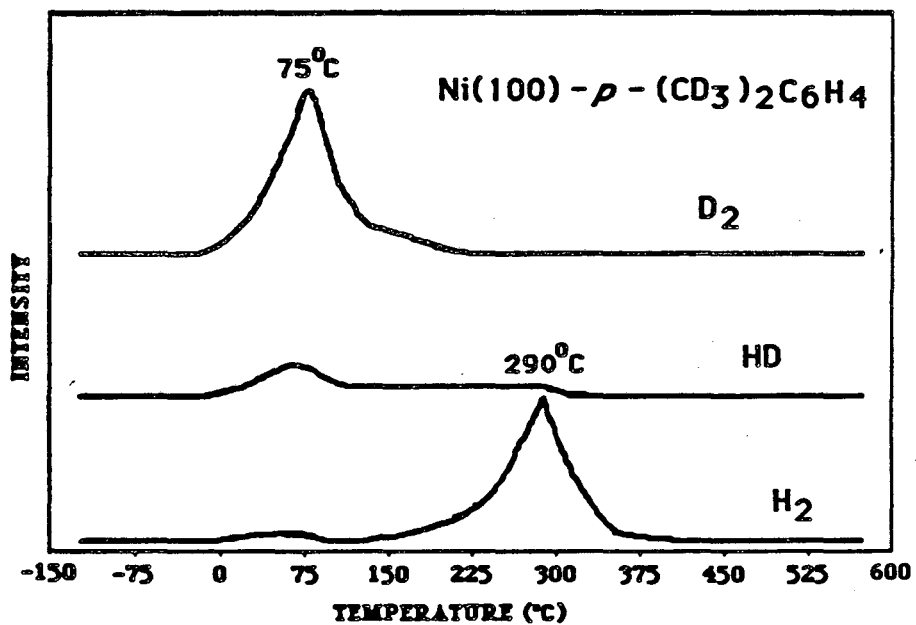
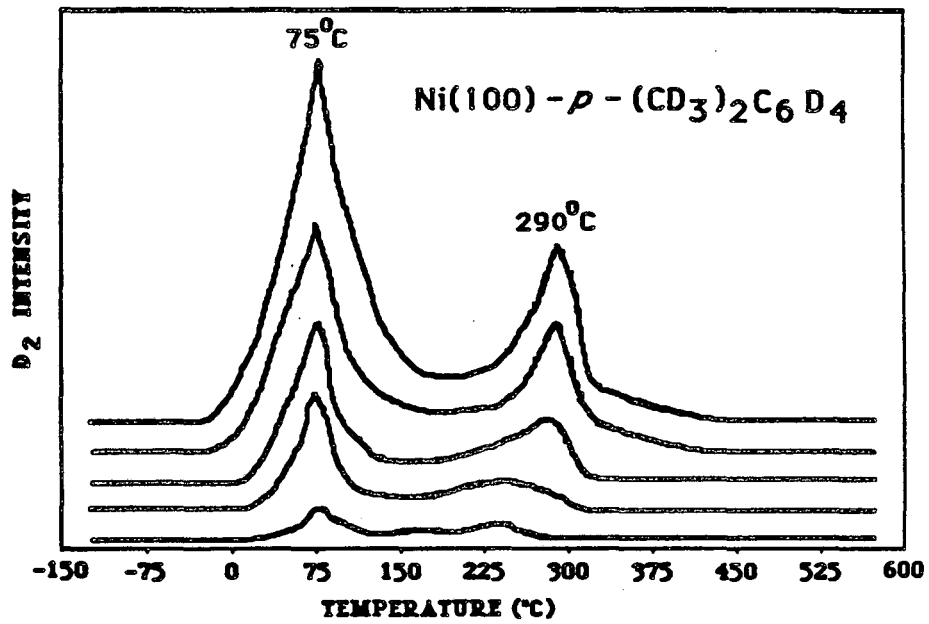
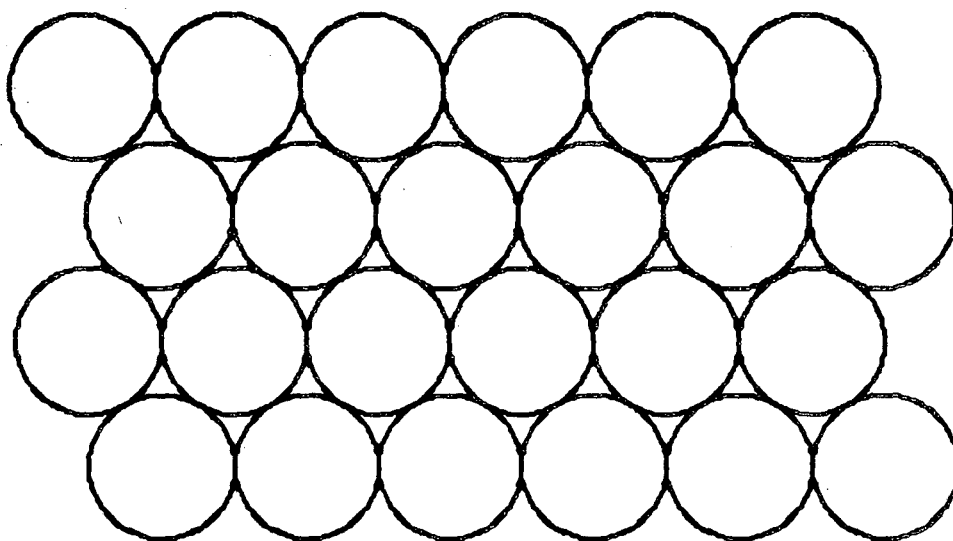
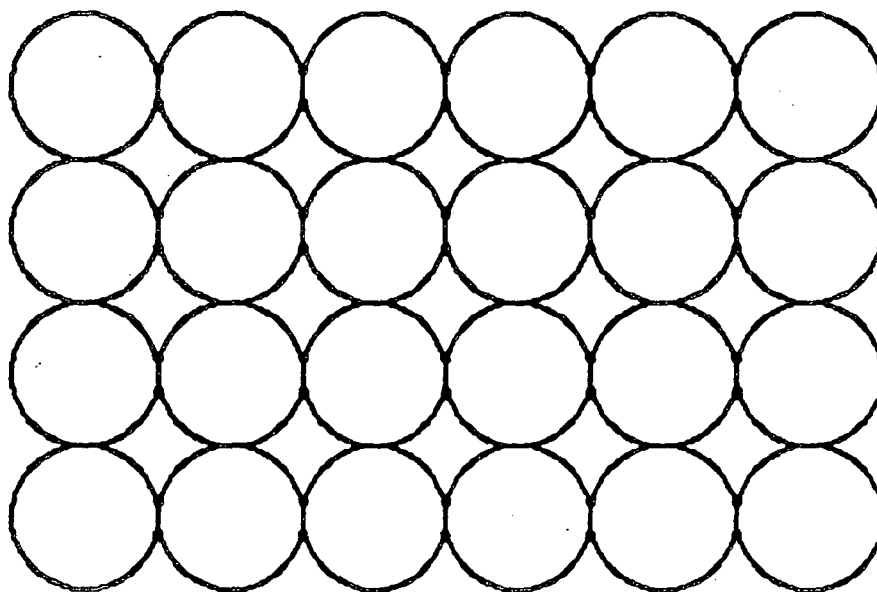


Figure 4-9. Nickel crystallizes in a face centered cubic lattice, so the (111) face of the crystal is hexagonal close packed and the (100) face has square, four-fold symmetry.

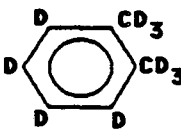
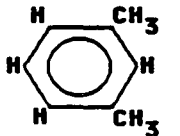
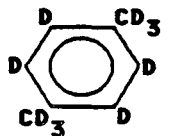
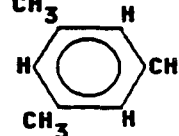




**Ni(111)**



**Ni(100)**

Adsorbate								
	1st Peak	2nd Peak	1st Peak	2nd Peak	1st Peak	2nd Peak	1st Peak	2nd Peak
Ni(100)	75°C	250°C	65°C	225°C	75°C	290°C	60°C	175°C
Ni(111)	105°C	222°C	110°C	189-330°C	114°C	223°C	105°C	~150°C

**Table 4-1.** Comparison of the peak maximum temperatures found in thermal desorptions of the xylenes off of Ni(100) and Ni(111). Desorptions done with specifically deuterated xylenes indicate that the first peak is due to aliphatic(methyl) C-D(C-H) bond breakage and the second peak is due to aromatic C-D(C-H) bond breakage. The comparison shows that Ni(100) breaks methyl C-D bonds more easily than Ni(111) but Ni(111) breaks aromatic C-D bonds more easily than Ni(100).

## Chapter Five

### $\pi$ - Bonding to Si and NiSi<sub>2</sub>

In an attempt to understand the surface chemistry of Si and NiSi<sub>2</sub>, thermal desorption spectra of C<sub>2</sub>D<sub>2</sub>, C<sub>2</sub>D<sub>4</sub>, C<sub>6</sub>H<sub>6</sub>, and pyridine on Si(100), NiSi<sub>2</sub>(100), Si(111) and NiSi<sub>2</sub>(111) were collected. Interesting chemisorption properties were seen and insight into the growth mechanism of NiSi<sub>2</sub> on Si is gained. The results are presented below.

#### Results - Si(100)

This section will deal primarily with thermal desorption experimental data, but it should be noted that both Auger electron spectroscopy and low energy electron diffraction (LEED) were performed as well. The Auger spectrum was characteristic of clean Si, though at times small amounts of carbon were present. The LEED pattern of Si(100), because of its reconstruction (which will be described in the discussion section), produced a sharp 2x2 pattern, the result of two (or more) domains of 1x2 reconstruction. No adsorbates studied produced any pattern different from this; the only effect was a dimming of the off-integral spots. Excessive Auger and LEED experiments were avoided because of the complications that electron beams cause when directed onto adsorbate covered Si surfaces.<sup>30,31</sup>

The thermal desorption spectra of acetylene, ethylene, benzene, and pyridine off of Si(100) are found in figures 5-1 - 5-4. A representative thermal desorption spectrum of C<sub>2</sub>D<sub>2</sub> off of Si(100) is shown in figure 5-1. Both molecular desorption of acetylene and the decomposition product, D<sub>2</sub>, are seen. The molecular peak appears at a relatively high temperature, 513°C, and the D<sub>2</sub> appears at a characteristically high hydrogen desorption temperature of 630°C.

Assuming a 1st order desorption process, the heat of adsorption of the acetylene molecule is 46 kcal/mole. The coverage used to obtain this spectrum is fairly high, near saturation.<sup>41</sup>

Figure 5-2 shows thermal desorption spectra of ethylene off of Si(100), starting with several different coverages. The remarkable thing about this spectrum is that there is essentially no  $D_2$  observed--only molecular desorption is seen. This peak appears at 370°C. The corresponding heat of adsorption is 37 kcal/mole.

Benzene also does not show any decomposition on the Si(100) surface(see figure 5-3). It desorbs molecularly at about 175°C. There is a high temperature shoulder to this peak which at low coverages is the sole peak. With pre-adsorption of small amounts of oxygen, this high temperature shoulder disappears. At high coverages, a low temperature shoulder appears off of the main 175°C peak. The 175°C peak indicates a heat of adsorption of 26 kcal/mole.

Finally, pyridine was adsorbed onto Si(100) and the subsequent thermal desorption spectrum is depicted in figure 5-4. The initial coverage was near saturation. Both molecular desorption is seen, with a peak maximum occurring at 195°C, and a decomposition product,  $D_2$ , is seen with a peak at -20°C. The molecular peak indicates a heat of adsorption of 27 kcal/mole. The fact that the decomposition product,  $D_2$ , desorbs at such a low temperature, -20°C, may be an indication that the deuterium atoms never touch the Si surface. Normally the Si-D(or H) bond is very strong.

### **NiSi<sub>2</sub>(100)**

The low energy electron diffraction pattern of NiSi<sub>2</sub>(100) was observed to consist of basically four-fold symmetry. There were, however, off integral dots seen(1/2,1/4, and others) of significant intensity, indicating that the NiSi<sub>2</sub>(100)

surface reconstructs in some fashion.

The thermal desorption spectrum of acetylene off of NiSi<sub>2</sub>(100) is seen in figure 5-5. The only desorption product seen was D<sub>2</sub>, indicating complete decomposition of the molecule. There are two peak maxima to be seen in this spectrum (initial coverage about at saturation). The first appears at around 225°C and the second at 400°C. It should be noted that the vertical scales on these different graphs, Si and NiSi<sub>2</sub>, are not comparable.

The thermal desorption of ethylene is depicted in figure 5-6. Here, as is the case with Si(100), only molecular desorption is seen. No decomposition takes place. However, as will be discussed later, much less ethylene adsorbs on NiSi<sub>2</sub>(100) than on Si(100). The desorption trace is very interesting, with first a small peak at about 75°C followed by a plateau which in turn is followed by a somewhat larger peak at about 355°C. The heats of adsorption corresponding to the 75°C peak and the 355°C peak are, respectively, 20 kcal/mole and 36 kcal/mole.

There is also no decomposition of benzene on NiSi<sub>2</sub>(100), as was the case with Si(100). The thermal desorptions of benzene, starting with increasing initial coverage are shown in figure 5-7. Here there are essentially two peak maxima which have a similar ratio to each other regardless of the initial coverage. The first peak occurs at 65°C followed by another, somewhat larger one at 160°C. There is also a high temperature region following the 160°C peak, which at high coverage looks like a broad shoulder. The heats of adsorption corresponding to these two peaks are 19 and 25 kcal/mole, respectively.

The thermal desorption of pyridine off of NiSi<sub>2</sub>(100) shows both molecular desorption and decomposition take place (see figure 5-8). The pyridine molecule desorbs at about 35°C, thus the heat of adsorption is 17 kcal/mole. The decomposition product, in this case H<sub>2</sub>, shows two peak maxima at 140°C and 340°C.

## NiSi<sub>2</sub>(100) Formation

The NiSi<sub>2</sub> (100) can be obtained (as is described in the experimental section) by first evaporating Ni atoms onto a clean and well-defined Si(100) surface and then heating at 750°C for 30 minutes. However, there is a critical amount of Ni atoms required before any silicide formation takes place. For example, if  $9.13 \times 10^{15}$  Ni atoms/cm<sup>2</sup> (13 monolayers using the definition given in the experimental section) are deposited onto the Si(100) surface, and the crystal brought up to 750°C for 30 minutes, there will be no sign of Ni on the surface. The Auger spectrum shows clean Si and the LEED pattern shows the 2x2 pattern characteristic of clean Si(100) prepared via Argon ion bombardment. The nickel atoms apparently diffuse into the bulk of the crystal. This process can be followed using Auger electron spectroscopy and the resultant data is presented in Table 5-1. This same amount of Ni can be evaporated onto the Si(100) surface, followed by annealing, for up to five times before any Ni signal is seen in the Auger spectrum.

If, on the other hand, 39 monolayers of Ni atoms are deposited on the surface in one clump, followed by annealing, the Ni signal remains in the Auger spectrum with a Si<sub>92</sub>/Ni<sub>61</sub> ratio of 25. The resulting LEED pattern is also more like that of NiSi<sub>2</sub>(100), with off integral dots, though they are of less intensity than with NiSi<sub>2</sub>(100). The thermal desorption spectra of acetylene, ethylene, and benzene off of this surface are shown in figures 5-9 - 5-11. All three spectra show characteristics of both the Si(100) surface and the NiSi<sub>2</sub>(100) surface, especially the acetylene thermal desorption. Here three D<sub>2</sub> peak maxima are observed, at 260, 410, and 575°C. Plus there is some molecular desorption occurring at 510°C, which only occurred on the Si surface and not on the NiSi<sub>2</sub> surface. If an even thicker layer of Ni atoms is deposited onto the Si(100)

surface ( $3.6 \times 10^{16}$  atoms/cm<sup>2</sup> and up), a complete NiSi<sub>2</sub> surface is formed, with a Si<sub>92</sub>/Ni<sub>61</sub> Auger peak ratio of 16 (characteristic of known NiSi<sub>2</sub>(100) on this same equipment) and a LEED pattern of NiSi<sub>2</sub>(100) is obtained.

### Results - Si(111)

After annealing to remove the oxide layer and bombarding the surface with Argon ions, the Auger spectrum contained only Si signals. After time a small amount of carbon accumulated on the surface but this did not affect the thermal desorption results. The argon ion bombarded surface demonstrated the characteristic 7x7 reconstruction. The 7x7 pattern remained even upon adsorption of all adsorbates studied, the only affect a dimming of the off-integral spots. This is in agreement with Chung et. al.,<sup>42</sup> who studied C<sub>2</sub>H<sub>2</sub> on Si(111).

Thermal desorption spectra were obtained for C<sub>2</sub>D<sub>2</sub>, C<sub>2</sub>D<sub>4</sub>, C<sub>6</sub>H<sub>6</sub>, and C<sub>5</sub>D<sub>5</sub>N off of Si(111) and are presented in figures 5-12 - 5-15. Multiple traces in the spectrum show the desorption curves starting at various exposures of the adsorbate to the surface. The smallest exposure is the lowest trace. As can be seen in figure 5-12, the only product detected desorbing from the surface during the C<sub>2</sub>D<sub>2</sub> thermal desorption was D<sub>2</sub>, indicating complete decomposition of the molecule. This differs from Chung, et. al.<sup>42</sup> who reported seeing molecular desorption. There are two D<sub>2</sub> peak maxima shown in figure 5-12, one at 340°C and the other at 650°C. At low coverages only the high temperature peak appears. These D<sub>2</sub> traces are very similar to plain hydrogen desorption off of Si(111).

Figure 5-13 shows the thermal desorption result of C<sub>2</sub>D<sub>4</sub> off of Si(111). Here the only D<sub>2</sub> peak that appeared was the high temperature one, with a maximum occurring at about 625°C. In addition to the D<sub>2</sub> desorption, however,

molecular desorption occurred as well. Here two peaks appeared. The first one, fairly small, occurred at about 60°C, and the second, the main peak, appears at 375°C. These two peaks correspond to heats of adsorption of 19 and 38 kcal/mole. There is apparently significant desorption occurring between these two peaks however, as well as a shoulder on the high temperature side of the 375°C peak, especially at high coverages. The D<sub>2</sub> peak maximum temperature drops as the coverage increases, which could be taken as an indication of 2nd order desorption kinetics. The thermal desorption results reported here are in very good agreement with those reported by Klimesch, et. al.<sup>43</sup> Like Klimesch, saturation really never was attained, though the high coverage trace presented should be fairly close.<sup>41</sup>

The thermal desorption spectra of benzene, C<sub>6</sub>H<sub>6</sub>, are shown in figure 5-14. At low coverages only the high temperature peak, located at 195°C, appears. The heat of adsorption for the benzene molecules located in this state is 27 kcal/mole. As the coverage is increased, benzene molecules fill in the higher energy adsorption state, and desorb at a lower temperature of around 100°C. The heat of adsorption for this state is 21 kcal/mole. The lower energy state, whose molecules desorb at 195°C, also fills more at higher coverages.

The thermal desorption results for pyridine off of Si(111) are shown in figure 5-15. Here saturation was definitely achieved, because peak areas changed very little even though exposures of pyridine to the Si(111) surface were changed significantly. Both molecular desorption and decomposition occur, with the decomposition product D<sub>2</sub> appearing at 615°C. A small D<sub>2</sub> peak maximum also appears at about 310°C. The molecular desorption peak appears at about 100°C, indicating a heat of adsorption of 21 kcal/mole.

### **NiSi<sub>2</sub>(111)**

The Auger electron spectrum for NiSi<sub>2</sub>(111) as performed with this



equipment gave a  $\text{Si}_{92}/\text{Ni}_{61}$  ratio of about 12-15. The low energy electron diffraction pattern is a sharp hexagonal  $1 \times 1$  pattern, characteristic of epitaxially grown  $\text{NiSi}_2(111)$ . The thermal desorption results are depicted in figures 5-16 - 5-19.

The only desorption product detected for the thermal desorption of acetylene,  $\text{C}_2\text{D}_2$ , is  $\text{D}_2$  (see figure 5-16), indicating complete decomposition of the molecules. There are two definite desorption maximum seen, one at  $380^\circ\text{C}$  and the other at  $585^\circ\text{C}$ . The higher temperature peak maximum drops in temperature as the coverage increases, while the lower temperature peak maximum stays at about the same temperature. This may be an indication that two different desorption processes are involved. A coverage dependent drop in peak maximum temperature is often taken to be 2nd order, while the lack of dependence taken to be 1st order. However, there are complications involved as is described in the introduction and the references cited therein. At higher coverages the  $380^\circ\text{C}$  peak rests on a broad, low intensity peak leading up to the  $585^\circ\text{C}$  peak.

The thermal desorption of  $\text{C}_2\text{D}_4$  off of  $\text{NiSi}_2(111)$  is shown in figure 5-17, and it is apparent that both molecular desorption and decomposition are involved. The decomposition product,  $\text{D}_2$ , has a peak maximum around  $585^\circ\text{C}$ , and the molecular desorption peak maximums are at  $65^\circ\text{C}$  and  $330^\circ\text{C}$ . The heats of adsorption corresponding to these two desorption temperatures are 19 and 35 kcal/mole. The spectrum of  $\text{C}_2\text{D}_4$  off of  $\text{NiSi}_2(111)$  is very similar to that of  $\text{C}_2\text{D}_4$  off of  $\text{Si}(111)$  (figure 5-13).

The thermal desorption spectra of benzene,  $\text{C}_6\text{H}_6$ , off of  $\text{NiSi}_2(111)$  is shown in figure 5-18. As has often been the case with benzene, two distinct peaks are seen, indicating two different reversible adsorption states. The high temperature state, which desorbs at about  $150^\circ\text{C}$ , has a heat of adsorption of around 24 kcal/mole. This state's population increases with coverage, though

not as dramatically as the lower temperature state, whose molecules desorb around 82°C. The heat of adsorption for this state is 20 kcal/mole. At low coverage, only the high temperature state is populated, but as coverage increases the population of the low temperature state grows larger than that of the high temperature state.

The thermal desorption of pyridine off of NiSi<sub>2</sub>(111) is shown in figure 5-19. Both decomposition and molecular desorption are occurring, though the amount of molecular desorption is fairly small. The molecular peak occurs at about 35°C, corresponding to a relatively low heat of adsorption of 17 kcal/mole. The decomposition product, in this case D<sub>2</sub>, desorbs in two different temperature regions, especially at high coverage. These temperature regions are around 210°C and 560°C. At low coverage the high temperature peak is the only one detected.

### **NiSi<sub>2</sub>(111) formation**

The extremely close lattice constants of Si and NiSi<sub>2</sub> allow a very ordered NiSi<sub>2</sub>(111) surface to be made via evaporation of Ni onto a Si(111) surface followed by annealing. Complete NiSi<sub>2</sub>(111) coverage of the surface can be achieved with an initial deposition of at least  $5.48 \times 10^{16}$  Ni atoms/cm<sup>2</sup>. The LEED pattern obtained, as has been described previously, is a very sharp hexagonal 1x1 pattern. As was the case in the formation of NiSi<sub>2</sub>(100), a critical number of atoms of Ni were required in order to detect NiSi<sub>2</sub>(111) formation. The deposition of  $9.13 \times 10^{15}$  atoms of Ni/cm<sup>2</sup>, followed by annealing of the Si crystal at 750°C for 30 minutes, resulted in a clean Si surface by Auger electron spectroscopy. With the deposition of a Ni layer only slightly thicker than this, followed by annealing, the Ni Auger signal remains in the spectrum, and apparently silicide formation begins. Deposition of  $1.37 \times 10^{16}$  Ni atoms/cm<sup>2</sup>,

followed by annealing, leaves a surface showing a  $\text{Si}_{92}/\text{Ni}_{61}$  Auger signal ratio of about 35 and a LEED pattern of  $1 \times 1$ , with faint lines between dots. When this deposition is followed by another  $1.37 \times 10^{16}$  Ni atoms/cm<sup>2</sup>, followed by annealing and then another deposition of  $2.74 \times 10^{16}$  Ni atoms/cm<sup>2</sup> and annealing, a  $\text{Si}_{92}/\text{Ni}_{61}$  Auger peak ratio of 24 is obtained. A LEED pattern that is  $1 \times 1$ , with maybe some lines between dots, is found. The addition of another  $2.74 \times 10^{16}$  Ni atoms/cm<sup>2</sup> followed by annealing leads to a complete silicide surface, with a  $\text{Si}_{92}/\text{Ni}_{61}$  ratio of 14 and a very sharp hexagonal  $1 \times 1$  LEED pattern.

$\text{C}_2\text{D}_2$  thermal desorptions were performed at each of the Ni deposition stages, and the size of the 380°C peak relative to the higher temperature peak measured. The data are summarized in Table 5-2. The size of the 380°C peak grew, relative to the higher temperature peak, with increasing Ni deposition, reaching its maximum relative size with the complete  $\text{NiSi}_2(111)$  surface present.

## Discussion

There are several points present in the data that require discussion, and they will be addressed in the following order. First an analysis of the clean silicon surfaces will be presented, taking into consideration the known surface chemistry of silicon. Next will be a discussion on the formation of  $\text{NiSi}_2$ , and how it relates to silicide formation in general. Following this will be comparisons between silicide and silicon surface chemistry, and what the results imply as far as surface science in general is concerned. Finally, a comparison of  $\text{NiSi}_2(100)$  and  $\text{NiSi}_2(111)$  will be undertaken, followed by some general conclusions.

### Si(100) and Si(111)

The first step to be taken in discussing the chemistry of any surface is a

description of the surfaces involved, especially when they are as complex as the Si surfaces. Silicon is a semiconductor and crystallizes in a diamond lattice structure with a lattice constant of 5.43Å. The Si atoms are held together by covalent bonding, usually considered to be  $sp^3$  hybrids, resulting in highly directional bonds that cause reconstruction on the Si surface.

The ideal Si(100) surface, without the reconstruction, is portrayed in figure 5-20(a). When the surface is formed, however, two  $sp^3$  bonds per surface atom must be broken, and the surface reconstructs in an attempt to fulfill the bonding requirements of the surface Si atoms. One bond per surface Si atom bonds with a neighboring surface atom, drawing them closer together, and the other bond per surface atom remains a dangling bond.<sup>44</sup> The two surface atoms do not draw together in an equal fashion, one ends up lower than the other, forming asymmetric dimers.<sup>45</sup> The result of this reconstruction is the doubling of the length of the unit cell in one direction, giving a 2x1 reconstruction. Domains of the 2x1 reconstruction yield the 2x2 LEED pattern observed. The number of surface atoms for the Si(100) surface is  $6.78 \times 10^{14}$  atoms/cm<sup>2</sup>, and the surface is a relatively open one, with a Si-Si nearest neighbor distance of 3.84Å.

The reconstruction of the Si(100) surface is understood fairly well, but this is not the case for the 7x7 reconstruction found on Si(111). The ideal Si(111) surface is pictured in figure 5-21(a). There are two models of reconstruction proposed for this surface. The first is the presence of double-layer islands present on the Si(111) surface.<sup>46</sup> The islands are triangular in shape and raised from the surface by (100) microfacets, which easily could be asymmetric dimers as found on the Si(100) surface. The other model is labeled the Triangle-Dimer Stacking-Fault model<sup>47</sup> and consists of triangular shaped subunits with dimers along the edges and deep apex holes. The key aspect in each of these models is that there are large areas of "ideal" surface, where the hexagonal Si(111) surface holds true. The single  $sp^3$  dangling bond per surface atom is perpendicular to the surface so interaction between the surface atoms are weaker than is the case with the Si(100) surface.<sup>44</sup> Thus much of this surface is

close packed with a Si-Si distance of  $3.84\text{\AA}$ , though there are also other geometries present on the Si(111) surface. There are  $7.84 \times 10^{14}$  surface atoms/cm<sup>2</sup> on the Si(111) surface.

Most of the Si surface-adsorbate studies done have involved hydrogen and/or water on Si; important systems in silicon technology. There are other adsorbates that have been studied, some of the more simpler ones being N<sup>48,49</sup>, NO<sup>50,51</sup>, NH<sub>3</sub><sup>51</sup>, H<sub>2</sub>S<sup>52</sup>, HCl and HBr<sup>53</sup>, CO<sup>54</sup>, and PH<sub>3</sub>.<sup>55</sup> However, it is H<sub>2</sub>, H<sub>2</sub>O, and O<sub>2</sub> that have received the most attention.

Hydrogen on Si(100) is particularly interesting. The first surface species to form is the monohydride, with the dangling bond of the Si surface atoms used for bonding. The LEED pattern of the (100) surface becomes sharper because the assymetry of the dimer formation becomes symmetric. The next step, which occurs with increasing H atom exposure (in order to achieve hydrogen adsorption, the H<sub>2</sub> molecule must first be predissociated on a hot filament--H<sub>2</sub> itself does not adsorb on silicon),<sup>56</sup> is the formation of the dihydride, which uses the bridging bond of the surface atoms. Upon completion of the formation of this species, the reconstruction of the surface disappears, and the ideal four-fold symmetry is seen in the LEED pattern.<sup>57</sup> Heating the Si crystal (at 320°C) will remove first the dihydride species, converting it to monohydride and the reconstruction will reappear. Further heating at a higher temperature (700°C) removes the hydrogen from the surface. Thermal desorption experiments (heating rates .4 - 3 °K/sec)<sup>58</sup> showed two different peaks, one at about 475°C and the other at about 525°C, and the authors related them to the di and monohydrides, respectively. Thermal desorption spectra of hydrogen off of Si(100) surface done by this author were limited to desorptions after long periods of time whereupon H<sub>2</sub> and other contaminants adsorbed to the surface. Presumably the hydrogen molecules were dissociated by the ion gauge filament, or at times the mass spectrometer filament. In these cases only one peak at 600°C was detected. The difference could be due to different temperature

measurement techniques or to vastly different heating rates.

The chemistry of hydrogen on Si(111) is interesting at high exposures. In the early stages of adsorption, Si-H bonds form. With increasing hydrogen atom exposure, Si-Si bonds break and SiH<sub>4</sub> desorbs from the surface.<sup>14</sup> Hydrogen thermal desorption off of Si(111) done by this author, again limited to background hydrogen atom adsorption, showed a single peak at 650°C. This probably corresponds to low hydrogen atom coverage.

The adsorption of water on Si surface has been the topic of many papers.<sup>16,59,60,61,62,63</sup> Apparently molecular adsorption occurs with the oxygen atom down toward the surface. The interaction of the molecule with the surface is so strong that at low coverage no H-bonded water clusters form as is the case with Cu.<sup>16</sup> Dissociation of the molecule occurs with heating, forming SiO<sub>2</sub> species and atomic oxygen and hydrogen on the surface. Eventually both hydrogen and oxygen desorb at high temperatures. Si obviously interacts very strongly with simple adsorbates such as hydrogen, oxygen, and water. In fact, Si tends to interact very strongly with all the small molecules that have been studied, so these small molecules tend to not be good probes of the differences in the surface chemistry between Si and NiSi<sub>2</sub>.

Larger molecules, particularly those that  $\pi$ -bond to surfaces, do not interact quite as much, though for the smallest molecule studied and presented in this thesis, C<sub>2</sub>D<sub>2</sub>, this obviously is not true (C<sub>2</sub>D<sub>2</sub> decomposed significantly, if not completely). Some of these molecules have been looked at previously. EELS studies of acetylene on Si(111) show that the molecule most likely sits between two Si atoms in a bridge position.<sup>42</sup> The use of ethylene on Si(111) and Si(100) at high temperatures to form a graphitic layer has shown that the (100) surface is more active<sup>64</sup>--it has a lower activation energy for ethylene decomposition. Thermal desorption experiments of ethylene on Si(111) have been done previously,<sup>43</sup> and the results presented here closely parallel these reported results. Some early work using ellipsometry concluded that benzene lay parallel

to the Si(111) surface,<sup>65</sup> the same orientation benzene has on metal surfaces. Finally, pyridine adsorption on Si(111) was studied using UPS, and it was found that the most likely geometry for the pyridine ring was with the ring tilted with respect to the surface, with the nitrogen atom down on the surface. Both the lone pair orbital on the nitrogen and the  $\pi$ -system of the ring were involved in bonding, though the former more so.<sup>66</sup>

Comparison of the thermal desorption of acetylene,  $C_2D_2$ , off of Si(100) and Si(111)(figures 5-1 and 5-12, respectively) shows that the Si(100) surface interacts to a lesser degree than the Si(111).<sup>67</sup> A reasonable amount of molecular desorption takes place on the (100) surface, and this does not happen on the (111) surface. The hydrogen desorption detected for each surface corresponds to the expected thermal desorption of each crystal after exposure to deuterium gas. The high temperature peak maximum at 650°C in the (111) spectrum is the same as background  $H_2$ , and the 630°C peak in the (100) spectrum is close to that for background  $H_2$  off of Si(100), at least with this same equipment.

The thermal desorptions for ethylene off of the two surfaces also provides an interesting comparison(figures 5-2 and 5-13). Here there is no decomposition of  $C_2D_4$  on Si(100), though there is a significant amount on Si(111). This would seem to indicate, once again, that the (100) surface is interacting much less with the ethylene molecule than the (111) surface. However, there is significant molecular desorption of  $C_2D_4$  off of Si(111) at lower temperatures, even as low as 60°C, which argues against this conclusion. There may be multiple adsorption sites on the (111) surface, and only one(a reversible one) on the (100) surface. This would account for the observed results.

Benzene thermal desorption off of the two surfaces(figures 5-3 and 5-14) are very similar. There is one dominant state available on the Si(100) surface and at least two significant states available on the Si(111) surface, but benzene interacts to approximately the same degree with both surfaces. It does not

decompose to any significant degree on either surface.

Some decomposition of pyridine does occur on both surfaces, as can be seen in figures 5-4 and 5-15. Molecular desorption does occur for both surfaces as well, with the desorption off of Si(100) occurring 95° higher than Si(111)(195°C vs. 100°C), indicating greater interaction between pyridine and the Si(100) surface. It is odd, however, that the D<sub>2</sub> desorption off of Si(100) occurs at such a low temperature. As mentioned earlier, this may happen if the D atoms never reach the Si(100) surface. If they did, a desorption peak up around 600°C would be expected. This is the case on the Si(111) surface.

The adsorbates used in these studies are all capable of  $\pi$ -bonding to a surface, and if we assume this is the case on the Si surface, then the bonding most likely involves the sp<sup>3</sup> dangling bond projecting from the surface. These dangling bonds overlap with the  $\pi$  bonds of the adsorbate molecules, forming *mu*-type bonds. In the case of pyridine, some bonding through the lone pair orbital on the nitrogen atom also must be involved.

In general, it appears that the Si(111) surface is more reactive to adsorbates than the Si(100) surface. This is the opposite of what one finds, for example, in fcc metals, where the (100) surface is usually more reactive. In the Si case both surfaces are fairly open, due to the relatively open structure of the diamond lattice. The nearest neighbor distance is 3.84Å, as opposed to about 2.5Å for Ni. The reason for the greater reactivity of the Si(111) surface may be due to the fact that the dangling bond of the Si(111) surface projects out from the surface at a 90° angle, while those of the Si(100) surface project out at a much smaller angle.<sup>44</sup> Thus overlap of this dangling bond with an adsorbate orbital may be less on the Si(100) surface than on the Si(111) surface. The difference in interaction of the two surfaces with adsorbates is not very great, however, and non-existent for benzene, though the major desorption peak is at a lower temperature for the (111) surface than for the (100) surface.

### **NiSi<sub>2</sub> Formation**



The easiest way, although not the only way, to form crystalline  $\text{NiSi}_2$  is to form it epitaxially on a silicon crystal surface. This was the procedure used in the experiments described in this thesis. It is possible to form silicides by depositing silicon onto a metal surface and then annealing. In this case the final silicide obtained is usually the metal rich silicide, which in the case of nickel would be  $\text{Ni}_3\text{Si}$ .<sup>68</sup> This would not grow epitaxially on Si so crystallinity would be lost. The use of  $\text{SiH}_4$  adsorbed on metal surfaces is yet another way to create a silicide surface, and this has been investigated on Pt.<sup>69</sup>

There have been basically two areas of research concerning silicide formation on a silicon surface. The first is the growth kinetics and mechanisms of bulk formation of epitaxial silicide. The second area is in ultra-thin metal layer reactions with a silicon substrate. Investigators are interested in this latter area for the microelectronics industry. With the reduction of device size, the lower limit of the number of metal atoms necessary to achieve silicide behavior is being explored.

When a relatively large amount of metal is evaporated onto a Si substrate, meaning, for example, 100Å and up, and then the sample is annealed, the final silicide formed is usually the silicon rich silicide, in this case  $\text{NiSi}_2$ . However, this is not the first silicide formed in the formation process. One model proposes that at first a nickel-silicon glassy membrane forms,<sup>70,71</sup> and it is from this glassy membrane that various silicides begin to form. The composition of the glass is probably close to the lowest-temperature eutectic in the binary system,<sup>72</sup> so the first phase to form is usually the one nearest this stoichiometry (In this case  $\text{Ni}_2\text{Si}$ ).<sup>73</sup> Another suggestion is that the first phase to form is the congruently melting phase neighboring the central eutectic, in the phase diagram, which is closest in composition to the diffusing species.<sup>74</sup> The main diffusing species in the Ni/Si system is Ni,<sup>75</sup> so the first phase to form is  $\text{Ni}_2\text{Si}$ . The next phase to

form in silicide formation is at the interface between  $\text{Ni}_2\text{Si}$  and the remaining element, Si, and is the nearest congruently melting compound richer in Si.<sup>76</sup> In this case the next phase to form is NiSi. Finally, at a high enough temperature,  $\text{NiSi}_2$  will form.

The above sequence of silicide formation was found empirically, and it obviously correlates in some manner with the eutectic points in the phase diagram. In fact, eutectic points are generally very important in thin film growth. This is most likely due to the fact that it is at compositions near eutectic points that the lowest interfacial free energy exists, facilitating nucleation of the corresponding silicide. That the first phase formed near the eutectic point is the one dominant in the main diffusing species indicates the importance of kinetic factors in the order of the phase formation.<sup>74,76</sup> So even though the most thermodynamically stable phase is  $\text{NiSi}_2$ , the first phase to form is  $\text{Ni}_2\text{Si}$ , due to the kinetic factors involved, primarily diffusion.

Many silicides, including  $\text{Ni}_2\text{Si}$  and NiSi, form via diffusion-controlled kinetics.<sup>77</sup> This is obviously not the case for  $\text{NiSi}_2$ , where at the high temperature necessary for formation diffusion is not a significant factor. No change is observed in the NiSi phase until, at about 750-800°C, small islands of  $\text{NiSi}_2$  form and spread through the whole thickness of the film. Obviously the formation of  $\text{NiSi}_2$  is nucleation controlled.

Nucleation theory leads to the activation energy for nucleation,  $\Delta G^*$ , being proportional to  $\sigma$ , the specific surface energy of the interface, cubed, and inversely proportional to the square of  $\Delta g$ , the chemical free energy per unit volume of product formed:<sup>78</sup>

$$\Delta G^* \propto \sigma^3 / \Delta g^2$$

For formation of a nucleus of NiSi<sub>2</sub>, the  $\Delta g$  between NiSi<sub>2</sub> and NiSi must be considered, and for these two compounds the difference in the energy of formation is very low:

$$\Delta g = g^f_{\text{NiSi}_2} - g^f_{\text{NiSi}} \approx 0$$

This small  $\Delta g$  factor then causes the energy of activation,  $\Delta G^*$ , for the formation of NiSi<sub>2</sub> to be quite large. This is why such a large temperature is required to form NiSi<sub>2</sub>. At the temperature of formation, diffusion of Ni is so fast that once nucleation takes place, NiSi<sub>2</sub> forms very rapidly.<sup>77</sup>

If the temperature of formation is in a range where diffusion is just possible, then complex kinetics are involved in the silicide formation. This is the case for CoSi<sub>2</sub>, where the formation temperature is around 500°C. Here diffusion and nucleation effects are superimposed in the kinetic behavior.<sup>79</sup>

Once the NiSi<sub>2</sub> has formed on the Si surface, an interface forms between the Si and NiSi<sub>2</sub> layers. Because of the almost identical lattice constants (only .4% mismatch), the interface formed can be very, very sharp, especially on the (111) surface. This sharpness allows very good epitaxial growth of NiSi<sub>2</sub> on Si(111) resulting in the sharp LEED pattern seen. When NiSi<sub>2</sub> is grown on Si(100), the resulting interface is not nearly as sharp as in the (111) case. Here there exist many facets, which are believed to be (111) planes, extended over hundreds of Å.<sup>80</sup> This may be the underlying cause of the reconstruction seen in the LEED pattern of the NiSi<sub>2</sub>(100) surface when epitaxially grown on the Si(100) surface.

Interestingly, the geometry and morphology of a silicide surface tends to reflect that of the silicon/silicide interface.<sup>80</sup> At the interface an electric barrier is created called the Schottky barrier. This occurs when a metal is brought into

contact with a semiconductor. The height of the Schottky barrier is very dependent on the nature of the metal/semiconductor (in this case NiSi<sub>2</sub>/Si) interface, more than the bulk qualities of the epitaxial layer.<sup>81,82</sup> Because the barrier height is very similar between Si and the nickel silicides, it has been suggested that the interfacial region is also very similar,<sup>83</sup> but this is difficult to confirm.

### Critical Thickness

In order to form any NiSi<sub>2</sub> at all, a critical number of Ni atoms must accumulate on the surface. On both the Si(100) and Si(111) surface unless a sufficient number of Ni atoms were deposited on the surface (2.7-3.6x10<sup>16</sup> and 1.37x10<sup>16</sup> Ni atoms/cm<sup>2</sup> for Si(100) and Si(111) respectively), no Ni remained after annealing. Apparently the Ni diffused into the Si crystal. Other investigators have come to the same conclusion and found that for Ni thicknesses less than the critical thickness, the 2x1 LEED pattern and the surface state (seen via ultraviolet photoelectron spectroscopy) reappear.<sup>76,84,85</sup> A similar thing has been reported for the Si(111) surface,<sup>86</sup> though the picture is less clear. Here, depending on the amount of Ni and the length of annealing time, various different LEED patterns have been seen.<sup>86,87,88</sup> Some investigators report diffusion from the surface while others report formation of NiSi<sub>2</sub> itself, of either type A or type B<sup>89,90</sup> (type B NiSi<sub>2</sub> has a lattice vector which is rotated 180° about the Si surface normal, the lattice vector of type A is not rotated). This unclear picture correlates well with the finding of a smaller critical thickness of Ni on Si(111) than on Si(100). Smaller amounts of Ni do react more readily with the (111) surface. This, combined with the differences in annealing times and temperatures, may account for the range of reports concerning critical thickness on Si(111).

The presence of a critical thickness for silicide formation is possible because diffusion of the metal through Si occurs readily. The diffusion coefficient

in high purity Si is large enough that Ni atoms can diffuse through a Si wafer in a matter of minutes. The presence of dopant will affect the diffusion of Ni,<sup>91</sup> though for thin layers the presence of dopant does not prevent the diffusion of Ni from the surface at high temperatures. Diffusion of thin layers of metal into the Si crystal have been reported for Ag<sup>92</sup> on Si (100), and Ag, Al, Ni, Pd, Pt, Ta, V<sup>93</sup>, and Au<sup>71</sup> on Si(111). After annealing with each of these metals, the clean Si surface LEED pattern was obtained. Again, these reported results depend on the time and temperature used in annealing.

### **Metal - Silicon Interaction at Room Temperature**

Because of the importance to the electronics industry of the reaction between metals and Si at very low coverages, many thin layer studies have been done at room temperature. Even at these low temperatures, interaction between the metals and silicon is seen.<sup>71</sup> The ability of some metals, Ni among them, to occupy the interstitial voids in the Si lattice with little activation energy makes this possible.<sup>84</sup> Once the metal is inside the lattice, weakening of the Si-Si bonds occurs and compound formation takes place.

Thus the first thing to happen when depositing Ni on Si(100) is the formation of a diffusion layer, where the Ni atoms diffuse into the interstitial voids in the lattice.<sup>84,94,95</sup> This diffusion layer does not destroy the 2x1 LEED pattern or the surface states seen in ultra-violet photoelectron spectroscopy.<sup>96</sup> With increasing Ni deposition, a thin layer of Ni<sub>2</sub>Si nucleates, and on top of this Ni metal forms.<sup>96</sup> The composition in the first few layers shifts gradually from the diffusion layer to the Ni metal layer, as can be seen by X-ray photoelectron spectroscopy.<sup>81</sup> On the Si(111) face, the first few Ni atoms again penetrate into the Si lattice and occupy the interstitial positions.<sup>81</sup> With increasing coverage, islands of Ni<sub>2</sub>Si form (as will be discussed in the next section), and then a film of Ni metal will form on top of that. All of this interaction occurs at room temperature.

Ni is not alone in interacting with Si at low coverages at room temperature. Pd interacts strongly with the Si(111) surface, at first just chemisorbing on the surface, but with increasing coverage interfacial intermixing occurs between the Si and Pd,<sup>97</sup> perhaps nucleating Pd<sub>2</sub>Si.<sup>86</sup> Upon heating the Pd partially diffuses into the bulk.<sup>98,99</sup> CoSi<sub>2</sub> forms at room temperature with low coverage. Higher coverage results in a cobalt film, though there may be some Si dispersed in this film.<sup>100</sup> Silver will embed itself under the top layer of Si atoms, but the interaction appears to be weak, although the LEED pattern is affected.<sup>101</sup> The weak Ag-Si interaction correlates with the fact that no silver silicides are known. Metals other than the noble and near-noble metals also will interact with Si at room temperature, but not to as great a degree. Si on W(110) will form WSi<sub>2</sub>, until halted by oxide formation.<sup>102</sup> Titanium does not interact much at low coverages, but with enough Ti atoms present, Si and Ti will form TiSi at the interface.<sup>103</sup> Yb only interacts to a small extent; it primarily remains on the surface.<sup>104</sup> Molybdenum apparently does not interact at all<sup>105</sup>, as is the case with vanadium,<sup>106</sup> at room temperature. In general, the refractory metals do not react with Si at room temperature to the extent that the noble and near-noble metals do.

There have been various models proposed to account for both the critical thickness phenomenon and the low temperature silicide formation (or metal-silicon interaction). One such model is the interstitial model, where the metal atoms enter the interstitial sites of the Si lattice, and sufficient numbers of atoms will cause weakening of the Si-Si bonds due to charge transfer.<sup>107</sup> Then reaction can take place. Another proposed model is the screening model,<sup>71</sup> where the covalent bonding between Si atoms is shielded by the mobile free electrons in the adsorbed metal layer. Thus Si-Si bonds are weakened and reaction occurs. A thick enough metal layer must be present in order for the electrons to move freely in the z direction. Yet a third model is the metal cluster model,<sup>108</sup> where clustering of enough metal atoms on the Si surface releases sufficient energy to allow metal-silicon reaction. This model requires metal atom

island formation on the surface and will be discussed in more detail in the next section.

### Island Formation

The thermal desorption spectra of acetylene, ethylene, and benzene (figures 5-9 - 5-11) off of a Si(100) surface with  $2.7 \times 10^{16}$  Ni atoms/cm<sup>2</sup>, along with the corresponding LEED pattern and Auger spectrum, suggest NiSi<sub>2</sub> island formation on the Si(100) surface. Particularly for the C<sub>2</sub>D<sub>2</sub> case, features of both the NiSi<sub>2</sub>(100) and Si(100) C<sub>2</sub>D<sub>2</sub> are seen. The D<sub>2</sub> peaks at 260 and 410°C are due to decomposition on NiSi<sub>2</sub>(100) and the molecular peak at 510°C must come from Si(100). No molecular desorption was found with NiSi<sub>2</sub>(100). Other investigators have hinted at the possibility of NiSi<sub>2</sub>(100) island formation on Si(100), through the use of LEED.<sup>109</sup> Here, although they obtained a 2x1 pattern after annealing, the I-V (intensity vs. voltage) curves were very different from those of clean Si(100). One possibility they suggest is NiSi<sub>2</sub>(100) 1x1 with bare regions of Si(100)2x1.

The same situation exists on the Si(111) surface. Table 5-2 shows this. The pattern of the Si<sub>92</sub>/Ni<sub>61</sub> Auger signal ratio decreasing with increasing Ni deposition and anneals, suggests that island growth of NiSi<sub>2</sub>(111) on Si(111) is occurring. Each Ni deposition should have been sufficient to completely cover the Si crystal surface many times over, yet clean Si behavior is seen--especially at the lower depositions. Also, in the thermal desorption spectra of C<sub>2</sub>D<sub>2</sub> the 380°C peak area increases relative to the higher temperature peak area with increasing Ni deposited. This points to NiSi<sub>2</sub> islands, as the 380°C peak is present only in NiSi<sub>2</sub>(111)- C<sub>2</sub>D<sub>2</sub> thermal desorptions (see Table 5-2).

Island formation on Si(111) has been observed by other investigators as

well. The "1x1" surface of Ni on Si(111) has been attributed to small domains with  $19^{1/2}$  by  $19^{1/2}$ (Ni) symmetry with the rest of the surface 7x7 domains where no Ni is present.<sup>110</sup> Transmission electron microscopy has been used to see Ni<sub>2</sub>Si islands with lateral sizes between 50 and 100Å, and thicknesses of around 9Å.<sup>111</sup> Ni<sub>2</sub>Si islands also have been seen for ultra-thin Ni layers using medium energy ion scattering.<sup>112</sup> The islands have remained Ni<sub>2</sub>Si because they were room temperature experiments and so no diffusion or further reaction occurred. The islands are also apparently covered with Si atoms, which may account for results which show formation of NiSi<sub>2</sub> first.<sup>89</sup> Van Loenen, et. al., besides seeing Ni<sub>2</sub>Si islands at room temperature, also saw NiSi<sub>2</sub> islands on Si(111) after annealing.<sup>113</sup> The number of Ni atoms/cm<sup>2</sup> required for island formation was less in their studies than in the authors, but nevertheless, island formation was observed.

Island formation, especially for room temperature deposits, is not limited to Ni.<sup>114</sup> Many metals, when deposited on Si, form islands at medium to high metal coverage. Island formation has been observed in the cases of Au,<sup>71,76,115,116</sup> Cu,<sup>76,117,118,119</sup> Ag,<sup>76,92,120,121,122,123</sup> Bi,<sup>124</sup> WSi<sub>2</sub>,<sup>125</sup> In,<sup>126</sup> and Co,<sup>127</sup> on silicon and Sn and Al on GaAs.<sup>108</sup> Pd, for some reason, does not appear to form islands.<sup>86</sup> It may be that Pd interacts so strongly with the Si surface so no surface migration, necessary for island formation, takes place. In the case of Cu on Si(111), island formation does not occur until the first monolayer of Cu has either dispersed itself on the surface or interacted with the surface atoms--whichever causes the 5x5 LEED pattern seen with a monolayer of Cu. This pattern was observed by this author when Cu diffused through the crystal to the surface. Obviously this means that the surface energy of Cu or of the Cu-Si compound formed is lower than that of the clean Si surface. Additional Cu atom deposition brings on island formation. In fact most island formation on Si does not occur until the metal-silicon interaction takes place. This is why island formation does not occur until medium to high coverages of metal are present. In



the nickel case it is probably that the first few Ni atoms interact with the Si surface atoms, even to the extent of slipping under the top layers of Si. This has been observed by many investigators, as was mentioned earlier. Then upon additional Ni deposition, islands of Ni form, providing sufficient energy for the formation of Ni<sub>2</sub>Si, as is discussed next.<sup>111</sup>

The idea of metal cluster formation releasing sufficient energy for reactions or diffusion to take place<sup>112</sup> explains both the observation of island formation and the requirement that a critical number of atoms be deposited before compound formation with annealing can occur. This is an especially useful concept if the first metal atoms that arrive to the Si surface diffuse under the surface to a small extent, as was suggested above. The energy associated with cluster formation is:

$$\Delta(n,m) = E_b^{(n)} - E_{ad}^{(m)}$$

with  $E_{ad}^{(m)}$  the energy required to desorb  $m$  atoms from their sites and  $E_b^{(n)}$  the energy released upon the formation of an  $n$ -atom cluster. This energy is released and available for surface chemical reactions. Unless sufficient numbers of adsorbate(Ni) atoms have been deposited on the Si surface, there is not sufficient energy available for compound formation. If the first Ni atoms diffuse into the Si, then it just takes that many more before reaction can occur. This accounts for the necessity of a critical number of Ni atoms deposited before any compound forms--the critical thickness. The clustering theory also accounts very nicely for the observation of islands of nickel silicide on silicon. With enough Ni atoms present, Ni clusters form, releasing enough energy to form Ni<sub>2</sub>Si at the cluster sites.

## Summary

Upon deposition of Ni, the first Ni atoms apparently diffuse into the Si crystal, at least to a small extent. If annealing is done at this point, the Ni atoms diffuse further into the bulk, particularly if dealing with a Si(100) surface. The extent of diffusion depends on annealing time and temperature. With larger amounts of deposited Ni, clusters of Ni atoms form, releasing sufficient energy to form Ni<sub>2</sub>Si islands, which are covered with a layer of Si atoms. Upon annealing, the Ni<sub>2</sub>Si islands first turn into NiSi then NiSi<sub>2</sub> islands. The remaining Ni atoms which resided in the near surface region diffuse far into the bulk. The NiSi<sub>2</sub> islands existence on both the Si(100) and Si(111) surfaces are demonstrated by the evidence given earlier (figure 5-9 and Table 5-2). With thick enough Ni layers deposited, the Ni<sub>2</sub>Si islands grow together to form a solid sheet of Ni<sub>2</sub>Si, which upon annealing converts to NiSi<sub>2</sub>, as is seen for thick Ni layer silicide formation.

### Bulk NiSi<sub>2</sub>

NiSi<sub>2</sub> crystallizes in the CaF<sub>2</sub> structure where the Si atoms form a simple cubic lattice with the Ni atoms occupying every other cube. The lattice constant is 5.40Å, very close to Si, which is what enables epitaxial growth. Each Si atom is surrounded by 4 nickel atoms at a distance of 2.34Å, 6 second nearest neighbor silicon atoms 2.70Å away, and 8 third nearest neighbor silicon atoms at a distance of 3.82Å. Each Ni atom is surrounded by 8 silicon atoms at a distance of 2.34Å, and then 12 second nearest neighbor Ni atoms at a distance of 3.82Å.<sup>128</sup> NiSi<sub>2</sub> is a metal with a resistivity of 40 μΩcm.<sup>71</sup>

An interesting point to consider is the type of bonding involved between Ni and Si in NiSi<sub>2</sub>. Is it ionic or covalent? Monitoring NiSi and NiSi<sub>2</sub> formation with X-ray photoelectron spectroscopy, it appears that charge transfer from Ni to Si is occurring,<sup>81</sup> though calculations show minimal ionicity.<sup>129</sup> The Ni xy, xz, and yz d orbitals bond with the Si sp<sup>3</sup> hybrid orbitals. In fact the projected Si s and p

components of the density of states do look remarkably similar to pure Si, with the  $sp^3$  hybrid signature.<sup>129</sup> The remaining d orbitals on Ni, the  $x^2-y^2$  and  $z^2$ , form a nonbonding band well below the Fermi level.<sup>128,130,131</sup> In fact the metallic nature of  $NiSi_2$  is due to s and p type free electrons. The bonding picture is not as simple as with Si, where the bonding and antibonding bands are clear cut. The linking of eight Si  $sp^3$  hybrids through a single Ni atom has the effect of smearing out the Si  $sp^3$  related density of states. The gap found in Si no longer exists, and a partially filled band exists at the Fermi level. This accounts for the metallic nature of  $NiSi_2$ .

### **$NiSi_2$ Surfaces**

Given that  $NiSi_2$  has a  $CaF_2$  crystal structure, it is easy to determine what the ideal surface looks like. The only question is which element, Si or Ni, is the top layer. In the  $NiSi_2(111)$  case, LEED intensity vs. voltage calculations show that silicon is the top layer<sup>87</sup> and has hexagonal symmetry as depicted in figure 5-21. The sharp  $1 \times 1$  LEED pattern demonstrates that no reconstruction is occurring on this surface. The Si-Si distance on the surface is  $3.82\text{\AA}$ , which is very close to the ideal Si(111) surface Si to surface Si distance of  $3.84\text{\AA}$ .

The Si - Si distance on the surface of ideal  $NiSi_2(100)$  is much smaller, only  $2.70\text{\AA}$ , and is smaller than that found on the ideal Si(100) surface ( $3.84\text{\AA}$ ) as can be seen in figure 5-20. However, both of these surfaces reconstruct. The Si(100) surface forms asymmetric dimers, so two of the surface atoms would be drawn together, leaving larger distances between the dimers. The reconstruction on the  $NiSi_2(100)$  surface has not been determined. That it reconstructs is obvious, for many off-integral dots are seen in the LEED pattern. Work done with intensity vs. voltage curves indicate a very interesting configuration is likely for this surface. These investigators assumed that the reconstruction was relatively weak. The

model that best fit their data was an adatom model, with a silicon perched on top of the surface, higher than the surface Si atoms (1.05Å), but located directly above the second layer Ni atoms (2.4Å above). In addition, the Si surface layer was slightly buckled.<sup>85</sup>

Some work has been done on the surface chemistry of NiSi<sub>2</sub>. Oxidation of NiSi<sub>2</sub> has been investigated due to Si oxidation procedures done in the electronics industry. It was found that the metal atoms act as a catalyst for oxidation, helping to split the O-O bond, but not ending up oxidized themselves.<sup>132,133</sup> Oxygen and other small molecule adsorption on NiSi<sub>2</sub>(111) were studied by Dubois and Nuzzo using electron energy loss spectroscopy.<sup>134</sup> They found that the surface acted similarly to Si(111) in many respects. H<sub>2</sub> and N<sub>2</sub> would not adsorb molecularly, O<sub>2</sub> desorbed associatively, interacting with both Ni and Si, however. CO did adsorb, at first molecularly, but shortly is dissociated. CO<sub>2</sub> apparently adsorbs dissociatively, with desorption of CO leaving an atom of oxygen behind. They also found that methanol would form a methoxide species (the OCH<sub>3</sub> group bonded to the surface oxygen end down), and this also has been seen on Si(111).<sup>135</sup>

### **NiSi<sub>2</sub>(111) vs. Si(111) Surface Chemistry**

The similarity of the surfaces of Si(111) and NiSi<sub>2</sub>(111) is reflected in the thermal desorption spectra of C<sub>2</sub>D<sub>2</sub>, C<sub>2</sub>D<sub>4</sub>, C<sub>6</sub>H<sub>6</sub>, and C<sub>5</sub>D<sub>5</sub>N off of these two surfaces, as can be seen in figures 5-12 - 5-19. The thermal desorption spectra of acetylene show the greatest differences (figures 5-12 and 5-16). Here decomposition is the only reaction occurring since D<sub>2</sub> is the only gas detected

desorbing from the surface. The high temperature peak is about 65°C lower off of NiSi<sub>2</sub>(111) than Si(111), but this just corresponds to the desorption of free H<sub>2</sub> off of these two surfaces. The main difference in these two spectra is the presence of the 380°C peak in the NiSi<sub>2</sub>(111) spectrum. This may be due to a Ni-D bond, but the EELS work mentioned earlier<sup>134</sup> shows no Ni-H bond formation upon H<sub>2</sub> adsorption.

The rest of the thermal desorption spectra show essentially no differences at all. However, note that the desorption temperatures for NiSi<sub>2</sub>(111) are consistently lower than for Si(111). The exact same crystal and thermocouple were used for each surface, so this effect should be real. Also, the amount desorbing is roughly the same for both surfaces (the vertical scales on the figures are completely arbitrary, not related to one another in any way).

The similarities between the thermal desorption spectra of NiSi<sub>2</sub>(111) and Si(111) can be explained easily by the fact that the two surfaces are almost identical. Each surface consists of Si atoms in a hexagonal arrangement with similar Si-Si distances. It is true that the Si(111) surface reconstructs into a 7x7 arrangement, but even with this rearrangement large areas of ideal 1x1 surface exist, as was mentioned earlier. This probably explains the similarity in peak shape and height found in the thermal desorptions of C<sub>2</sub>D<sub>4</sub>, C<sub>6</sub>H<sub>6</sub>, and C<sub>5</sub>D<sub>5</sub>N off of Si(111) and NiSi<sub>2</sub>(111).

The difference (lower D<sub>2</sub> desorption temperature for NiSi<sub>2</sub>(111)) found in these spectra is somewhat more difficult to explain. Since all of these adsorbate molecules are donor molecules<sup>136</sup> it may be that the charge transfer from Ni to Si seen by some investigators could cause weaker bonding between the Si surface atoms and the adsorbate molecules.

### **NiSi<sub>2</sub>(100) vs. Si(100) Surface Chemistry**

Unlike the (111) faces of Si and NiSi<sub>2</sub>, the thermal desorption spectra of C<sub>2</sub>D<sub>2</sub>, C<sub>2</sub>D<sub>4</sub>, C<sub>6</sub>H<sub>6</sub>, and pyridine off of Si(100) and NiSi<sub>2</sub>(100) show some dramatic differences (see figures 5-1 - 5-8). Looking at acetylene, there is molecular desorption off of Si(100) which is not present with NiSi<sub>2</sub>(100). However the desorption temperature of the decomposition product is much lower for NiSi<sub>2</sub> than for Si. The thermal desorption of hydrogen off of Si(100) is about 50°C higher than off of NiSi<sub>2</sub> (550° vs 600°), but the C<sub>2</sub>D<sub>2</sub> deuterium comes off much lower on NiSi<sub>2</sub>(100).

The ethylene spectra of Si(100) and NiSi<sub>2</sub>(100) are very similar, at least as far as peak shape and temperature are concerned. The amount of ethylene desorbing from the NiSi<sub>2</sub>(100) surface is much, much smaller than for Si(100) which will be discussed more later. The 75°C peak found with NiSi<sub>2</sub> may or may not be significant, but if it is it just demonstrates the presence of a low temperature state on NiSi<sub>2</sub>(100) that is not present on Si(100). Benzene also shows a low temperature (high energy) state present on the NiSi<sub>2</sub>(100) surface which is not on the Si(100) surface. This peak is seen growing in at about 65°C.

Pyridine desorption is very different on these two surfaces as well. For Si(100) the D<sub>2</sub> desorption occurs at such a low temperature that it seems likely the D atoms never reach the Si surface. For NiSi<sub>2</sub>, the decomposition product (in this case H<sub>2</sub>) desorption is complex, with the two higher temperature peaks seen in figure 5-8. The molecular peaks for Si and NiSi<sub>2</sub> show a much lower peak maximum for NiSi<sub>2</sub>(100) than Si(100).

The amount of molecules desorbing from the surfaces of NiSi<sub>2</sub>(100) and Si(100), which is an indication of the amount that was initially adsorbed, are vastly different, as can be seen in Table 5-3 (again, the vertical scales for the thermal desorption figures are not related to one another). This is most dramatic

for ethylene,  $C_2D_2$ . These figures, taken with the molecular peak maxima temperatures found through the thermal desorptions, lead to the general conclusion that the  $NiSi_2(100)$  surface is much less reactive than the  $Si(100)$  surface. The adsorbates bond less strongly to  $NiSi_2(100)$  than to  $Si(100)$ . Why is this the case?

As was mentioned for the (111) surfaces, the presence of Ni may mean that the surface Si atoms have more electron density on them than in Si. This would account for weaker binding on the  $NiSi_2(100)$  surface. However, looking at the actual surface configurations also can explain this phenomena, as well as the drastically reduced amount of adsorption on  $NiSi_2(100)$ . As figure 5-20 shows, the Si-Si distance of the ideal  $NiSi_2(100)$  surface is actually smaller than that found on ideal  $Si(100)$ . This alone could be used to rationalize the reduced reactivity of the  $NiSi_2(100)$  surface. The more open surface can allow the adsorbate molecule to coordinate with a larger number of surface atoms. However, in the case of  $NiSi_2(100)$ , it appears that additional Si atoms are present, residing above the surface on top of the Ni sites. This would then further inactivate the surface (helping to satisfy the surface dangling bonds), similar to sulfur poisoning of a noble metal,<sup>137</sup> and essentially no adsorbate could reach the Ni atoms (present in the second layer anyway). This surface geometry and Si atom nature, along with the possible Ni electron donation to the Si atoms, accounts for the reduced reactivity of the  $NiSi_2(100)$  surface compared to the  $Si(100)$  surface.

### **$NiSi_2(111)$ vs. $NiSi_2(100)$ Surface Chemistry**

The most significant difference between the thermal desorptions off of  $NiSi_2(111)$  and  $NiSi_2(100)$  is the temperature at which the decomposition

product,  $H_2$  or  $D_2$ , desorbs from the surface. In the case of  $NiSi_2(111)$  the  $D_2$  that desorbs from the surface does so at temperatures which are consistent with free  $H_2$  desorption. For the  $NiSi_2(100)$  case  $D_2$  (in the case of  $C_2D_2$ ) and  $H_2$  (in the case of  $C_5H_5N$ ) desorb at temperatures that are well below the desorption temperature of free hydrogen. This may be due to the effect of the residual carbon left on the surface from decomposition. The  $NiSi_2(100)$  surface, with additional adatom Si atoms sitting in what are perhaps potential C atom sites, may not have available sites for hydrogen adsorption, hence they desorb. Doing two thermal desorption experiments in a row, without cleaning the surface, should provide clues as to whether this is possible. However, at the high temperatures attained in the flash, carbon apparently diffused into the bulk, for there was no discernable change in the Auger spectrum.

Other than hydrogen desorption temperature, there is not much difference between the thermal desorption spectra of  $NiSi_2(100)$  and  $NiSi_2(111)$ . The ethylene spectra look very similar except for some decomposition on the (111) plane, and the benzene spectra look similar as well.



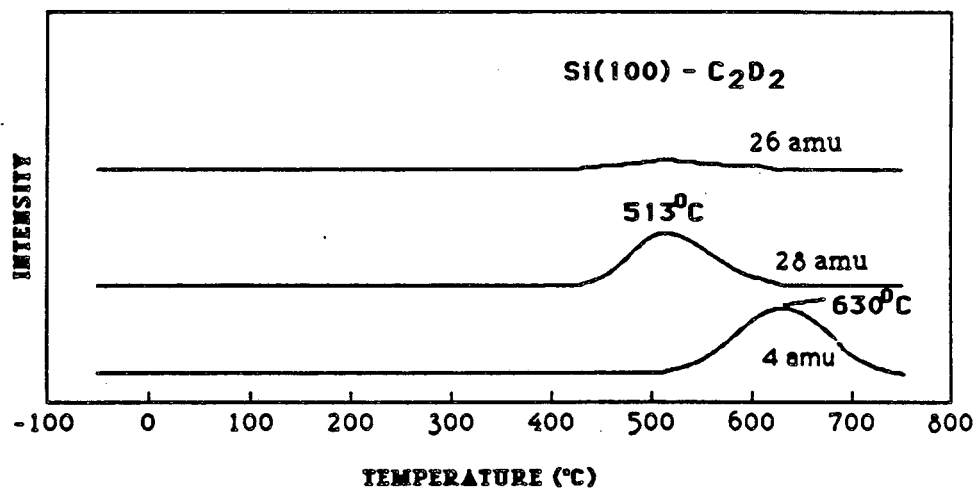


Figure 5-1. Thermal desorption spectrum of deuterated acetylene off of Si(100). Both acetylene(molecular desorption) and deuterium(due to acetylene decomposition) are seen desorbing from the surface. The high temperature deuterium peak seen is characteristic of hydrogen desorption off of Si(100).

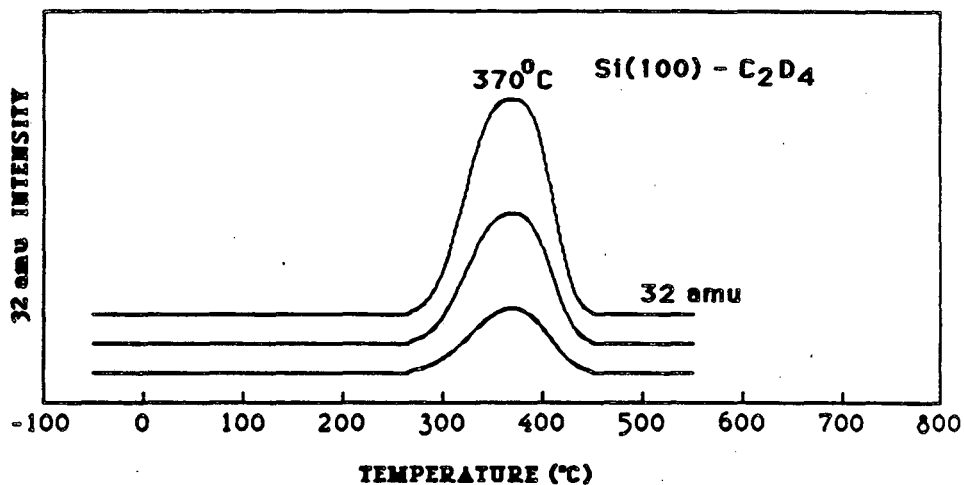


Figure 5-2. Thermal desorption spectra of deuterated ethylene off of  $Si(100)$ , starting with several different coverages. Only molecular desorption is observed--no decomposition of ethylene on  $Si(100)$  occurred.

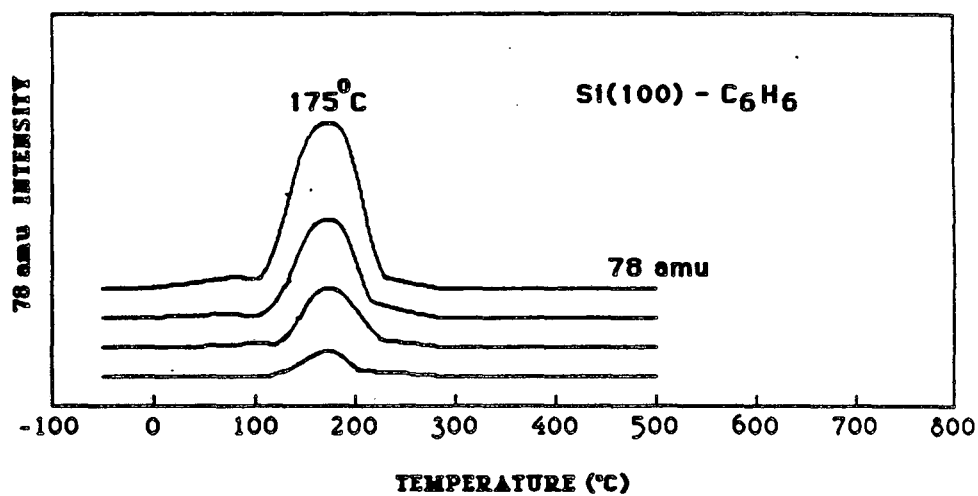


Figure 5-3. Thermal desorption spectra of benzene off of Si(100), starting with several different coverages. Here, as was the case with ethylene, only molecular desorption is observed. Benzene did not decompose on the Si(100) surface.

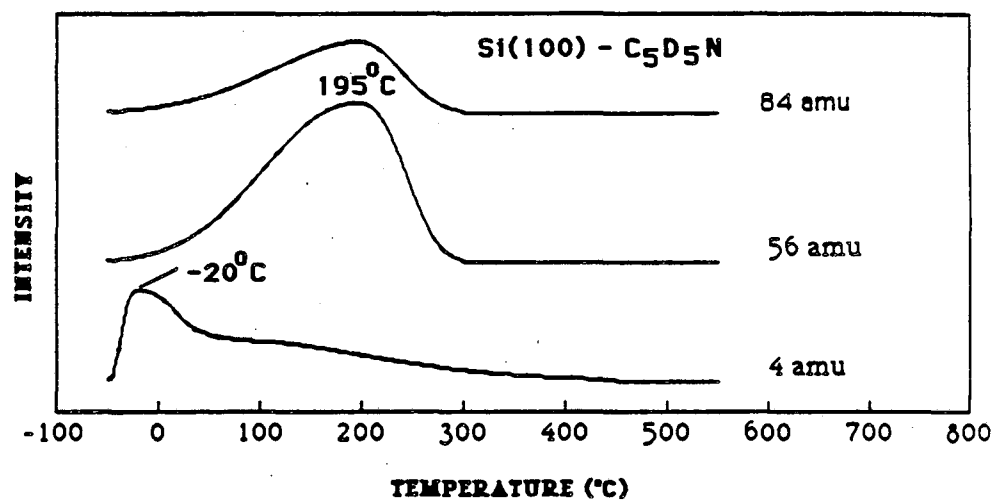


Figure 5-4. Thermal desorption spectrum of deuterated pyridine off of Si(100). Initial coverage was near saturation. Both deuterium and molecular pyridine desorbed, indicating only partial decomposition of pyridine occurred on the Si(100) surface. The low desorption temperature of the deuterium suggests the D atoms never reached the Si(100) surface before desorbing.

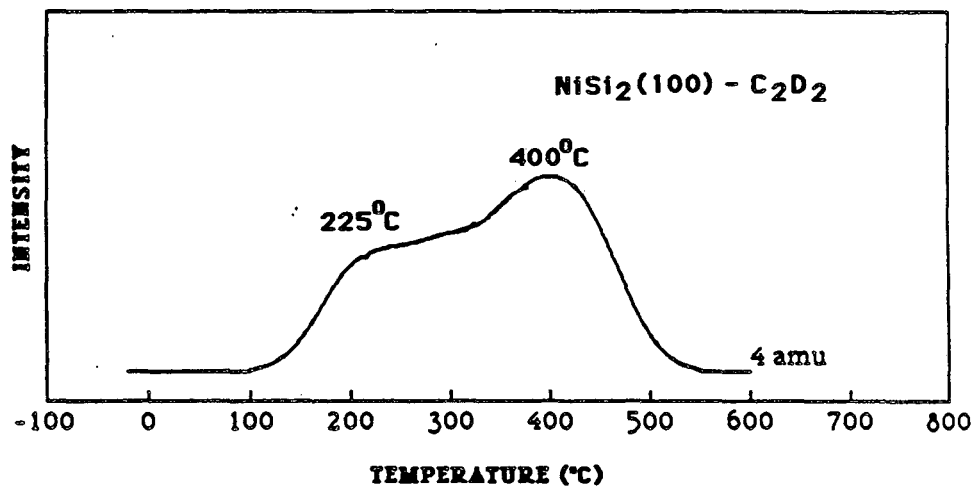


Figure 5-5. Thermal desorption spectrum of deuterated acetylene off of NiSi<sub>2</sub>(100). Only the decomposition product, D<sub>2</sub>, was seen. Characteristic D<sub>2</sub> desorption off of NiSi<sub>2</sub>(100) occurs at much higher temperature.

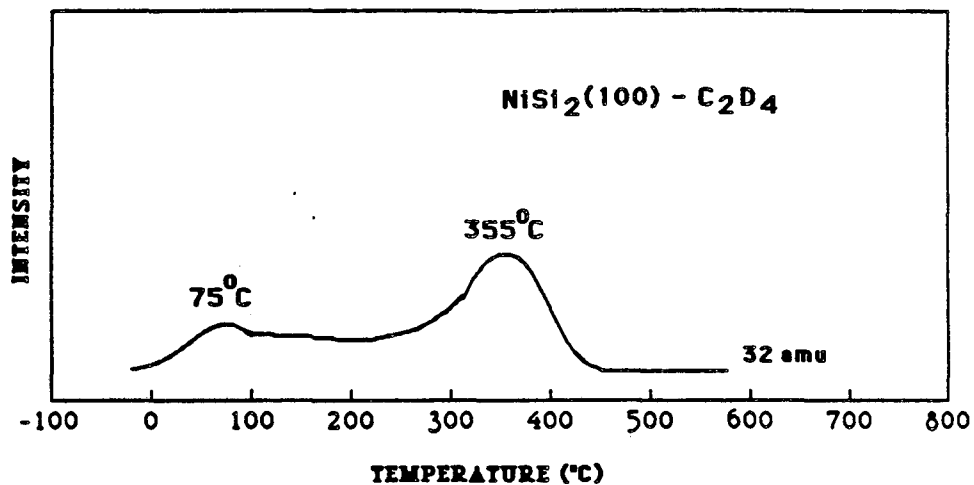


Figure 5-6. Thermal desorption spectrum of deuterated ethylene off of NiSi<sub>2</sub>(100). Only molecular desorption of ethylene was observed, indicating no decomposition of the molecule occurred.

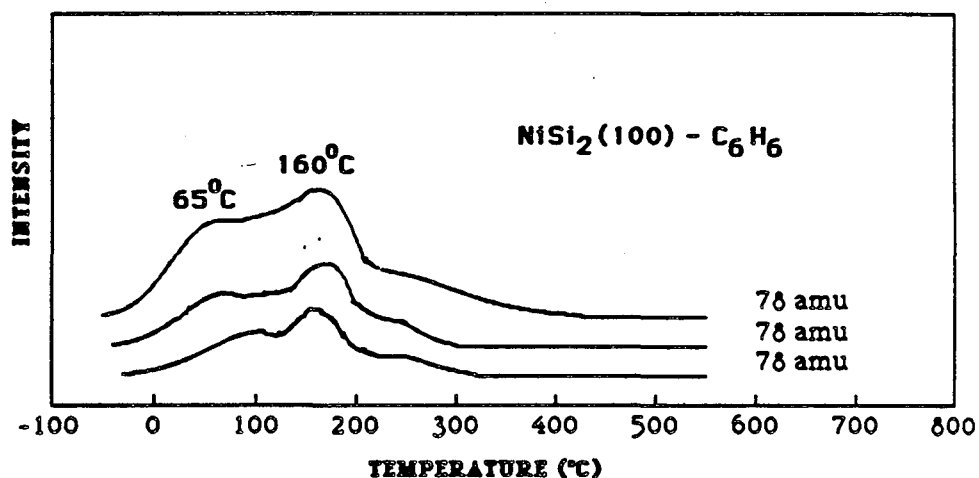
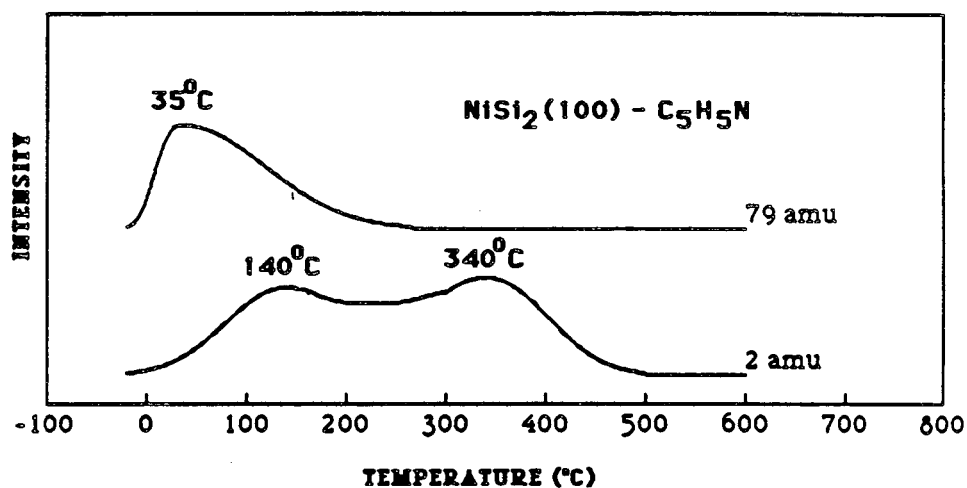


Figure 5-7. Thermal desorption spectra of benzene off of NiSi<sub>2</sub>(100), starting with three different coverages. The two main peaks indicate that two different adsorption states exist for benzene on NiSi<sub>2</sub>(100). Equal population of each state regardless of initial coverage suggests little surface diffusion of benzene on this surface.



**Figure 5-8.** Thermal desorption spectrum of pyridine off of NiSi<sub>2</sub>(100), starting with near saturation coverage. Both molecular desorption and hydrogen desorption are observed, indicating partial decomposition of pyridine on NiSi<sub>2</sub>(100).



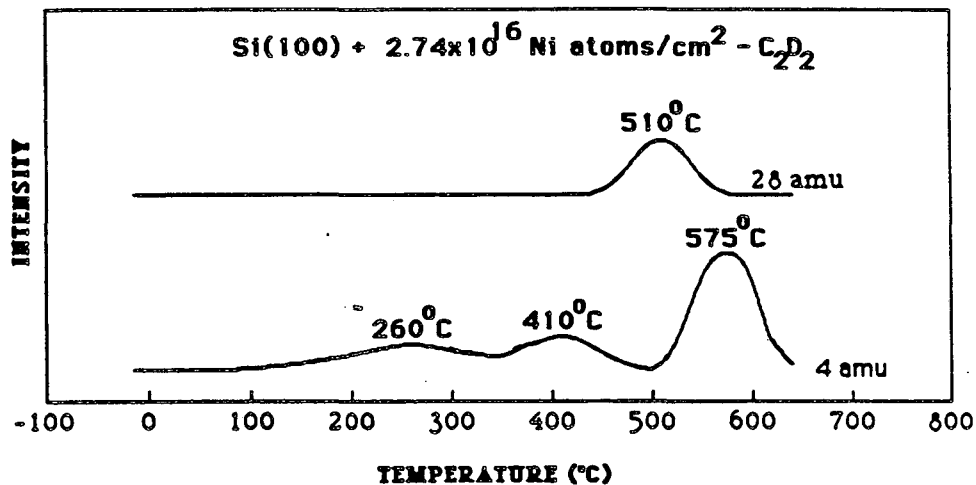
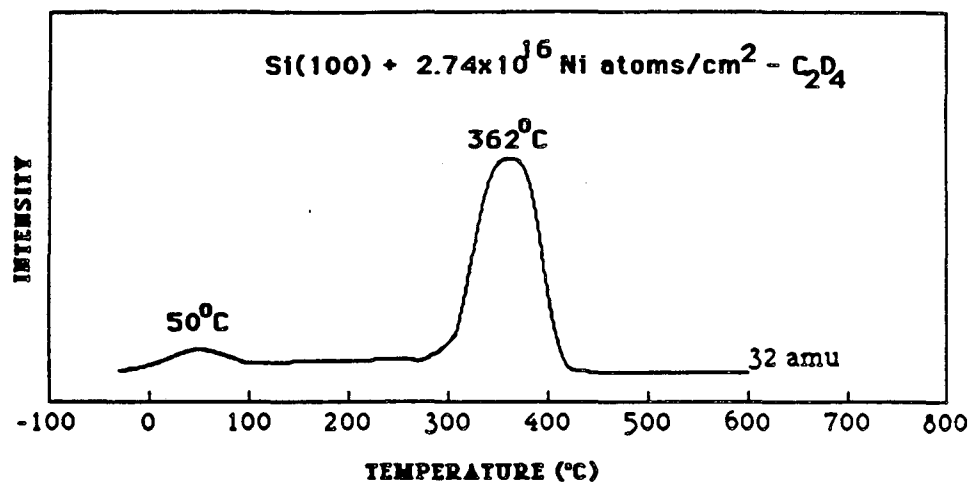


Figure 5-9. Thermal desorption spectrum of deuterated acetylene off of Si(100) with  $2.74 \times 10^{16}$  Ni atoms/cm<sup>2</sup> previously deposited and annealed. The spectrum contains features characteristic of both Si(100) and NiSi<sub>2</sub>(100) acetylene thermal desorptions, indicating NiSi<sub>2</sub>(100) island growth.



**Figure 5-10.** Thermal desorption spectrum of deuterated ethylene off of Si(100) with  $2.74 \times 10^{16}$  Ni atoms/cm<sup>2</sup> previously deposited and annealed. NiSi<sub>2</sub>(100) island growth is hinted at by the presence of features characteristic of both NiSi<sub>2</sub>(100) and Si(100).

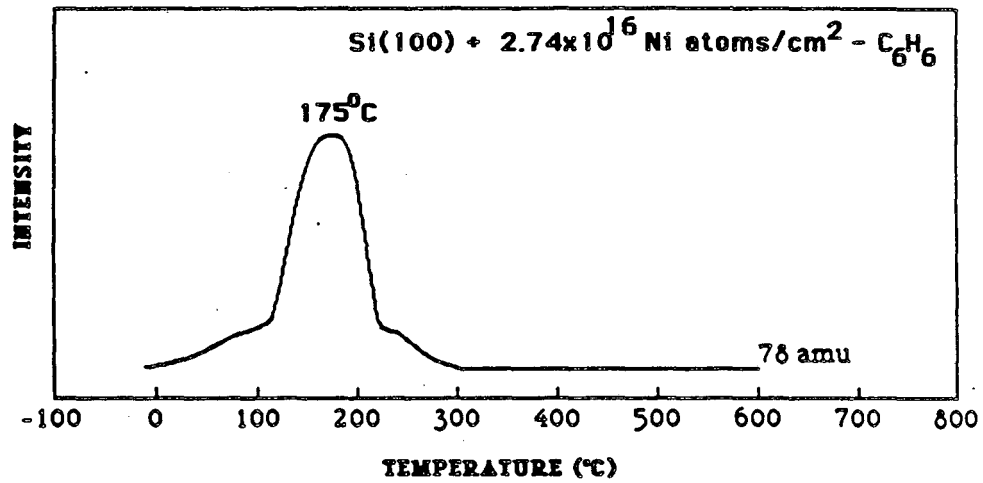


Figure 5-11. Thermal desorption spectrum of benzene off of Si(100) with  $2.74 \times 10^{16}$  Ni atoms/cm<sup>2</sup> previously deposited and annealed. Although not as clear as the acetylene case, the spectrum is different enough from that of pure Si(100) to suggest NiSi<sub>2</sub>(100) island growth.

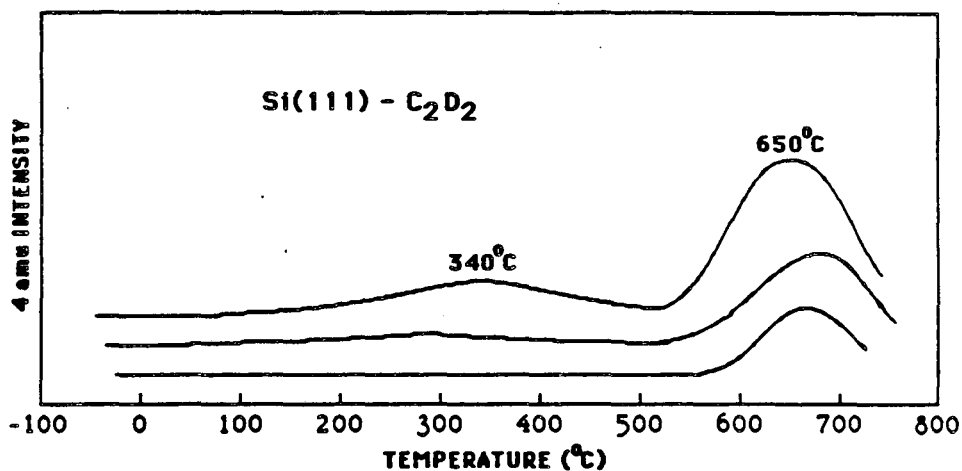


Figure 5-12. Thermal desorption spectra of acetylene off of Si(111) starting with several different coverages. Only deuterium desorption was detected, indicating the acetylene completely decomposed on Si(111). The spectra are characteristic of deuterium desorption from Si(111).

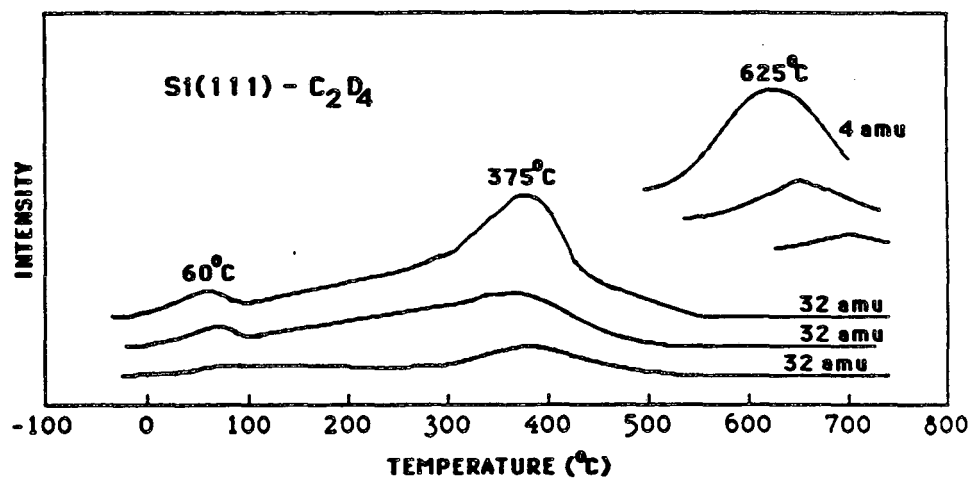


Figure 5-13. Thermal desorption spectra of deuterated ethylene off of Si(111), starting with three different coverages. Both deuterium and ethylene desorption are observed, indicating only partial decomposition of the ethylene occurred on this surface.

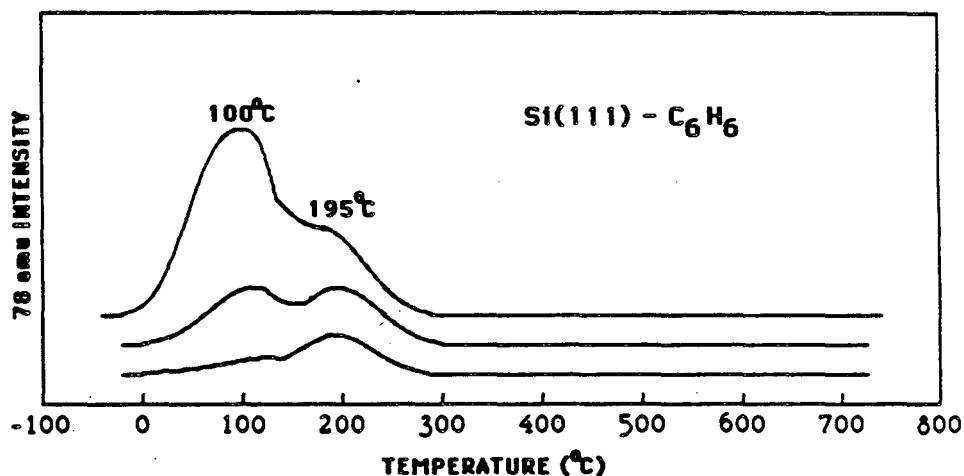
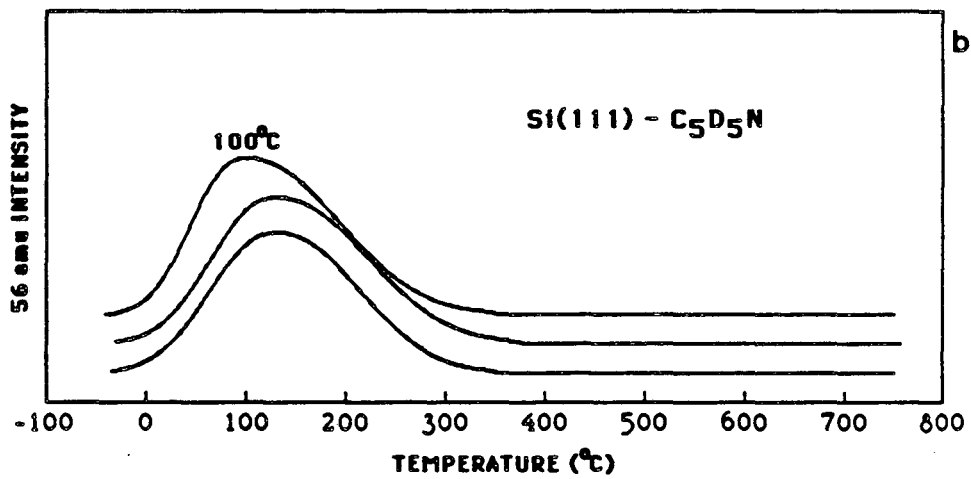
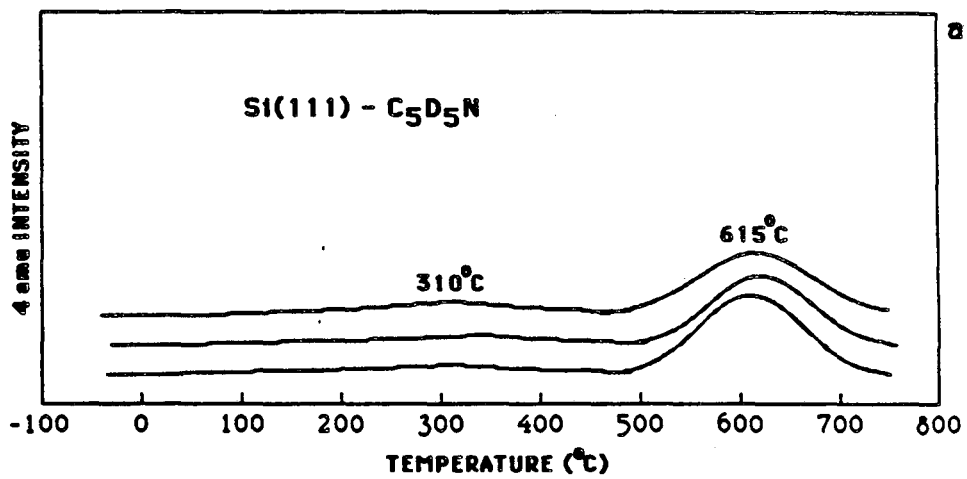


Figure 5-14. Thermal desorption spectra of benzene off of Si(111), starting with three different coverages. No decomposition of benzene occurred in this case--only molecular desorption was observed. At low coverages only the high temperature peak is seen. At higher coverages the lower temperature peak grows in. This indicates two different adsorption states for benzene on Si(111).

Figure 5-15. Thermal desorption spectra of deuterated pyridine off of Si(111), starting with three different coverages. Both decomposition and molecular desorption occur. In (a), the decomposition product,  $D_2$ , is depicted. The spectra found here are characteristic of free hydrogen desorption off of this surface. In (b), the molecular peak is shown for the three spectra. The peak maximum temperature for molecular desorption occurs at  $100^\circ\text{C}$ .





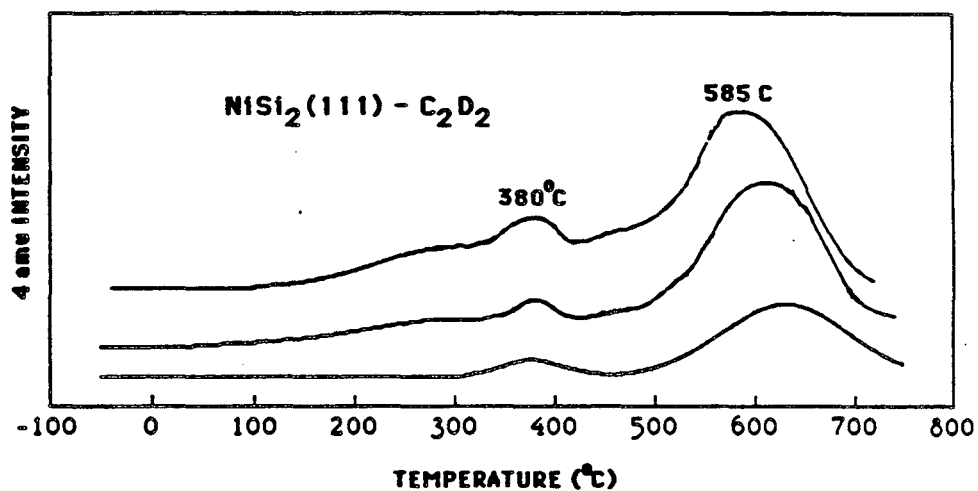


Figure 5-16. Thermal desorption spectra of deuterated acetylene off of NiSi<sub>2</sub>(111), starting with three different coverages. The only gas detected desorbing from the surface was D<sub>2</sub>, indicating complete decomposition of the molecule. The 380°C peak is the only feature that distinguishes these spectra from hydrogen desorption off of NiSi<sub>2</sub>(111).

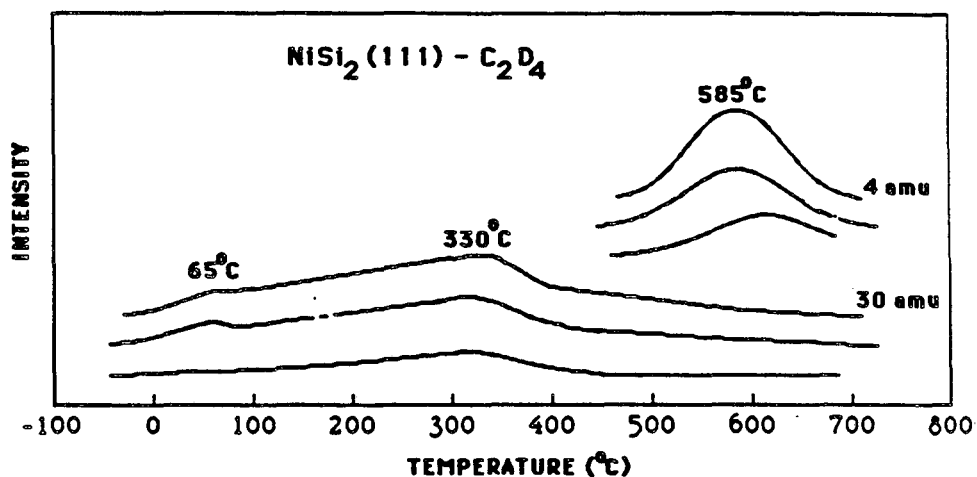


Figure 5-17. Thermal desorption spectra of detuerated ethylene off of NiSi<sub>2</sub>(111), starting with three different coverages. Both ethylene and D<sub>2</sub> are detected desorbing from the surface, indicating only partial decomposition of the ethylene occurred.

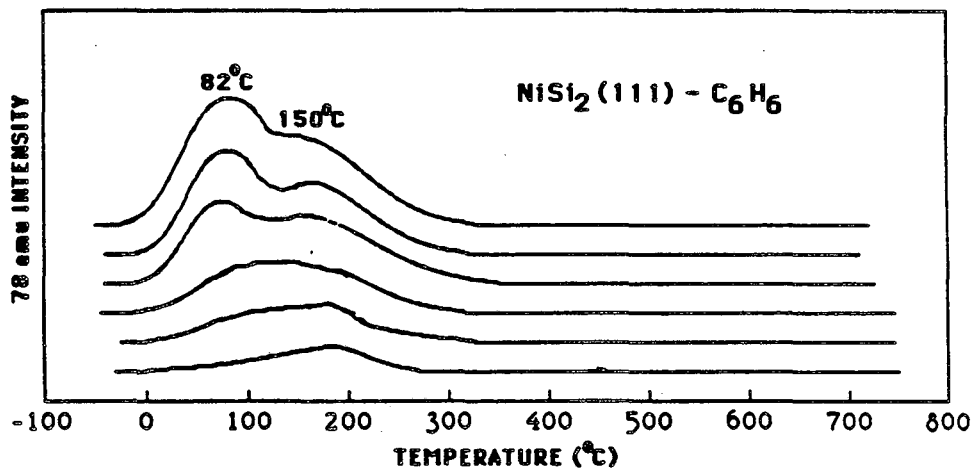


Figure 5-18. Thermal desorption spectra of benzene off of  $NiSi_2(111)$ , starting with several different coverages. Only benzene desorption occurred, indicating no decomposition of the molecule took place. The two peaks present in the spectrum suggest two different adsorption states for benzene on  $NiSi_2(111)$ .

Figure 5-19. Thermal desorption spectra of deuterated pyridine off of  $\text{NiSi}_2(111)$ , starting with two different coverages. Both decomposition and molecular desorption occur. In (a), the decomposition product,  $\text{D}_2$ , is depicted. The spectra found here are characteristic of free hydrogen desorption off of this surface. In (b), the molecular peak is shown for the two spectra. The peak maximum temperature for molecular desorption occurs at  $35^\circ\text{C}$ , much lower than was the case for the  $\text{Si}(111)$  surface.

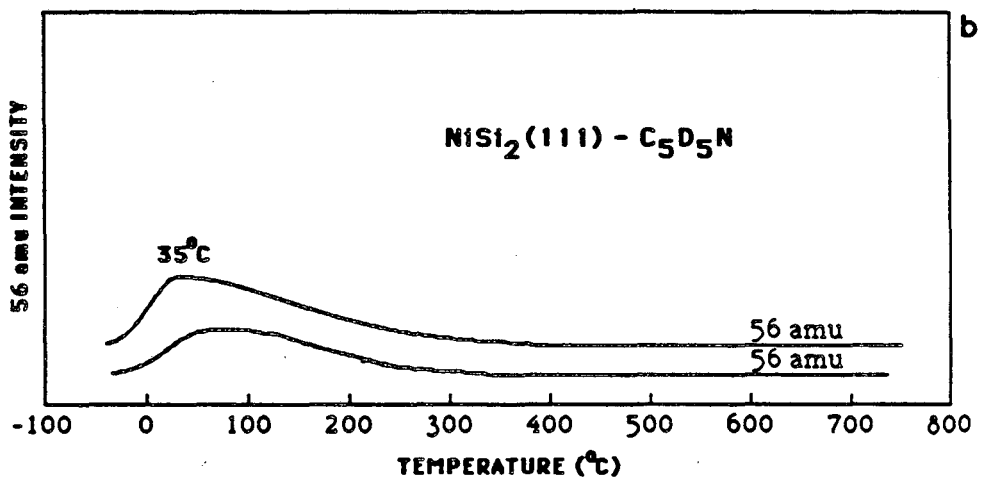
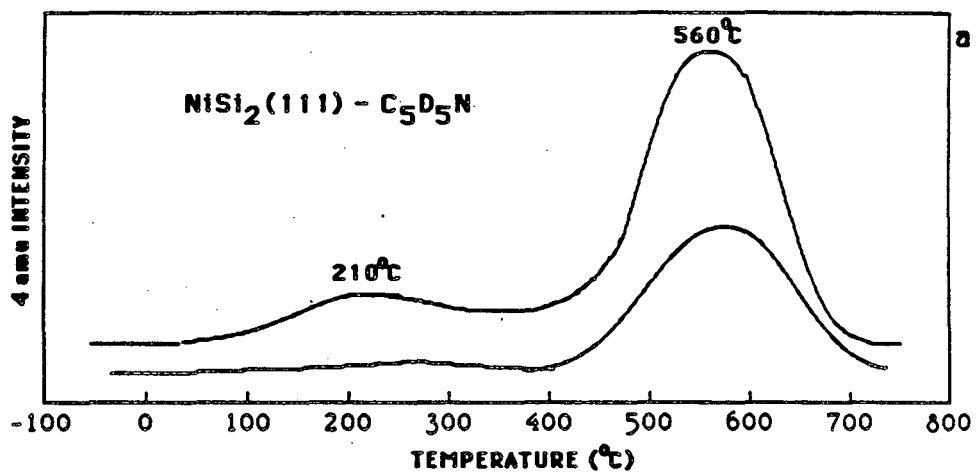
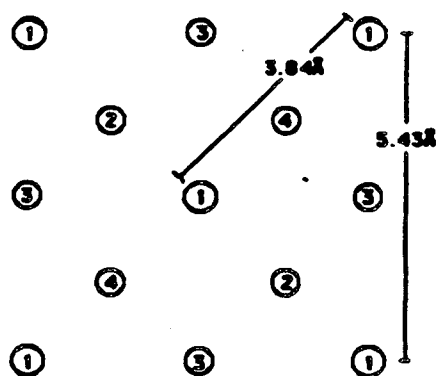


Figure 5-20. Side and top views of ideal Si(100) and NiSi<sub>2</sub>(100)

surfaces. Both surfaces reconstruct. The numbers indicate which layer the represented atom belongs in: 1 being the top layer, 2 the second layer down, etc.... The second layer in NiSi<sub>2</sub>(100) consists of Ni atoms.

Note that the surface Si atom distance is actually smaller on NiSi<sub>2</sub>(100) than on Si(100).

Si(100)



NiSi<sub>2</sub>(100)

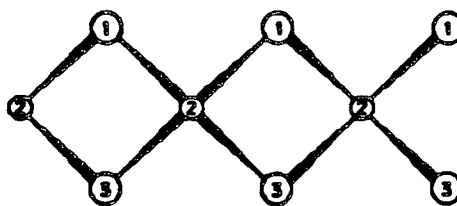
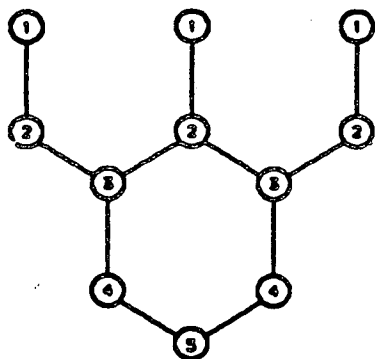
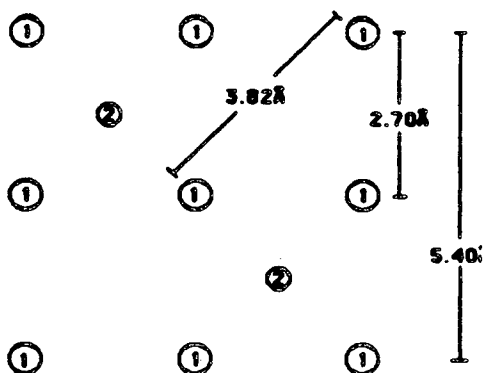
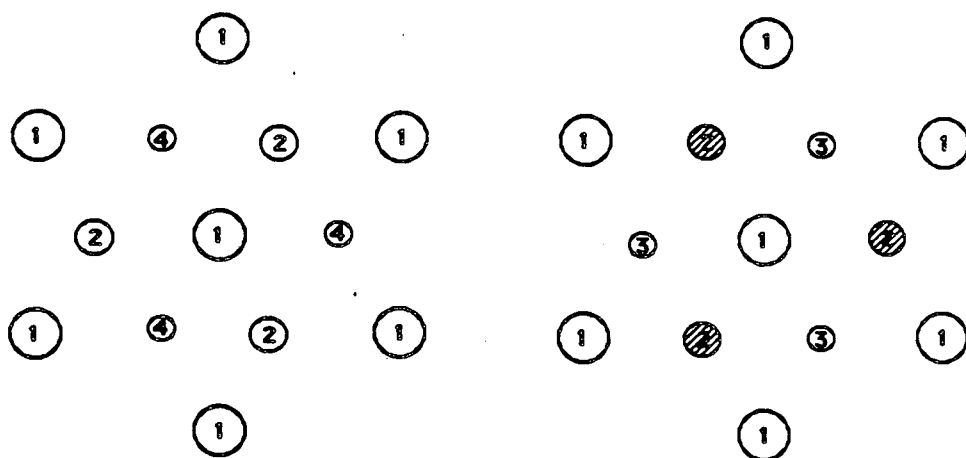


Figure 5-21. Side and top views of ideal Si(111) and NiSi<sub>2</sub>(111) surfaces. The Si(111) surface reconstructs. The numbers indicate which layer the represented atoms belong in: 1 is for the top layer, 2 for the second layer down, etc.... The second layer in NiSi<sub>2</sub>(111) consists of Ni atoms. The top layers of Si atoms on both surfaces are essentially identical.





$\text{Si}(111)$

$\text{NiSi}_2(111)$

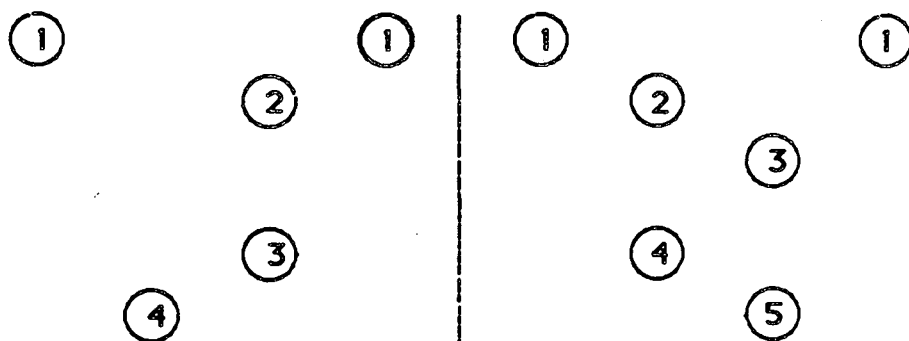


Table 5-1. When small amounts of Ni are deposited onto the Si(100) surface (in this case  $9.13 \times 10^{15}$  Ni atoms/cm<sup>2</sup>), and the crystal slowly heated, diffusion of the Ni into the Si occurs. Eventually the clean Si surface Auger electron spectrum and LEED pattern are regained.

Temperature(°C)	Si <sub>92</sub> /Ni <sub>61</sub> Auger Ratio	LEED Pattern
-45	infinite	2x2 sharp
-45	1.4	none
0	.95	
50	1	
100	1.3	
150	1.6	
200	2	
250	2	
300	3	
350	3.2	
400	5.8	1x1 diffuse
450	6	
500	7	1x1
550	34	
600	43	
650	55	
700	infinite	2x2 sharp
750	infinite	

Table 5-2. The size of the 380°C peak for C<sub>2</sub>D<sub>2</sub> thermal desorptions(found only with the NiSi<sub>2</sub>(111) surface and not with the Si(111) surface) grows relative to the high temperature peak(found on both surfaces) with increasing Ni acculmulation. Each Ni deposition was followed by a high temperature anneal necessary to form NiSi<sub>2</sub>. The data indicate that NiSi<sub>2</sub>(111) islands form on the Si(111) surface with small Ni depositions.

Ni Atoms Deposited (/cm <sup>2</sup> )	Total Accumulated (/cm <sup>2</sup> )	Si92/Ni61 Auger Ratio	LEED Pattern	Size of 380°C Peak Relative to High Temperature Peak
0	0	infinite	7x7	0%
1.37X10 <sup>16</sup>	1.37X10 <sup>16</sup>	35	1x1 (faint lines)	9%
1.37x10 <sup>16</sup>	1.37x10 <sup>16</sup>			
2.74x10 <sup>16</sup>	5.48x10 <sup>16</sup>	24	1x1 (possibly faint lines)	20%
2.74x10 <sup>16</sup>	8.22x10 <sup>16</sup>	14	1x1	36%

<b>Areas</b>			
	<u>amu</u>	<u>Si(100)</u>	<u>NiSi<sub>2</sub>(100)</u>
C <sub>2</sub> D <sub>2</sub>	4	414	113
	28	92	-
C <sub>2</sub> D <sub>4</sub>	32	1360	233
C <sub>6</sub> H <sub>6</sub>	78	652	429
C <sub>5</sub> D <sub>5</sub> N	4	606	495(2 amu)
	56	796	228(52 amu)
	84	398	175(79 amu)

Table 5-3. A comparison of the peak areas found under the thermal desorption peaks for the various adsorbates shows that saturation coverage on NiSi<sub>2</sub>(100) is much less than on Si(100). This is particularly true for ethylene. The masses listed in parentheses are present because perdeutero pyridine was used on NiSi<sub>2</sub>(100) while perdeutero pyridine was used on Si(100).

## Chapter Six

### Conclusions

The Ir and Ni experiments reported and discussed in this thesis show how thermal desorption spectroscopy and isotopic labeling can be useful in deciphering complicated reaction mechanisms of large molecules on metal surfaces. Of course, it is necessary to use adsorbate molecules where isotopic labeling is possible and will demonstrate something--molecules with distinctive atoms. Methyl-substituted benzenes, with their aliphatic and aromatic hydrogen atoms, were ideal for this type of study.

The decomposition of methyl-substituted benzenes on metal surfaces proceeds in a step-wise fashion, with methyl(aliphatic)C-H bonds breaking prior to aromatic C-H bonds. The mechanism of decomposition is not necessarily the same on every surface, as is demonstrated by the thermal desorption spectra of *p*-xylene off of Ni(100) and Ir(111) surfaces.

In order for thermal desorption spectroscopy to show regiospecific bond breakage, the temperatures at which the different bonds break must be sufficiently different. This was the case for Ni(100) but not for Ni(111), demonstrating that different surface orientations affect certain types of bonds more than others. The (100) surface breaks aliphatic C-H bonds more easily than the (111) surface, but the (111) surface breaks aromatic C-H bonds easier than the (100) surface. This latter effect is most likely due to the symmetry of the (111) surface and the six-member aromatic ring being the same. The other factor which helps demonstrate regiospecific bond breakage is the symmetry of the adsorbate molecule. Higher symmetry means fewer different interactions with the surface, so the thermal desorption spectrum is simpler. The peaks are better resolved. This is why *p*-xylene showed regiospecific bond breakage more clearly than *o*- or *m*-xylene.

The Si/NiSi<sub>2</sub> experiments demonstrated several different things. They confirmed that the top layer of the NiSi<sub>2</sub> surface is Si; the surface chemistry of

NiSi<sub>2</sub> was similar to Si in more respects than would be the case were Ni in the top layer. They also showed that the underlying Ni has only a small effect on Si surface chemistry. This was particularly true for Si(111), where NiSi<sub>2</sub>(111) has almost the exact same surface geometry. Only a small decrease in surface reactivity was noted.

This information has far-reaching implications. It suggests that, in some cases, bulk contaminants of crystals will not have any appreciable effect on the surface chemistry and can be ignored. It also suggests that oxidizing only the near-surface region is sufficient to mimic true oxide behavior--if crystallinity can be achieved.

The other important point brought out by the Si/NiSi<sub>2</sub> studies was that NiSi<sub>2</sub> forms islands on the Si surface. This was demonstrated clearly by thermal desorption spectroscopy, where thermal desorption spectra features characteristic of each surface appeared in the same spectrum. The use of thermal desorption spectroscopy to demonstrate island growth is quite useful.

Given the adsorbates used in this thesis, methyl-substituted benzenes, acetylene, ethylene, benzene, and pyridine, it is most likely that they are  $\pi$ -bonding to the surfaces studied. The d orbitals of the metal atoms and the sp<sup>3</sup> dangling bond of the Si atoms are both capable of  $\pi$ -bonding to these adsorbates. This would place the initial bonding geometry of these molecules, other than pyridine, parallel to the surface. Pyridine most likely bonds through both the nitrogen lone pair and the aromatic ring, leading to the tilted geometry suggested in reference 66.



### References and Notes

1. Pierre Laszlo, Acc. Chem. Res., **19**, 121-127(1986).
2. Taylor, et. al., J. Am. Chem. Soc., **98**, 6750(1976).
3. A definition of chemisorption, taken from reference 10, is when "an atom or molecule is bound to a surface through overlapping of one or more of its electron orbitals." This differs from the other type of adsorption, physical adsorption, where the attractive force between adsorbate and surface is Van der Waals interactions. Chemisorption is the formation of an actual chemical bond between adsorbate and surface.
4. C.M. Friend and E.L. Muetterties, J. Am. Chem. Soc., **103**, 773-779(1981).
5. (a) Hans Conrad zur Loye and A.M. Stacy, submitted to J. Phys. Chem. (b) H. Praliaud and G.A. Martin, J. Catal. **72**, 394-396(1981).
6. T. Gentle, Surface Chemistry of Palladium, Ph.D. Thesis, Lawrence Berkeley Laboratory and the University of California, Berkeley, 1984.
7. Solomon, et. al., J. Am. Chem. Soc., **102**, 6752-6761(1980).
8. Rebecca Rawls, Chem. Eng. News., **June 23, 1986**, 35-36.
9. David R. Nelson, Scientific American, **255(2)**, 42(1986).
10. Alfred Clark, The Chemisorptive Bond, Academic Press, New York, 1974.

11. The density gradient is  $d[\ln N(E)]/dE$ . A positive density gradient means that there is an increasing number of states available at that particular energy.
12. Roy S. Morrison, "Semiconductor Surfaces" in Treatise on Solid State Chemistry, Vol. 6B Surfaces II., ed. Hannay, Plenum Press, New York, page 203(1976).
13. Shen-Shu Sung and Roald Hoffmann, J. Am. Chem. Soc., 107, 578-584(1985).
14. H. Kobayashi, K. Edamoto, M. Onchi, and M. Nishijima, J. Chem. Phys., 78(12), 7429-7436.
15. M. Henzler, Surf. Sci., 25, 650-680(1971).
16. Dieter Schmeisser, Surf. Sci., 137, 197-210(1984).
17. J.A. Appelbaum and D.R. Hamann, "Chemisorption on Semiconductor Surfaces" in Topics in Current Physics: Theory of Chemisorption, ed. by J.R. Smith(1980).
18. Norman P. Lieske, J. Phys. Chem. Solids, 45(8/9), 821-870(1984).
19. B.E. Koel, J.E. Crowel, B.E. Bent, C.M. Mate, and G.A. Somorjai, J. Phys. Chem., 90, 2949-2956(1986).
20. P.A. Redhead, Vacuum, 12, 203(1962).
21. David A. King, Surf. Sci., 47, 384-402(1975).

22. Frances M. Lord, Surf. Sci., 43, 173-182(1974).
23. John L. Falconer and Robert J. Madix, J. Catal., 48, 262-268(1977).
24. L.A. Petermann, "Thermal Desorption Kinetics of Chemisorbed Gases" in Progress in Surface Science, Vol. 3, ed. by Davison, page 1(1973).
25. C.M. Chan, R. Aris, and W.H. Weinberg, Appl. Surf. Sci., 1, 360(1978).
26. J.M. Soler and N. Garcia, Surf. Sci., 124, 563-570(1983).
27. The use of  $10^{13} \text{ sec}^{-1}$  for the frequency factor can be a large source of error in the calculation. It is a general estimate at best. Frequency factors can range from  $10^8 \text{ sec}^{-1}$  to  $10^{15} \text{ sec}^{-1}$ .
28. Farrokh Mohammadi, Solid State Technology, Jan. 1981, p. 65.
29. R.T. Tung, J.M. Poate, J.C. Bean, J.M. Gibson, and D.C. Jacobson, Thin Solid Films, 93, 77-9(1982).
30. B.A. Joyce and J.H. Neave, Surf. Sci., 34, 401-419(1973).
31. R.E. Kirby and D. Lichtman, Surf. Sci., 41, 447-466(1974).
32. R.E. Kirby and J.W. Dieball, Surf. Sci., 41, 467-74(1974).
33. B.E. Nieuwenhuys, D.E. Hagen, G. Rovida, and G.A. Somorjai, Surf. Sci., 59, 155-176(1976).

34. J.U. Mack, E. Bertel, and F.P. Netzer, Surf. Sci., 159, 265-282(1985).
35. Due to heater wire background desorption, the initial part of the thermal desorption spectra was often very noisy. This may have prevented the detection of molecular desorption, even from a physisorbed state, from the Ir(111) surface.
36. K. Christmann, O. Schober, G. Ertl, and M. Neumann, J. Chem. Phys., 60(11), 4528(1974).
37. H. Jobic, B. Tardy, and J.C. Bertolini, Journal of Electron Spectroscopy and Related Phenomena, 38, 55-64(1986).
38. J.C. Bertolini, G. Dalmai-Imelik, and J. Rousseau, Surf. Sci., 67, 478-488(1977).
39. T.N. Rhodin and G. Ertl., The Nature of the Surface Chemical Bond, North-Holland Publishing Co., New York(1979).
40. G.A. Somorjai, Adv. Cat., 26, 1-68(1977).
41. Saturation coverage was considered achieved when no larger amount of adsorbate desorbed from the surface despite a large increase in the exposure given.
42. Yip Wah Chung, Wigbert Siekhaus, and G.A. Somorjai, Surf. Sci., 58, 341-348(1976).
43. P. Klimesch, G. Meyer, and M. Henzler, Surf. Sci., 124, 336-350(1983).

44. I. Ivanov, A. Mazur, and J. Pollmann, Surf. Sci., 92, 365-384(1980).
45. D.J. Chadi, Phys. Rev. Lett., 43(1), 43-47(1979).
46. E.G. McRae, Surf. Sci., 124, 106-128(1983).
47. E.G. McRae, "Triangle-Dimer Stacking-Fault Model of the Si(111)7x7 Surface Bonding Configuration" in The Structure of Surfaces, ed. by M.A. Van Hove and S.T. Tang, Springer Verlag, New York, p. 278(1984).
48. A.G. Schrott and S.C. Fain, Jr., Surf. Sci., 123, 204-222(1982).
49. A.G. Schrott, Q.X. Su, and S.C. Fain, Jr., Surf. Sci., 123, 223-230(1982).
50. M. Nishijima, H. Kobayashi, K. Edamoto, and M. Onchi, Surf. Sci., 137, 473-490(1984).
51. T. Isu and K. Fujiwara, Solid State Communications, 42(6), 477-479(1982).
52. K. Fujiwara and H. Ogata, Surf. Sci., 72, 157-166(1978).
53. M. Miyamura, Y. Sakisada, M. Nishijima, and M. Onchi, Surf. Sci., 72, 243-252(1978).
54. H. Frederick Dylla, John G. King, and Mark J. Cardillo, Surf. Sci., 74, 141-167(1978).
55. A.J. van Bommel and J.E. Crombeen, Surf. Sci., 36, 773-777(1973).
56. That H<sub>2</sub> does not adsorb on Si surfaces is due to the high activation energy

of H<sub>2</sub> dissociation, since the Si-H bond itself is very strong. It may be that because Si, unlike transition metals, does not have occupied d orbitals; there is no electron density at a high enough energy to transfer to the  $\sigma^*$  orbital of the H<sub>2</sub> molecule. Thus no destabilization of the H<sub>2</sub> molecule by the Si surface occurs.

57. J.S. Schaefer, F. Stuck, J.A. Anderson, G.J. Lapeyre, and W. Gopel, Surf. Sci., **140**, 207-215(1984).
58. Jin Xiaofeng, Feng Yiqing, Zhuang Chengqun, and Wang Xun, "The Thermal Desorption Spectra of Hydrogen Chemisorption on Si(100) Clean Surface," in Proceedings of the 17th International Conference on the Physics of Semiconductors, ed. by Chadi and Harrison, Springer-Verlag, p. 117(1985).
59. D. Schmeisser, F.J. Himpsel, and G. Hollinger, Phys. Rev. B, **27**(12), 7813-7816(1983).
60. Kenzo Fujiwara, Surf. Sci., **108**, 124-134(1981).
61. S. Ciraci, S. Erkoc, and S. Ellialioğlu, Solid State Communications, **Vol. 45**(1), 35-38(1983).
62. K. Fujiwara and H. Ogata, Surf. Sci., **86**, 700-705(1979).
63. M. Nishijima, K. Edamoto, Y. Kubota, H. Kobayash, and M. Onchi, Surf. Sci., **158**, 422-437(1985).
64. F.W. Smith, Surf. Sci., **80**, 388-393(1979).

65. F. Meyer, Surf. Sci., 27, 107-116(1971).
66. M.N. Piancastelli, G. Margaritondo, and J.E. Rowe, Solid State Communications, 45(3), 219-221(1983).
67. Here less interaction means less strongly bound adsorbates and less decomposition.
68. T.A. Nguyen, M. Azizan, R.C. Cint, and G. Chauvet, Surf. Sci., 162, 651-656(1985).
69. Yasuo Takahashi, Hiromu Ishii, and Junichi Murota, J. Appl. Phys., 58(8), 3190-3194(1985).
70. Akio Hiraki, Surf. Sci., 168, 74-99(1986).
71. Akio Hiraki, Surf. Sci. Reports, 3, 357-412(1984).
72. R.M. Walser and R.W. Bene', Applied Physics Letters, 28(10), 624-625(1976).
73. Max Hansen and Kurt Anderko, Constitution of Binary Alloys, McGraw-Hill Book Company Inc., New York, page 1039(1958).
74. Maria Ronay, Applied Physics Letters, 42(7), 577-579(1983).
75. F. d'Heurle, S. Petersson, L. Stolt, and B. Strizker, J. Appl. Phys., 53(8), 5678-5681(1982).
76. C. Calandra, O. Bisi, and G. Ohavian, Surface Science Reports, 4,

271-364(1985).

77. F.M. d'Heurle and P. Gas, Journal of Materials Research, 1986.
78. V. Raghavan and Morris Cohen, "Solid State Phase Transformations" in Treatise on Solid State Chemistry, Vol. 5: Changes of State, ed. by Hannay, Plenum Press, New York(1976).
79. F.M. d'Heurle, C.S. Petersson, Thin Solid Films, 128(3-4), 283-297(1985).
80. K.C.R. Chiu, J.M. Poate, J.E. Rowe, T.T. Sheng, and A.G. Cullis, Appl. Phys. Lett., 38(12), 988-990(1981).
81. N.W. Cheung, P.J. Grunthaner, F.J. Grunthaner, and J.M. Mayer, J. Vac. Sci. Technol., 18(3), 917-923(1981).
82. P.S. Ho, M. Liehr, P.E. Schmid, F.K. Legoues, E.S. Yang, H.L. Evans, and X. Wu, Surf. Sci., 168, 184(1986).
83. Yu-Jeng Chang and J.L. Erskine, Physical Review B, 28(10), 5766.
84. Yu-Jeng Chang and J.L. Erskine, Physical Review B, 26(8), 4766-4769(1982).
85. S.C. Wu, Z.Q. Wang, Y.S. Li, F. Jona, and P.M. Marcus, Solid State Communications, Vol. 57(8), 687-690(1986).
86. J.G. Clabes, Surf. Sci., 145, 87-100(1984).
87. W.S. Wang, F. Jona, and P.M. Marcus, Physical Review B, 28,



7377-7380(1983).

88. D. Morgen, W. Worth, and E. Umbach, Surf. Sci., 152/153, 1086-1095(1985).
89. F. Comin, J.E. Rowe, and P.H. Citrin, Phys. Rev. Lett., 51, 2402(1983).
90. R.T. Tung, J.M. Gibson, and J.M. Poate, Phys. Rev. Lett., 50(6), 429.
91. R.D. Thompson, D. Gupta, and K.N. Tu, Physical Review B., 33(4), 2636-2641(1985).
92. M. Hanbucken and H. Neddermeyer, Surf. Sci., 114, 563-573(1982).
93. W.S. Yang, S.C. Su, and F. Jona, Surf. Sci., 169, 383-393(1986).
94. N.W. Cheung, and J.W. Mayer, Phys. Rev. Lett., 46(10), 671-674(1981).
95. O. Bisi, L.W. Chiao, and K.N. Tu, Surf. Sci., 152/153, 1185-1190(1985).
96. Yu-Jeng Chang and J.L. Erskine, J. Vac. Sci. Technol. A, 1(2), 1193-1197(1983).
97. K. Okuno, T. Ito, M. Iwami, and A. Hiraki, Solid State Communications, 44(2), 209-212(1982).
98. Yasufumi Yabuuchi, Fumiya Shoji, Kenjiro Oura, Tervo Hanawa, Yozo Kishikawa, and Satosh Okada, Jap. J. Appl. Phys., 21(12), L752-L754(1982).

99. S. Okada, K. Oura, T. Hanawa, and K. Satoh, Surf. Sci., 97, 88-100(1980).
100. C. Pirri, J.C. Peruchetti, G. Gewinner, and J. Derrien, Phys. Rev. B, 29(6), 3391-3397(1984).
101. Yasushi Terada, Tohru Toshizuka, Kenjiro Oura, and Tervo Hanawa, Surf. Sci., 114, 65-84(1982).
102. Shang - Lin Weng. Phys. Rev. B., 29(4), 2363-2365(1984).
103. M. Iwami, S. Hashimoto, and A. Hiraki, Solid State Communications, 49(5), 459-462(1984).
104. G. Rossi, J. Nogami, I. Lindau, and Z. Braicovich, J. Vac. Sci. Technol. A, 1(2), 781-784(1983).
105. H. Balaska, R.C. Cinti, T.T.A. Nguyen, and J. Derrien, Surf. Sci., 168, 225-233(1986).
106. J.G. Clabes, G.W. Rubloff, and T.Y. Tan, Phys. Rev. B., 29(4), 1540.
107. K.N. Tu, Appl. Phys. Lett., 27, 221(1975).
108. Alex Zunger. Phys. Rev. B, 24(8), 4372-4391(1981).
109. Koki Takita, et. al., Jap. J. Appl. Phys., Vol 24(12), L932-L934(1985).
110. Y.J. Chabal, R.J. Culbertson, L.C. Feldman, and J.E. Rowe, J. Vac. Sci. Technol., 18(3), 880-882(1981).

111. E.J. van Loenen, J.F. van der Veen, and F.K. LeGoues, Surf. Sci., 157, L373-L378(1985).
112. E.J. van Loenen, J.W.M. Frenken, and J.F. van der Veen, Appl. Phys. Lett., 45(1), 41-43(1984).
113. E.J. van Loenen, A.E.M.J. Fischer, and J.F. van der Veen, Surf. Sci., 154, 52-69(1985).
114. Kasturi L. Chopra, Thin Film Phenomena, McGraw-Hill Book Co., New York, 1969.
115. V.G. Lifshits, V.B. Akilov, and Y.L. Gavriljok, Solid State Communications, 40, 429-432(1981).
116. P. Perfetti, S. Nannarone, F. Patella, and C. Quaresima, Phys. Rev. B, 26(3), 1125-1138(1982).
117. M. Hanbucken, J.J. Metois, P. Mathiez, and F. Salvan, Surf. Sci., 162, 622-627(1985).
118. E. Daugy, P. Mathiez, F. Salvan, and J.M. Layet, Surf. Sci., 154, 267-283(1985).
119. I. Abbati, M. Grion, J. Vac. Sci. Technol., 19(3), 631(1981).
120. M. Hanbucken and G. LeLay, Surf. Sci., 168, 122-132(1986).
121. E.J. van Loenen, M. Iwami, R.M. Tramp, and J.F. van der Veen, Surf. Sci., 137, 1-22(1984).

122. Keiji Horioka, Hiroshi Iwasaki, Shigemitso Maruno, Sung - Te Le, and Shogo Nakamura, Surf. Sci., 136, 121-132(1984).
123. Mitsuchika Saitoh, Fumiya, Shoji, Kenjiro Oura, and Tervo Hanawa, Surf. Sci., 112, 306-324(1981).
124. Akira Kawazu, Tatsuo Otsuki, and Goroh Tominaga, Japanese Journal of Applied Physics, 20(3), 553-560(1981).
125. W.T. Lin, and L.J. Chen, J. Appl. Phys., 58(4), 1515(1985).
126. J. Knall, J.E. Sundgen, G.V. Hansson, and J.E. Greene, Surf. Sci., 166, 512-538(1986).
127. C. Pirri, J.C. Peruchetti, G. Gewinner, and D. Polmont, Solid State Communications, 57(5), 361-364(1986).
128. Y.J. Chabal, D.R. Hamann, J.E. Rowe, and M. Schluter, Phys. Rev. B, 25(12), 7598-7602(1982).
129. J. Tersoff, and D.R. Hamann, Phys. Rev. B, 28, 1168-1170(1983).
130. J.H. Weaver, A. Francios, and V.L. Moruzzi, Phys. Rev. B, 29(6), 3293-3302(1984).
131. M. Azizan, R. Baptist, G. Chavet, and T.A. Nguyen Tan, Solid State Communications, 57(1), 1-3(1986).
132. S. Valeri, U. del Pennino, P. Lomellini, and G. Ottaviani, Surf. Sci., 161,

1-11(1981).

133. S. Valeri, U. del Pennino, P. Lomellini, and P. Sassaroli, Surf. Sci., 145, 371-389(1984).
134. L.H. Dubois and R.G. Nuzzo, J. Am. Chem. Soc., 105, 365-369(1983).
135. O. Bisi, L.W. Chiao, and K.N. Tu, Surf. Sci., 152/153, 1185-1190(1985).
136. Gabor A. Somorjai, Chemistry in Two Dimensions: Surfaces, Cornell University Press, 1981.
137. E.L. Muetterties, R.M. Wexler, T.M. Gentle, K.L. Shanahan, D.G. Klarup, A.L. Johnson, V.H. Grassian, K.B. Lewis, T.G. Rucker, and R. Lum, "Thiophene Coordination Chemistry of Group VIII Metal Surfaces", in preparation.

This report was done with support from the Department of Energy. Any conclusions or opinions expressed in this report represent solely those of the author(s) and not necessarily those of The Regents of the University of California, the Lawrence Berkeley Laboratory or the Department of Energy.

Reference to a company or product name does not imply approval or recommendation of the product by the University of California or the U.S. Department of Energy to the exclusion of others that may be suitable.

*LAWRENCE BERKELEY LABORATORY  
TECHNICAL INFORMATION DEPARTMENT  
UNIVERSITY OF CALIFORNIA  
BERKELEY, CALIFORNIA 94720*